

**BIOACTIVITY-GUIDED EXTRACTION AND
FRACTIONATION OF *ONOSMA BRACTEATUM* WITH
SPECIFIC REFERENCE TO
ITS ANTI-CANCER ACTIVITY AGAINST LUNG CELL
CANCER**

A Thesis submitted to Gujarat Technological University

for the Award of

Doctor of Philosophy

in

PHARMACY

by

Rajapara Arunabahen Mavjibhai

149997390002

under supervision of

Prof. (Dr) Mamta B. Shah



**GUJARAT TECHNOLOGICAL
UNIVERSITY AHMEDABAD**

April-2024

**BIOACTIVITY-GUIDED EXTRACTION AND
FRACTIONATION OF *ONOSMA BRACTEATUM*
WITH SPECIFIC REFERENCE TO
ITS ANTI-CANCER ACTIVITY AGAINST LUNG
CELL CANCER**

A Thesis submitted to Gujarat Technological
University

for the Award of

Doctor of Philosophy

in

PHARMACY

by

Rajapara Arunabahen Mavjibhai

149997390002

under supervision of

Prof. (Dr) Mamta B. Shah



**GUJARAT TECHNOLOGICAL
UNIVERSITY AHMEDABAD**

April-2024

©Rajapara Arunabahen Mavjibhai

DECLARATION

I declare that the thesis entitled **Bioactivity guided extraction and fractionation of *Onosma bracteatum* with specific reference to its anti-cancer activity against lung cell cancer** submitted by me for the degree of Doctor of Philosophy is the record of research work carried out by me during the period from 2014 to 2024 under the supervision of **Prof. (Dr) Mamta B. Shah** and this has not formed the basis for the award of any degree, diploma, associateship, fellowship, titles in this or any other University or other institution of higher learning.

I further declare that the material obtained from other sources has been duly acknowledged in the thesis. I shall be solely responsible for any plagiarism or other irregularities, if noticed in the thesis.

Signature of the Research Scholar:..........Date: 30-04-2024

Name of Research Scholar: Rajapara Arunabahen Mavjibhai

Place: Ahmedabad

CERTIFICATE

I certify that the work incorporated in the thesis **Bioactivity-guided extraction and fractionation of *Onosma bracteatum* with specific reference to its anti-cancer activity against lung cell cancer** submitted by **Ms. Rajapara Arunabahen Mavjibhai** was carried out by the candidate under my supervision/guidance. To the best of my knowledge: (i) the candidate has not submitted the same research work to any other institution for any degree/diploma, Associateship, Fellowship or other similar titles (ii) the thesis submitted is a record of original research work done by the Research Scholar during the period of study under my supervision, and (iii) the thesis represents independent research work on the part of the Research Scholar.

Signature of Supervisor:..........30-04-2024

Name of Supervisor: Prof. (Dr) Mamta B. Shah

Place: Ahmedabad

COURSE-WORK COMPLETION CERTIFICATE

This is to certify that Ms. Rajapara Arunabahen Mavjibhai enrolment no. 149997390002 is a PhD scholar enrolled for PhD program in the branch Pharmacy of Gujarat Technological University, Ahmedabad.

(Please tick the relevant option(s))

- He/She has been exempted from the course-work (successfully completed during M.Phil Course)
- He/She has been exempted from Research Methodology Course only (successfully completed during M.Phil Course)
- He/She has successfully completed the PhD course work for the partial requirement for the award of PhD Degree. His/ Her performance in the course work is as follows-

Grade Obtained in Research Methodology (PH001)	Grade Obtained in Self Study Course (Core Subject) (PH002)
CC	AA



Supervisor's Sign.....

Name of Supervisor : Prof. (Dr) Mamta B Shah

Place: Ahmedabad

ORIGINALITY REPORT CERTIFICATE

It is certified that PhD Thesis titled **Bioactivity-guided extraction and fractionation of *Onosma bracteatum* with specific reference to its anti-cancer activity against lung cell cancer** by **Rajapara Arunabahen Mavjibhai** has been examined by us.

We undertake the following:

- a. Thesis has significant new work/ knowledge as compared already published or are under consideration to be published elsewhere. No sentence, equation, diagram, table, paragraph or section has been copied verbatim from previous work unless it is placed under quotation marks and duly referenced
- b. The work presented is original and own work of the author (i.e. there is no plagiarism). No ideas, processes, results or words of others have been presented as Author own work.
- c. There is no fabrication of data or results which have been compiled / analyzed.
- d. There is no falsification by manipulating research materials, equipment or processes, or changing or omitting data or results such that the research is not accurately represented in the research record.
- e. The thesis has been checked using **Orkund** (copy of originality report attached) and found within limits as per GTU Plagiarism Policy and instructions issued from time to time (i.e. permitted similarity index $\leq 10\%$).

Signature of the Research Scholar:..........Date: 30-04-2024

Name of Research Scholar: Rajapara Arunabahen Mavjibhai

Place: Ahmedabad

Signature of Supervisor:..........Date: 30-04-2024













Name of Supervisor: Prof. (Dr) Mamta B. Shah

Place: Ahmedabad

Document Information

Analyzed document	Onosma_Thesis pdf.pdf (D168914882)
Submitted	5/30/2023 7:29:00 AM
Submitted by	L. M. College of Pharmacy
Submitter email	mph228owner@gtu.edu.in
Similarity	3%
Analysis address	mph228owner.gtuni@analysis.arkund.com

Sources included in the report

SA	Gujarat Technological University / Compiled.docx Document Compiled.docx (D156882033) Submitted by: mph228owner@gtu.edu.in Receiver: mph228owner.gtuni@analysis.arkund.com	 1
SA	FINAL COPY THESIS.pdf Document FINAL COPY THESIS.pdf (D164651452)	 1
SA	Uday Vegad_Synopsis.pdf Document Uday Vegad_Synopsis.pdf (D157425286)	 7
SA	RKU_Veena_Patel_Thesis.docx Document RKU_Veena_Patel_Thesis.docx (D35537485)	 5
SA	THISIS.pdf Document THISIS.pdf (D140256475)	 4
SA	Dipanwita Ghoshal Ph.D Thesis - PHYTOCHEMICAL AND PHARMACOLOGICAL SCREENING OF IXORA PAVETTA.docx Document Dipanwita Ghoshal Ph.D Thesis - PHYTOCHEMICAL AND PHARMACOLOGICAL SCREENING OF IXORA PAVETTA.docx (D164944425)	 1
SA	FINAL THESIS 1-2.docx Document FINAL THESIS 1-2.docx (D164550106)	 4
W	URL: https://www.cell.com/cell-reports/pdf/S2211-1247(22)00525-3.pdf Fetched: 10/24/2022 7:11:21 AM	 1
SA	Gujarat Technological University / Nisha Bagda .pdf Document Nisha Bagda .pdf (D75434908) Submitted by: bagdanisha13@gmail.com Receiver: mph265owner.gtuni@analysis.arkund.com	 1
SA	final_intro_prachi_with_abstract_1__1_.pdf Document final_intro_prachi_with_abstract_1__1_.pdf (D139327818)	 3
SA	tribulosin- AJRC.docx Document tribulosin- AJRC.docx (D42555637)	 4
SA	Mali_Prashant_Yuvaraj_Ph.D_Thesis_02.pdf Document Mali_Prashant_Yuvaraj_Ph.D_Thesis_02.pdf (D111954648)	 1

**PhD THESIS Non-Exclusive License to GUJARAT TECHNOLOGICAL
UNIVERSITY**

In consideration of being a PhD Research Scholar at GTU and in the interests of the facilitation of research at GTU and elsewhere, I, Rajapara Arunabahen Mavjibhai having 149997390002 hereby grant a non-exclusive, royalty free and perpetual license to GTU on the following terms:

- a) The University is permitted to archive, reproduce and distribute my thesis, in whole or in part, and/or my abstract, in whole or in part (referred to collectively as the “Work”) anywhere in the world, for non-commercial purposes, in all forms of media;
- b) The University is permitted to authorize, sub-lease, sub-contract or procure any of the acts mentioned in paragraph (a);
- c) The University is authorized to submit the Work at any National / International Library, under the authority of their “Thesis Non-Exclusive License”;
- d) The Universal Copyright Notice (©) shall appear on all copies made under the authority of this license;
- e) I undertake to submit my thesis, through my University, to any Library and Archives. Any abstract submitted with the thesis will be considered to form part of the thesis.
- f) I represent that my thesis is my original work, does not infringe any rights of others, including privacy rights, and that I have the right to make the grant conferred by this non-exclusive license.
- g) If third party copyrighted material was included in my thesis for which, under the terms of the Copyright Act, written permission from the copyright owners is required, I have obtained such permission from the copyright owners to do the acts mentioned in paragraph (a) above for the full term of copyright protection.
- h) I understand that the responsibility for the matter as mentioned in the paragraph (g) rests with the authors / me solely. In no case shall GTU have any liability for any acts / omissions / errors / copyright infringement from the publication of the said thesis or otherwise

- i) I retain copyright ownership and moral rights in my thesis, and may deal with the copyright in my thesis, in any way consistent with rights granted by me to my University in this non-exclusive license.
- j) GTU logo shall not be used /printed in the book (in any manner whatsoever) being published or any promotional or marketing materials or any such similar documents.
- k) The following statement shall be included appropriately and displayed prominently in the book or any material being published anywhere: “The content of the published work is part of the thesis submitted in partial fulfilment for the award of the degree of Ph.D. in Pharmacy of the Gujarat Technological University”.
- l) I further promise to inform any person to whom I may hereafter assign or license my copyright in my thesis of the rights granted by me to my University in this nonexclusive license. I shall keep GTU indemnified from any and all claims from the Publisher(s) or any third parties at all times resulting or arising from the publishing or use or intended use of the book / such similar document or its contents.
- m) I am aware of and agree to accept the conditions and regulations of Ph.D. including all policy matters related to authorship and plagiarism.

Date: 30-04-2024

Place: Ahmedabad



Signature of the Research Scholar



Signature of Supervisor

THESIS APPROVAL FORM

The viva-voce of the PhD Thesis submitted by Smt. Rajapara Arunabehn Mavjlbhal (Enrollment No.149997390002) entitled Bioactivity-guided extraction and fractionation of *Onosma bracteatum* with specific reference to its anti-cancer activity against lung cell cancer was conducted on 30th April 2024 at Gujarat Technological University

(Please tick any one of the following option)

The performance of the candidate was satisfactory. We recommend that he/she be awarded the PhD degree

Any further modifications in research work recommended by the panel after 3 months from the date of first viva-voce upon request of the Supervisor or request of Independent Research Scholar after which viva-voce can be re-conducted by the same panel again.

(briefly specify the modifications suggested by the panel)

The performance of the candidate was unsatisfactory. We recommend that he/she should not be awarded the PhD degree.

(The panel must give justifications for rejecting the research work)

Name and signature of Supervisor with seal

MBSLah

1) (External examiner 1) Name and Signature

Jagannath Sahu 30.4.24

2) (External examiner 2) Name and Signature

[Signature]

30/4/24

ABSTRACT

Onosma bracteatum Wall. (Boraginaceae) is a perennial, hairy herb mainly distributed in the highlands of India and Nepal, specifically in the North-Western Himalayas of Jammu & Kashmir, Himachal Pradesh, and Uttar Pradesh. It is a highly valuable medicinal herb widely utilized by the tribes of the Western Ghats for treating various ailments such as fever, cough, bronchitis, rhinitis, stomatitis, jaundice, constipation, epilepsy, kidney disease, and weakness of cardiac muscles. The plant is rich in pyrrolizidine alkaloids, quinones, coumarins, flavonoids, sterols, phenolics, saponin, and fat and fixed oil.

The plant was evaluated for pharmacognostic study which includes macro and microscopic evaluation, determination of physicochemical parameters, preliminary qualitative and quantitative phytochemical study. Bioactivity guided approach is used to evaluate anticancer activity and isolation of phytoconstituents. *In vitro* cytotoxicity of the total methanolic extract was examined using the brine shrimp lethality assay and two lung cancer cell lines (A549 and NCI-H23). Successive solvent extraction was performed using petroleum ether, chloroform, ethyl acetate, butanol, and water solvents. All the extracts were evaluated using the brine shrimp lethality assay, and active extracts from this assay were further tested for *in vitro* cytotoxicity against the two lung cancer cell lines (A549 and NCI-H23). The combination of petroleum ether and chloroform extracts was assessed for apoptosis profiling on both cell lines. Active extracts were subjected to chromatographic fractionation, and the obtained fractions were subsequently evaluated for *in vitro* anticancer activity. The active fraction was further subjected to compound isolation. The identification of the isolated compound was carried out through TLC (thin-layer chromatography) and characterized using IR (infrared), NMR (nuclear magnetic resonance), and Mass spectroscopy techniques. Phytochemical profiling of the extract and fractions was carried out using HR-LCMS (high-resolution liquid chromatography-mass spectrometry). Additionally, the identification of compounds was also performed from the extracts by partitioning with solvents. A simple and validated HPTLC (high-performance thin-layer chromatography) method and HPTLC-MS method were developed to estimate the identified compounds derived from *O. bracteatum*.

The characteristic features required for the quality evaluation of *O. bracteatum*, including morphological, microscopical, and physico-chemical

parameters, were systematically recorded. The total methanolic extract exhibited significant cytotoxicity on both *Artemia Salina* and lung cancer cell lines. Among the solvent extracts, pet ether and chloroform demonstrated potent cytotoxicity against the lung cancer cell line. Furthermore, the combination of petroleum ether and chloroform extract exhibited synergistic action in the comprehensive apoptosis profile study. A total of six fractions were collected from column chromatography from petroleum ether extract, with fractions five and six displaying potent activity in the apoptosis profile (MTT assay, wound healing assay, annexin-V assay, caspase 3/7 assay, and comet assay). Fractions one to four, however, showed no activity in the comet assay. The compound 17-(5,6-dimethylhept-3-en-2-yl)-10,13-Dimethyl-4,10,12,13,14,15,16,17-octahydro-1H-Cyclopenta[a]phenanthrene (C-1) was isolated from the PF5 fraction, while 1,7-dihydroxy-3-methyl-9H-xanthene-9-one (C-2) was isolated from fraction PF6. The concentration of C-2 in the plant was found to be 0.17% w/w using the HPTLC method. HR-LCMS results indicated that PF4, PF5, and PF6 primarily contain phenolics, flavonoids, shikonin, coumarins, and xanthone compounds. Validated and simultaneous HPTLC methods were developed for the quantitative and qualitative analysis of phytoconstituents in *O. bracteatum*. The methods revealed the presence of β -sitosterol and lupeol at 0.1021% w/w and 0.1352% w/w, respectively, in the pet ether extract, and (+)catechin, (-)epicatechin, and kaempferol at 0.0577% w/w, 0.0318% w/w, and 0.0286% w/w, respectively, in the total methanolic extract.

Thus, it can be concluded that the drug extracts of *O. bracteatum*, either alone or in combination, can be used in the treatment of lung cancer.

Key words: *Onosma bracteatum*, Apoptosis, Bioactivity guided fractionation, chromatography, Boraginaceae, HR-LCMS, Lung cancer, Cytotoxicity

ACKNOWLEDGEMENT

Pursuing a dissertation project is both an arduous and gratifying experience. It is akin to climbing a high peak, step by step, accompanied by adversity, challenges, frustrations, encouragement, and the generous help of many individuals. When I found myself at the summit, enjoying the beautiful scenery, I realized that it was indeed a result of teamwork that brought me there. Although words cannot fully express my gratitude to all those who assisted me, I would like to extend my heartfelt thanks to each and every one of them. Words always fall short in capturing the true essence of one's intentions.

I first and foremost express my revered regard and obeisance to the ALMIGHTY GOD with whose blessings I was able to complete my project work.

*My heart full gratitude goes to my Research Supervisor **Prof. (Dr) Mamta Shah, Professor**, L.M College of Pharmacy. Her vigilant supervision, continuous moral support, encouragement, systemic planning and kindness enabled me to complete this thesis. There is no limit to the ecstasy experienced during this piece of work, which was carried out under the supervision of Mamta madam.*

*I am extremely thankful and grateful to my Doctoral Progress Committee members, **Dr. Kilambi Pundrikakshudu and Dr. N. R. Sheth**, for their mentorship and valuable guidance throughout my journey of research.*

*I express my gratitude to **Dr. Mahesh Chabbria**, Principal of L.M. College of Pharmacy in Ahmedabad, for providing the necessary facilities that contributed to the successful completion of this project work.*

*I am sincerely grateful to **Dr. V.P. Bhatt**, Scientist at the Herbal Research and Development Institute, for their invaluable contribution in collecting and conducting the primary authentication of the plant.*

*I am obliged to **Dr. Anuradha Gajjar**, Head -Department of Pharmaceutical Analysis for permission to perform HPTLC, HPLC and for guidance in performing analysis.*

*I am thankful to faculty members of Department of Pharmacognosy, L.M. Collage Of Pharmacy - **Dr. Preeti Verma, Dr. Karuna Modi, and Dr. Krupa Gadhvi** for helping me*

during my entire research work.

I would like to express my thanks to Miss Nupoor Gandhi, a research scholar at L.M. College of Pharmacy in Ahmedabad, for her assistance in conducting HPTLC analysis of my extracts.

Special thanks to non-technical, Ramchandra Yadavji, Sureshbhai and Siddhnathji for helping me during my entire work and study and also thankful to Bharatbhai, Prakash kaka, Chiragbhai, Vinu kaka, Raju kaka, Yogeshbhai, and Dharmeshbhai for their help.

In preparing this dissertation I have received great help from many of my professors, friends, and colleagues in a number of ways, whom I might have missed inadvertently. I take this opportunity to thank all of them.

I dedicate this research work to my parents, who provided me with education, unwavering support, and constant encouragement to pursue my studies. I am immensely grateful to my in-laws, beloved husband, Mr. Vipul Kaila, and my loving daughter, Nairuti, for their patience and understanding, allowing me the necessary time to complete this endeavor.

I am indebted to all my family members, friends and well-wishers who directly or indirectly involved in the completion of this endeavour.

Aruna M Rajapara

TABLE OF CONTENT

Sr. No.	Title	Page No.
1	Introduction	1-17
2	Review of Literature	18-26
3	Material & Methods	27-65
4	Results & Discussion	66
	4.1 Identification, Collection, and Authentication of the Plant Material	66
	4.2 Assessment of quality of plant materials	66
	4.2.1 Morphology of stem, root, and flower of <i>O. bracteatum</i>	66
	4.2.2 Microscopical study (Powder study)	67
	4.2.3 Proximate Analysis	68
	4.3 Phytochemical studies	68
	4.3.1 Preliminary Profile	68
	4.3.1.1 Preparation of extract and qualitative phytochemical study	69
	4.3.1.2 Quantitative phytochemical study	70
	4.4 In vitro Antioxidant assay of TME	70
	4.4.1 Phosphomolybdenum assay	70
	4.4.2 DPPH scavenging assay	70
	4.4.3 Nitric oxide scavenging assay	70
	4.5 Preliminary cytotoxicity assay of TME	71
	4.5.1 Brine Shrimp lethality assay	71
	4.5.2 MTT assay on cell line (A549 and NCI-H23 cell line)	72
	4.6 Yield of extracts	73
	4.7 In vitro antioxidant activity of Extracts	74
	4.7.1 Phosphomolybdenum assay	74
	4.7.2 DPPH scavenging assay	75
	4.7.3 Nitric oxide scavenging assay	75

4.8 In vitro cytotoxicity assay of Extracts	76
4.8.1 Brine shrimp lethality assay	76
4.8.2 MTT assay on A549 and NCI-H23 cell lines	77
4.9 Apoptosis profile of mixture of A1 and A2 on A549 and NCI-H23 cell line	80
4.9.1 MTT assay	80
4.9.2 Wound healing assay or scratch assay	81
4.9.3 Annexin V assay	82
4.9.4 Caspase 3/7 activity	84
4.9.5 comet assay	86
4.10 preparations of fractions	87
4.11 Apoptosis profile of Fractions on A549 and NCI-H23 cell line	88
4.11.1 Cytotoxicity of Fractions by MTT assay	88
4.11.2 Wound healing assay or scratch assay	91
4.11.3 Annexin V assay	91
4.11.4 Caspase 3/7 Assay	95
4.11.5 Comet assay	96
4.12 Identification and characterization of compound C-1 isolated from fraction PF5	99
4.12.1 Physical characteristic of compound C-1	99
4.12.2 Chemical characteristic of compound C-1	99
4.12.3 Spectroscopic analysis of compound C-1	100
4.12.3.1 IR Spectra of C-1	100
4.12.3.2 Mass spectra of C-1	100
4.12.3.3 NMR spectra of C-1	101
4.12.4 Probable structure of compound C-1	102
4.13 Identification and characterization of compound C-2 isolated from fraction PF6	102
4.13.1 Physical characteristic of compound C-2	102

4.13.2	Chemical characteristic of compound C-2	102
4.13.3	Spectroscopic analysis of compound C-2	103
4.13.3.1	IR Spectra of C-2	103
4.13.3.2	Mass Spectra of C-2	104
4.13.3.3	NMR Spectra of C-2	104
4.13.4	Probable structure of compound C-2	106
4.13.5	Quantification of C-2 by HPTLC Method	106
4.14	HRLC-MS study of A1+A2 and PF1 to PF6	107
4.15	Identification and estimation of compounds from extract A1	116
4.15.1	Identification of β -sitosterol and Lupeol in PEF by TLC	116
4.15.2	Estimation of β -sitosterol and Lupeol in PEF by HPTLC	116
4.15.2.1	Calibration curves of β -sitosterol and Lupeol	116
4.15.2.2	Validation of HPTLC method for β -sitosterol and Lupeol	117
4.15.2.3	Quantification of β -sitosterol and lupeol	119
4.16	Identification and estimation of compounds from MEF	122
4.16.1	Identification of (+)catechin and (-)epicatechin in MEF by TLC	122
4.16.2	Identification of (+)catechin and (-)epicatechin in MEF by Mass	123
4.16.3	Estimation of (+)catechin and (-)epicatechin in MEF by HPTLC	123
4.16.3.1	Calibration curve of (+)catechin and (-)epicatechin	123
4.16.3.2	Validation of HPTLC method for (+)catechin and (-)epicatechin	124
4.16.3.3	Quantification of (+)catechin and (-)epicatechin	125
4.17	Identification and estimation of compound from MEF	128
4.17.1	Identification of kaempferolin MEF by TLC	128
4.17.2	Identification of kaempferol in MEF by Mass	129
4.17.3	Estimation of kaempferol in MEF by HPTLC	129
4.17.3.1	Calibration curve of kaempferol	130

	4.17.3.2 Validation of HPTLC method for kaempferol	130
	4.17.3.3 Quantification of kaempferol	131
5	Summary & Conclusion	137-139
	Appendix A	
	List of publications	

LIST OF ABBREVIATION

%	Percentage
μ	Micro
μL	Microliter
α	Alpha
β	Beta
C	Celsius
Gm	Gram
hr	Hour
IU	International Unit
kg	Kilogram
mg	Milligram
min	Minute
mL	Milliliter
nm	Nanometer
°	Degree
ppm	Parts per million
w/v	Weight by volume
w/w	Weight by weight
L	Litre
#	Mesh size
pH	Potential of hydrogen
Ng	Nanogram
M	Molar
mM	Milimolar
Sec	Second
mA	Miliampere
m/z	Mass to charge ratio
v/v	Volume by volume
Mm	Milimeter
Cm	Centimeter
nLs ⁻¹	Nano liter per second
N	Number
N	Normal
<	Less than
>	Greater than
SD	Standard deviation
Vs	Verses
Δ	Delta
R _f	Retention factor

LIST OF FIGURES

Figure No.	Description
Figure 1.1	Plant of <i>Onosma bracteatum</i>
Figure 3.1	Flow chart of preparation of Fractions
Figure 3.2	Scheme for Apoptosis profile and Isolation of compounds from active fractions
Figure 3.3	Scheme for separation of compounds on TLC from A1 extract
Figure 3.4	Scheme for separation of compounds on TLC from TME
Figure 4.1	Morphology of <i>O. bracteatum</i> a) Stem b) Root c) Flower
Figure 4.2	Powder characteristics of <i>O. bracteatum</i>
Figure 4.3	DPPH and NO scavenging activity of TME
Figure 4.4	Plot of log concentration of TME versus percent shrimp mortality after 24hr of exposure
Figure 4.5	Graph of sample concentration vs % inhibition of A549 cells treatment with TME of <i>O. bracteatum</i>
Figure 4.6	Graph of sample concentration vs % inhibition of NCI-H23 cells treatment with TME of <i>O. bracteatum</i>
Figure 4.7	DPPH and Nitric oxide scavenging activity of A1 to A5 extract
Figure 4.8	Plot of log concentration of A1, A2, A3, A4, A5 and potassium dichromate versus percent shrimp mortality after 24 h of exposure
Figure 4.9	Effect of extract A1 on A549 cell
Figure 4.10	Effect of extract A2 on A549 cell
Figure 4.11	Effect of extract A4 on A549 cells
Figure 4.12	Effect of extract A1 on NCI-H23 cells
Figure 4.13	Effect of extract A2 on NCI-H23 cells
Figure 4.14	effect of extract A4 on NCI-H23 cells
Figure 4.15	effect of mixture of A1 and A2 on A549 cell lines
Figure 4.16	effect of mixture of A1 and A2 on NCI-H23 cell line
Figure 4.17	cell migration of mixture of A1 and A2 on A549 and NCI-H23 cell lines
Figure 4.18	Apoptosis profile of mixture of A1 and A2 using Annexin V on A549 cell line

Figure 4.19	Graphical representation of stages of apoptosis
Figure 4.20	Apoptosis profile of mixture of A1 and A2 using Annexin V on NCI-H23 cell lines
Figure 4.21	Graphical representation of stages of apoptosis
Figure 4.22	Effects of mixture of A1 and A2 extract on the caspase activation in A549 cell line.
Figure 4.23	Effects of mixture of A1 and A2 extract on the caspase activation in NCI-H23 cell lines
Figure 4.24	Representative images of comets showing the genotoxic effect of mixture of A1 and A2 on A549 cells analysed by comet assay
Figure 4.25	Graphical representation of genotoxic effect of mixture of A1 and A2 on A549 cells analysed by comet assay
Figure 4.26	Representative images of comets showing the genotoxic effect of mixture of A1 and A2 on NCI-H23 cells analysed by comet assay
Figure 4.27	Graphical representation of genotoxic effect of mixture of A1 and A2 on NCI-H23 cells analysed by comet assay
Figure 4.28	% cytotoxicity of fractions on A549 cell line
Figure 4.29	% cytotoxicity of fractions on NCI-H23 cell lines
Figure 4.30	Cell migration effects of fractions with positive standard on A549 cell
Figure 4.31	Cell migration effects of fractions with positive standard on NCI-H23 cell
Figure 4.32	Apoptosis profile of fractions on A549 cell line
Figure 4.33	Graphical representation of stages of apoptosis
Figure 4.34	Apoptosis profile of fractions on NCI-H23 cell line
Figure 4.35	Graphical representation of stages of apoptosis
Figure 4.36	graphical representation of caspase 3/7 activity
Figure 4.37	Representative images of comets showing the genotoxic effect of Fractions on A549 cells analysed by comet assay
Figure 4.38	graphical representation of DNA fragmentation activity in A549 cell line
Figure 4.39	Representative images of comets showing the genotoxic effect of Fractions on NCI-H23 cells analysed by comet assay

Figure 4.40	graphical representation of DNA fragmentation activity in NCI-H23 cell line
Figure 4.41	TLC of compound C-1
Figure 4.42	IR spectra of Compound C-1
Figure 4.43	Mass spectra of compound C-1
Figure 4.44	H1-NMR Spectra of compound C-1
Figure 4.45	C13-NMR spectra of compound C-1
Figure 4.46	Structure of C-1
Figure 4.47	TLC of compound C-2
Figure 4.48	IR spectra of compound C-2
Figure 4.49	Mass spectra of compound C-2
Figure 4.50 (a), (b), (c), (d)	H1-NMR Spectra of compound C-2
Figure 4.51	Structure C-2
Figure 4.52 (A)	HPTLC study of C-2
Figure 4.52 (B)	Calibration curve of C-2
Figure 4.52 (C)	chromatogram of C-2
Figure 4.52 (D)	chromatogram of fraction PF6
Figure 4.53 (A)	chromatogram of mixture of A1 and A2
Figure 4.53 (B)	chromatogram of fraction PF1
Figure 4.53 (C)	chromatogram of fraction PF2
Figure 4.53 (D)	chromatogram of fraction PF3
Figure 4.53 (E)	chromatogram of fraction PF4
Figure 4.53	chromatogram of fraction PF5

(F)	
Figure 4.53 (G)	chromatogram of fraction PF6
Figure 4.54	TLC of PEF (C) with standard β -sitosterol (A) and Lupeol (B)
Figure 4.55	HPTLC chromatogram of standards β -sitosterol (s1 to s5) and lupeol (l1 to l5) and PEF(Petroleum ether extract fraction)
Figure 4.56	Densitometric chromatogram of standard β -sitosterol (BS), lupeol (LP) and Petroleum ether extract fraction (PEF)
Figure 4.57	Overlain spectra of β -sitosterol (A) and lupeol (B) with PEF
Figure 4.58	TLC of MEF (B) with standard (+)catechin (A) and (-)epicatechin (C)
Figure 4.59	Mass spectra of (+)catechin (A) and (-)epicatechin (B) from MEF
Figure 4.60	HPTLC chromatogram of standards (+)catechin (c1 to c5) and (-)epicatechin (e1 to e5) and MEF(Total methanolic extract fraction)
Figure 4.61	Densitometric chromatogram of standard (+)catechin and (-)epicatechin and total methanolic extract fraction (MEF)
Figure 4.62	Overlain spectra of (+)catechin (A) and (-)epicatechin (B) with MEF
Figure 4.63	TLC of MEF (B) with standard kaempferol (A)
Figure 4.64	Mass spectra of kaempferol from MEF
Figure 4.65	HPTLC chromatogram of standard kaempferol (k1 to k5) and MEF(Total methanolic extract fraction)
Figure 4.66	Densitometric chromatogram of standard kaempferol and total methanolic extract fraction (MEF)
Figure 4.67	Overlain spectra of kaempferol with MEF

LIST OF TABLES

Table No.	Description
Table 4.1	Physico-chemical parameters of <i>O.bracteatum</i>
Table 4.2	Qualitative phytochemical screening of <i>O. bracteatum</i>
Table 4.3	Quantitative phytochemical screening of <i>O. bracteatum</i>
Table 4.4	Total Antioxidant capacity of TME of <i>O.bracteatum</i>
Table 4.5	Effect of TME and Potassium dichromate on brine shrimp
Table 4.6	IC ₅₀ value of TME
Table 4.7	% Yield of extracts
Table 4.8	Total Antioxidant capacity of A1 to A5 of <i>O.bracteatum</i>
Table 4.9	EC ₅₀ value of A1 to A5 in DPPH assay
Table 4.10	EC ₅₀ value of A1 to A5 in nitric oxide scavenging assay
Table 4.11	Effect of A1, A2, A3, A4, A5 and potassium dichromate on brine shrimp
Table 4.12	IC ₅₀ value of A1, A2 and A4 extracts on A549 and NCI-H23 cells
Table 4.13	IC ₅₀ value of mixture of A1 and A2 on A549 cells and NCI-H23 cells
Table 4.14	% Yield of Fractions
Table 4.15	IC ₅₀ values of Fraction on A549 and NCI-H23 cells
Table 4.16	List of compounds identified in the mixture of A1 and A2 by Q-Exactive Plus Biopharma
Table 4.17	List of compounds identified in the PF1 by Q-Exactive Plus Biopharma
Table 4.18	List of compounds identified in the PF2 by Q-Exactive Plus Biopharma
Table 4.19	List of compounds identified in the PF3 by Q-Exactive Plus Biopharma
Table 4.20	List of compounds identified in the PF4 by Q-Exactive Plus Biopharma
Table 4.21	List of compounds identified in the PF5 by Q-Exactive Plus Biopharma

Table 4.22	List of compounds identified in the PF6 by Q-Exactive Plus Biopharma
Table 4.23	Calibration curve of β -sitosterol and Lupeol
Table 4.24	Intra and interday precision analysis of β -sitosterol, lupeol
Tablet 4.25	LOD, LOQ and recovery
Table 4.26	Quantification (n=3) data of Extract A1
Table 4.27	Summary of validation parameters for β -sitosterol and lupeol estimation by HPTLC
Table 4.28	Calibration curve of (+)catechin and (-)epicatechin
Table 4.29	Intra and interday precision analysis of (+)catechin and (-)epicatechin
Tablet 4.30	LOD, LOQ and recovery
Table 4.31	Quantification (n=3) data of MEF
Table 4.32	Summary of validation parameters (+)catechin and (-)epicatechin estimation by HPTLC
Table 4.33	Calibration curve of <i>kaempferol</i>
Table 4.34	Intra and interday precision analysis of kaempferol
Tablet 4.35	LOD, LOQ and recovery
Table 4.36	Quantification (n=3) data of MEF
Table 4.37	Summary of validation parameters kaempferol estimation by HPTLC

LIST OF APPENDICES

Appendix A: Authentication certificate of *Onosma bracteatum* Wall.

Chapter 1

Introduction

INTRODUCTION

1.1 INTRODUCTION TO CANCER

Cancer can be defined as a disease in which a group of abnormal cells grows uncontrollably without following the normal rules of cell division.¹ Normal cells are continuously subject to signals that recognize whether the cell should divide or differentiate into another new cell or die. Cancer cells develop a degree of autonomy from these signals, leading to uncontrolled growth and proliferation. If this uncontrolled growth of cell is to continue and spread, it can be fatal. Almost 90% of cancer-related deaths are due to tumor spreading - a process called metastasis.² Cancer is a multi-gene, multi-step disease originating from a single abnormal cell with an altered DNA sequence (mutation). Uncontrolled proliferation of these abnormal cells is followed by a second mutation leading to a slightly abnormal state. Consecutive rounds of mutation and selective growth of these cells result in the development of a tumor mass. Lung, prostate, colon, stomach, and hepatic cancer are the most common types of cancer in men, although breast, colon, lung, cervical, and thyroid cancer are the most frequent among women.³

Cancer is not a single disease but a complex of many diseases. About 200 distinct types of cancer have been identified. These can be divided into mainly four types: carcinomas, sarcomas, lymphomas, and leukemia. Carcinomas are tumors composed of epithelial cells of ectodermal or endodermal origin. Examples of carcinomas are solid tumors of nerve tissue and body surfaces and their adhering glands. These include cervical, breast, skin, and brain cancer. About 85% of cancers are carcinomas. Sarcomas are tumors composed of connective tissue cells, of mesodermal origin. They are solid tumors that grow from connective tissue, cartilage, bone, and muscles. Lymphoma is a cancer in which the lymph nodes and spleen produce too many lymphocytes. Hodgkin's disease is a type of lymphoma. Leukemia is the neoplastic growth of white blood cells and is characterized by unnecessary cell production.⁴

1.1.1 Causes of cancer^{2,4}

The first known report associations with cancer are the effects of lifestyle choices such as obesity, physical inactivity, diet, smoking, tobacco, and alcohol consumption. The risk of cancers is also enhanced by contagious agents including viruses such as hepatitis B virus (HBV), human papillomavirus (HPV), and human immunodeficiency virus (HIV). Cancer development and progression are due to exposure to cancer-causing agents (carcinogens, mutagens) and disclosure to high levels of UV radiation in the sun's rays, influenced by external environmental factors such as tobacco, chemicals, radiation and infectious organisms and intracellular factors such as inherited mutations, hormones, immune conditions, and mutations. There are several reasons for the increased incidence of cancer among older people: age-related alterations in the immune system (decreased immune surveillance); accumulation of random genetic mutations or lifetime exposure to carcinogens (especially for colon and lung cancers); hormonal changes or exposure; and longevity.

1.1.2 Mechanism of cancers⁵⁻⁷

Cancer is caused by specific DNA damage. Several common mechanisms cause DNA damage leading to certain malignancies. First, proto-oncogenes are activated by translocations. Second, proto-oncogenes are activated by point mutations. Third, the inactivation of a gene by mutation can result in tumors. Functional loss of these a tumor suppressor gene is found in many tumors such as colon and lung cancer. Cells can turn into cancer cells when mutations affect tumor suppressor genes or oncogenes.

DNA damage causes cancer development when defective DNA repair leads to chromosomal mutations that activate oncogenes or inactivate tumor suppressor genes. When DNA damage persists and disrupts replication or transcription, the DNA damage checkpoint triggers cellular senescence or apoptosis, inactivating or eliminating damaged cells and suppressing tumorigenesis. DNA repair mechanisms prevent cancer by preventing mutations. Therefore, DNA repair is essential to prevent tumor development.

1.1.3 Hallmarks of Cancer⁸⁻¹²

DNA mutations create defects in cellular regulatory circuitry that disrupt normal cell growth behavior. However, the complexity of this disease is not so simple at the cellular and molecular levels. The behavior of individual cells is not autonomous and usually depends on external signals from surrounding cells within the tissue or microenvironment. There are over 100 different types of cancer, and each particular organ may contain multiple subtypes of tumors. The 6 hallmarks of cancer are

- 1) Immortality: Continuous cell division and infinite replication
- 2) Generating 'Go' signals (growth factors from oncogenes)
- 3) Disabling 'Stop' signals (anti-growth signals from tumor suppressor genes)
- 4) Resistance to cell death (apoptosis)
- 5) Angiogenesis: Induction of new blood vessel growth
- 6) Metastasis: Spread to other sites

1) Immortality: continuous cell division and infinite replication¹³

Cancer cells are usually defined by their ability to divide uncontrollably. Telomeres play an important role in cell division. Telomeres are repetitive DNA sequences that protect the linear ends of chromosomes. After each round of cell division, telomere length gradually shortens until the cell stops dividing and enters senescence. Cancer cells prevent telomere shortening by producing the enzyme telomerase, which maintains telomere elongation and maintains length without losing DNA base pairs. Nearly 85-90% of all cancers have telomerase activation. Telomerase adds noncoding hexanucleotide repeats to the ends of telomere DNA, keeping the required length above a critical threshold, preventing erosion, and allowing unlimited replication capacity. Generating

2) Generating 'Go' signals (growth factors from oncogenes)^{14,15}

Oncogenes are the derivatives of normal cellular genes called proto-oncogenes. The conversion of proto-oncogenes to oncogenes is triggered by several factors such as mutations, chromosomal rearrangements, viral insertion, and gene amplifications. Proto-oncogenes encode proteins that stimulate cell cycle division, but mutant forms, called oncogenes and over-activate the stimulatory proteins, causing cell hyperproliferation. Oncogenes are gene that encodes a protein that can transform cells in culture or induce cancer in animals. A consequence of oncogenic transformation is that tumor cells become independent

of external growth signaling factors in any normal tissue microenvironment. Tumor cells can actively proliferate independently of growth factors. This autonomy of growth factor signaling leads to uncontrolled growth (e.g., in the absence of ideal conditions for cell division and stress) and increases the likelihood of acquiring additional mutations in the cell genome.

There are three main cellular strategies that cancer cells use to achieve growth factor autonomy.¹⁶

a) Alteration of extracellular growth signals: Platelet-Derived Growth Factor is a protein required by cells to stimulate cell division. PDGF normally binds to PDGF receptors in the extracellular domain to stimulate intracellular cell proliferation pathways. Certain cancers arise from the overproduction of the PDGF protein or when cells are infected with certain viruses that overproduce PDGF-like oncoproteins that also bind to PDGF receptors.

b) Alteration of transcellular mediators of those signals: The most common group of receptors involved in numerous types of cancers belongs to the family tyrosine kinase. These include the EGF, FGF, IGF, and PDGF receptors (Epidermal Growth Factor, Fibroblast Growth Factor, Insulin Growth Factor, and Platelet-Derived Growth Factor respectively).

c) Changes in intracellular signaling messengers that stimulate proliferation: The most common but most complex mechanism of cancer transformation derives from changes in components of the intracellular, cytoplasmic signaling cascade, within cells that receive input from the ligand-activated growth factor receptors on the cell membrane. Mutations in proteins of intracellular signaling cascade (adaptor proteins) are found in almost all human tumors.

3) Disabling 'Stop' signals (anti-growth signals from tumor suppressor genes)¹² TSGs (Tumour suppressor genes) encode proteins that usually inhibit cell division. Mutations that result in functional inactivation of these proteins are known as loss-of-function mutations because they remove the normal brakes on proliferative capacity. The functional activity of TS proteins may also be affected by inhibitory/competing oncoproteins or deregulation. A well-known example of a tumor suppressor protein is p53. Nearly 50% of all cancers have p53 mutations and nearly 80% of mutations in squamous cell carcinoma (SCC) involve p53. Mutations or losses of a function of this essential protein allow continuing cell division despite DNA damage. p53 is generally degraded in a normal cell.

However, conditions of cellular stress or DNA damage (eg. exposure to radiation or mutagens) result in the expression of intermediate proteins that stabilize the p53 protein. This stable p53 protein forms a tetramer (complex of four p53 proteins), that acts as a transcription factor and expresses genes involved in either arresting cell cycle progression, DNA repair (if the damage is minor) or induction of cell death (if the damage is too severe). However, in tumors, the loss of function of p53 removes this important guardianship, allowing the cells to continue dividing despite the DNA-damaging mutations.

4) Resistance to cell death (apoptosis)^{11,12}

Apoptotic cell death is part of normal growth and development. Tissue homeostasis is the balance between cell division and cell death in which the number of cells within the tissue remains relatively constant. When this balance is disrupted, the cells either a) divide faster than they die, leading to the development of cancer or b) die faster than they divide, leading to tissue atrophy. A deficiency of growth-stimulating factors, such as growth factors, can trigger apoptosis, and binding of specific external molecules (ligands) such as death ligands, can trigger intracellular apoptotic signaling. Apoptosis sensing relies on signals either exterior (extrinsic induction) or interior (intrinsic induction) to the cell. External signals include exposure to toxins, certain hormones, etc. that are communicated internally via receptors or transporters on the cell membrane. Internal signals, on the other hand, monitor response to stress and DNA damage. For example heat, radiation, hypoxia, GF deficiency, viral infection, or increased intracellular calcium all evoke apoptosis through internal signaling pathways. External apoptotic signaling is usually mediated by cell surface receptors that bind death or survival factors. For example, death signals are activated when the endogenous ligand (CD95L) binds to the CD95 receptor (also called Fas receptors) on the cell membrane. Other examples include the binding of tumor necrosis factor- α (TNF- α) to the TNF receptors (TNFR1) or the binding of FAS ligands to FAS receptors on the cell membrane. Loss of signals from the extracellular matrix and intercellular adhesion proteins also stimulates cell apoptosis. The Internal signals that trigger apoptosis converge on the mitochondria, which is the aerobic powerhouse of the cell. Cytosolic proteins, such as Bcl-2 family members, target mitochondria and cause organelles to swell or become leaky and releasing specific apoptotic effector proteins into the cytosol. Leaky proteins include SMACs

(secondary mitochondria-derived activators of caspases) that bind to IAPs (inhibitors of apoptosis proteins) and deactivate them, allowing apoptosis to proceed. Another important leaky protein is cytochrome c, which is released from the outer mitochondrial membrane through a channel called MAC (Mitochondrial apoptosis-inducing channel). In the cytosol, cytochrome c binds to Apaf-1 and ATP, which then binds to procaspase-9 to form a protein complex known as the apoptosome. Formation of this apoptosome is the last irreversible stage of apoptosis, wherein caspase-9 (initiator) activates the enforcer of apoptosis, effector caspase-3. These caspases (cysteiny aspartate-specific serine proteases) are end-effectors of apoptosis that perform cell death by selectively removing structurally important proteins and DNA.

5) Angiogenesis: Induction of new blood vessel growth¹²

Cells and tissues need oxygen and nutrients to survive and grow and therefore most cells lie within 100µm of a capillary blood vessel. Under most conditions, cells that line the capillaries – the endothelial cells- do not grow and divide. However, certain conditions such as during menstruation or wound healing trigger endothelial cell division and the growth of new capillaries, and this process is termed angiogenesis. Tumor cells release pro-angiogenic factors, such as vascular endothelial growth factor (VEGF), which diffuse into nearby tissues and bind to receptors on the endothelial cells of pre-existing blood vessels, leading to their activation. Such interactions lead to the secretion and activation of various soluble proteases (such as matrix metalloproteinases MMPs), which degrade the basement membrane and the extracellular matrix. The degradation allows activated endothelial cells to divide and migrate to the tumor. Integrin molecules help to pull the developing new blood vessel forward. Endothelial cells lie down on the new basement membrane and secrete growth factors, such as platelet-derived growth factor (PDGF), which attract supporting cells to stabilize the new vessel.

6) Metastasis: Spread to other sites^{17,18}

Solid tumors are normally part of normal tissues and under optimal conditions, can invade nearby tissues or pass throughout the circulatory system to colonize distant sites in the body. These secondary tumors – metastases – are responsible for nearly 90% of cancer-related deaths. The migration of cancer cells from the primary location to distant sites is a complex biological process that involves

changes at the molecular, cellular, and physical levels. In summary, the invasion and metastasis cascade usually includes the following steps:

- a. Local invasion: In this process, the little in situ tumor breaks through the basement membrane barrier.
- b. Intravascular invasion: Tumour cells migrate through the walls of the capillaries or lymphatic vessels into the circulatory system. This is a key step in this pathway and it involves a complex morphological change, in which the cancer cells acquire properties of invasiveness and cell motility. This allows the cancer cell to progress through the capillary walls and into the circulatory system.
- c. Transport: Cancer cells migrate through the blood or lymph until they are attached to a solid supporting tissue. Both blood and lymph are involved in transport, but most of the distant metastases are caused by circulation via the bloodstream. At this stage, most of the cancer cells can be lost or destroyed by hostile conditions. However, surviving cancer cells get lodged in the first set of capillaries they encounter (mainly because large cells block the small passageways of the capillaries) and form microthrombi.
- d. Extravasation: This final translocation step broadly resembles intravasation, which ultimately migrates to the tissues they are lodged in, usually the lungs, brain, or liver. The main difference is that the direction of movement is reversed. Cancer cells within microthrombi have been pushed through the capillary wall and into the tissue microenvironment.
- e. Formation of micrometastases: Upon extravasation, the cancer cells can reactivate the cell proliferation pathways and form small tumor masses that originate through the lumen of the capillaries or the vessel wall.
- f. Colonization: This is the most complex and difficult stage. This is mainly because the new environment does not always provide the survival and proliferation factors necessary for growth. Most cancer cells usually die or survive for long periods as micrometastases (which are much harder to detect).

1.1.4 Lung cancer

Globally, there were an estimated 20 million new cases of cancer and 10 million deaths from cancer. In 2023, 1,958,310 new cancer cases and 609,820 cancer deaths are projected to occur in the United States. Among all cancer, Lung cancer was the most commonly occurring cancer worldwide with 2.5 million new cases accounting for 12.4% of the total new cases. Lung cancer was the leading

cause of cancer death (1.8 million deaths, 18.7% of the total cancer deaths).¹⁹ It is categorized into mainly two types based on prognosis and treatment: non-small-cell lung cancer (NSCLC), which accounts for around 85% of cases, and the remaining 15% account for small-cell lung cancer (SCLC).²⁰

Current treatments available for lung cancer include surgery, radiotherapy, chemotherapy, targeted therapy, and/or immunotherapy, depending on the type and stage of cancer. Radiotherapy and chemotherapy have serious side effects due to their cytotoxicity to normal cells, whereas targeted therapy and immunotherapy have an inadequate target range and can be very expensive.²¹ In an attempt to overcome the limitations and drawbacks of these individual and combined cancer therapies, several anticancer molecules have been developed. The efficiency of most of these molecules is compromised by the ability of cancer cells to acquire drug resistance. Thus, continued research into developing new and unique anticancer drugs that are very potent, tumor-selective, and can overcome drug-resistant cancer cells is urgently needed.²² Natural products, particularly those derived from plants, have long played an important role in drug discovery.

1.2 NATURAL PRODUCTS

Natural products have been used since the dawn of civilization and the most common sources of medications include minerals, plants, and animals. Medicinal plants with a long history of ethnopharmacological use have been a valuable source of effective phytochemicals that provide beneficial effects against numerous diseases.²³ According to the World Health Organization (WHO), 80% of people still rely on plant-based traditional medicines for primary health care²⁴, and 80% of 122 plant-derived drugs were related to their original ethnopharmacological purpose.²⁵ The knowledge associated with traditional medicine has promoted further investigations of medicinal plants as potential medicines and has led to the isolation of many natural products that have become well-known pharmaceuticals. Many natural products isolated from higher plants have become clinical medicines and are still used today. Quinine and quinidine from *Cinchona*, morphine, and codeine from Corn poppy, digoxin from digitalis leaf, atropine and hyoscyne from Solanaceous plants, caffeine (*Coffea arabica*, *Thea sinensis*), digoxin (*Digitalis purpurea*), ephedrine (various species of

Ephedra), ergometrine (*Claviceps purpurea*), pilocarpine (*Pilocarpus jaborandi*), reserpine (*Rauwolfia serpentina*), etc. still in clinical use.²⁶

Approximately 25% of clinically used drugs are derived from plants, with more than 60% of these drugs having anticancer activity. Medicinal plants are often utilized in the form of concentrated extracts.²⁷ Modern medicines, however, requires the separation and purification of one or two active compounds that elicit the activity. Extracts with potential bioactivity are typically subjected to bioassay-guided isolation, which involves (i) extraction of metabolites using appropriate solvents, (ii) chromatographic fractionation of the resulting extract, (iii) bioassay screening of each fraction, (iv) isolation of the molecule(s) from bioactive fractions, and (v) identification of the isolated molecules and evaluation of their bioactivity

1.3 BIOACTIVITY GUIDED FRACTIONATION

Bioactivity-guided fractionation and isolation combined with chromatographic separation techniques are widely used. Fractionation of extracts is based on bioactivity rather than a class of compound of interest, which includes stepwise separation of the plant extract.²⁸⁻³⁰ Physicochemical properties and further fractionation and screening are followed based on bioactivity screening. In the first round, all the fractions are screened for bioactivity, and only fractions with significant activity are further processed until a getting of the pure isolate, is responsible for target biological activity. After active isolates are identified, chemical characterization and structural elucidation are performed.^{31,32} The biological activity-based isolation method has been used to discover a variety of plant-derived natural products, including anticancer drugs, camptothecin, and paclitaxel from *Camptotheca acuminata* and *Taxus brevifolia*, respectively. Other natural products or modified forms of natural products include the dopamine receptor agonist, morphine derivatives apomorphine, atropine derivative tiotropium, used to treat chronic obstructive pulmonary disease, galantamine obtained from *Galanthus nivalis* is selective anticholinesterase and artemether is antimalarial agent derived from artemisinin.^{28,32-34} The bioactivity-directed fractionation of natural products is a relatively new technology. In the experimental process, mainly two approaches are used to isolate the phytoconstituents.²⁸

a) Parallel Approach

This approach is selected when the plants used in the study have known biological activities from traditional or ethnopharmacological knowledge.

b) Sequential Approach

This approach is generally used when the plant selection is random and the biological activity of the selected plant is unknown.

In both approaches, the plant material extraction is performed using a variety of polar and non-polar solvents. However, their method of extraction and fractionation remains invariable. In general, the chemical classes of components present in an extract or fraction can be predicted depending on the polarity of the solvent used. Lipophilic compounds (less polar components) such as oils, fatty acids, steroids, hydrocarbons, and less polar terpenoids are extracted with non-polar solvents such as n-hexane and ether. On the other hand, intermediate polar compounds such as phenolics and alkaloids are generally present in ethyl acetate and chloroform extracts. Highly oxygenated and highly polar compounds such as sugars, flavonoids, glycosidic alkaloids, and low molecular weight carboxylic acids are commonly obtained in water or methanol/ethanol extracts²⁸.

1.4 HYPHENATED TECHNIQUES

After preliminary biological screening of the extracts, bioactive extracts were rapidly fractionated by chromatography, followed by liquid chromatography-mass spectrometry (LC-MS) and nuclear magnetic resonance (NMR) spectroscopy. After LC-MS analysis, new compounds in isolates are first differentiated from the known compounds by comparing the MS data with previously identified compounds available in the web libraries. LC-MS/MS is the most efficient analytical technique used for phytochemical profiling of the active fractions, which produced good chromatographic separation power with remarkable characterizing capacity of mass spectrometry. Spectroscopy is currently a major approach in the structural elucidation of phytochemicals. Characterization of the structure of pure bioactive molecules is performed by the data obtained from a various spectroscopic technique such as FT-IR spectroscopy, NMR spectroscopy, and mass spectrometry. In addition to these major techniques, data from X-ray diffraction, optical rotatory dispersion, and chemical analysis are also useful.³⁵

HPTLC is a powerful analytical method suitable for qualitative and quantitative analytical tasks. HPTLC is one of the most widely used analytical techniques in the field of the pharmaceutical industry, clinical chemistry, forensic chemistry, biochemistry, cosmetics, food and drug analysis, environmental analysis, etc.³⁶ In the pharmaceutical sector HPTLC is widely utilized for method development, adulterant detection in herbal products, pesticide residue, mycotoxins recognition, and quality control of herbal plants and health foods.³⁷ HPTLC is an analytical technique based on TLC, but it increases the resolution of the compounds to be separated and allows quantitative analysis of the compounds. Some improvements include the use of high-quality TLC plates with finer particle sizes for the stationary phase resulting in better resolution. Separation can be further improved by developing a plate, many times in a multiple development device.³⁸ As a result, HPTLC gives better resolution and a lower limit of detection (LODs). It is the only chromatographic method that can display the results as an image. Other advantages are simplicity, low costs, parallel analysis of samples, high sample volume, fast results, and the possibility of multiple detections.³⁹

1.5 INTRODUCTION TO PLANT: *Onosma bracteatum* Wall.

It is commonly used in Ayurvedic medicine, the traditional medical system of India, is commonly known as Goji, Gaozaban, or Sedge. *Onosma bracteata* Wall. (Boraginaceae) is distributed in India and Nepal at high altitudes and in Jammu & Kashmir, Himachal Pradesh, and Uttar Pradesh in the north-western Himalayas.^{40,41} It is a very valuable medicinal herb and is widely used by the tribes of the Western Ghats for fever, cough, bronchitis, rhinitis, stomatitis, jaundice, constipation, epilepsy, kidney disease & weakness of cardiac muscles.⁴²⁻⁴⁵

1.5.1 Synonyms⁴¹

Sansk. : Darvipatra, Gauajihva, Kharaparni, Gauji

Assam. : Lisanusaur

Beng. : Gojialata, Dadisha

Eng. : Cow's Tongue/ Lisanussoar, Sedge herb

Guj. : Bhonpathari, Galajibhi

Hindi. : Gaujaban, Gojiya

Kan. : ShankhaHuli, Aakalanalige, Gojaba

Mal. : Kozhuppu

Mar. : Govjaban, Paatharee
 Ori. : Kharsan, Kharaptra
 Punj. :Kazban
 Tam. : Kharaptra, Dharviptra, Kozha
 Tel. : Yeddunaluka
 Urdu. : Gaozaban

1.5.2 Taxonomical Classification⁴⁶

Kingdom : Plantae, Plants
 Subkingdom : Tracheophytes
 Super division : Angiosperms
 Division : Eudicots
 Class : Asterids
 Order : Boraginales
 Family : Boraienaceae
 Sub family : Boraginoideae
 Genus: Onosma
 Species: Bracteatum



Fig.1.1 Plant of *Onosma bracteatum* (1.5 cm is for Flower, 2.3X0.7cm is for Leaf)

1.5.3 Geographical Distribution:A perennial, hairy herb, mainly distributed in the highlands of India and Nepal, in North-Western Himalayas of Jammu & Kashmir, Himachal Pradesh and Uttar Pradesh. It usually grows in rock crevices in dry or moist and sunny weather and is popularly known as rock garden plant.^{41,42,47-49}

1.5.4 Description:^{41,47,49,50}

Leaf: Bilateral, lanceolate to ovate-lanceolate, acuminate showing tubercle-based hispid hairs on both surfaces; greenish to light yellow above and white below.

Flower: Purple, trumpet-shaped, in dense, glossy, glomerate clusters. The nut-lets are grey, rough, wrinkled, and bumpy.

Stem: Flat, erect, stout, with a rough surface having longitudinal wrinkles and covered with stiff, hispid hairs and cicatrices, greenish-yellow in color, short fracture; odor and taste none.

Root: Simple and infrequently branched, densely studded with calcareous tubercles and armed with bristles; purplish red from inside.

1.5.5 Medicinal Uses:^{40, 51-53}

Traditionally it is used for leprosy (kushtha), urinary tract disease (Mutrakricha), fever (Jihwaroga), dyspnoea, cough, as a tonic to build the body's immune system, asthma, bronchitis (Kasa, Shwasa, Pratishyaya), antispasmodic (Grahi), rheumatism, syphilis, cardio protectant (hridayaroga) and wound and skin diseases. It is the main ingredient in various Unani and Ayurvedic preparations (Kameeragaozabansada, Dawa-ul-miskMotadiJawahardar, Shahi, etc.) used in the treatment of hypertension, leprosy, rheumatism, and asthma.

REFERENCES

1. Cancer. *In* The Cell: A Molecular Approach, G.M. Cooper, 2nd edition. Sinauer Associates, Sunderland 2000.
2. M.G. Saria. Overview of Cancer. *In*Your guide to Cancer Prevention, J.L. Watson (eds), The Oncology Nursing Society,2000, pp.1-11
3. Wittekind C, & Neid M. Cancer Invasion and Metastasis. *Oncology*. 2005; 69(1): 14–16.
4. Meena M. Cancer notes. 2020.
5. Halazonetis T D, Gorgoulis V G, Bartek J. An Oncogene-Induced DNA Damage Model for Cancer Development. *Science*.2008; 319(5868):1352–1355.
6. Rieger PT. The biology of cancer genetics. *Semin Oncol Nurs*. 2004; 20(3):145-54.
7. Weinberg R. A. How Cancer Arises. *Sci. Am.*, 1996; 275(3): 62–70.
8. Macheret M, &Halazonetis T D. DNA Replication Stress as a Hallmark of Cancer. *Annu. Rev. Pathol*. 2015; 10(1), 425–448.
9. Hanahan D, & Weinberg R A. Hallmarks of cancer: the next generation. *Cell*. 2011; 144(5):646-74.
10. Harrington K J. Biology of cancer. *Medicine*. 2008; 36(1): 1–4.
11. Idikio H A. Human cancer classification: a systems biology- based model integrating morphology, cancer stem cells, proteomics, and genomics. *J Cancer*. 2011; 2:107-15.
12. Nenclares P, & Harrington K J. The biology of cancer. *Cancer Biol. Med*. 2020; 48(2):67-72.
13. Low K C, &Tergaonkar V. Telomerase: central regulator of all of the hallmarks of cancer.*Trends Biochem. Sci*. 2013; 38(9): 426–434.
14. Berthois Y, & Martin P M. Growth factors and oncogenes.*Biomed. Pharmacother*. 1989; 43,(9):635-639
15. Wong R S, & Passaro E J. Growth factors, oncogenes and the autocrine hypothesis. *Surg Gynecol Obstet*. 1989; 168(5):468-73.
16. Shrivastava R, & Bhadauria S. Role of Growth Factor Signaling in Cancer. *Def. Life SCI. J*.2016; 1(1):34-47.

17. Calibasi-Kocal G, & Basbinar Y. Cancer Metastasis. *In* Cancer Metastasis. BasbinarY, Calibasi-Kocal, G(ed) IntechOpen London 2018.
18. Hapach L A, Mosier J A, Wang W, Reinhart-King C A. Engineered models to parse apart the metastatic cascade. *npj Precis. Onc.* 2019; 3(20):1-8
19. Siegel R L, Miller K D, Wagle N S, Jemal A. Cancer statistics, 2023. *CA Cancer J Clin.* 2023; 73(1): 17-48.
20. Oser M G, Niederst M J, Sequist L V, Engelman J A. Transformation from Non-Small-Cell Lung Cancer to Small-Cell LungCancer: Molecular Drivers and Cells of Origin. *Lancet Oncol.* 2015; 16:165-172.
21. Lemjabbar H, & Basbaum C. Platelet-Activating Factor Receptor and ADAM10 Mediate Responses to Staphylococcus Aureus inEpithelial Cells. *Nat. Med.* 2002; 8: 41–46.
22. Wang X, Zhang H, Chen X. Drug Resistance and Combating Drug Resistance in Cancer. *Cancer Drug Resist.* 2019; 2: 141–160.
23. Newman D J, & Cragg G M. Natural Products as Sources of New Drugs from 1981 to 2014. *J. Nat. Prod.* 2016; 79: 629–661.
24. Farnsworth N R, Akerele R O, Bingel A S, Soejarto D D, Guo Z. Medicinal Plants in Therapy. *Bull. WHO.* 1985;63:965–981
25. Fabricant D S, & Farnsworth N R. The value of plants used in traditional medicine for drug discovery. *Environ. Health Perspect.* 2001;109:69–75
26. Wachtel-Galor S, & Benzie IFF. Herbal Medicine: An Introduction to Its History, Usage, Regulation, Current Trends, and Research Needs. *In*Herbal Medicine: Biomolecular and Clinical AspectsBenzie IFF, Wachtel-Galor S(ed). 2nd edition. CRC Press/Taylor & Francis Boca Raton (FL). 2011
27. Salem M A, Perez de Souza L, Serag A, Fernie A R, Farag M A, Ezzat S M, Alseekh S. Metabolomics in the Context ofPlant Natural Products Research: From Sample Preparation to Metabolite Analysis. *Metabolites* 2020; 10(37):1-30
28. Najmi A, Javed S A, Al Bratty M, Alhazmi H A. Modern Approaches in the Discovery and Development of Plant-Based Natural Products and Their Analogues as Potential Therapeutic Agents. *Molecules.* 2022;27(2):349
29. Koehn F E, & Carter G T. The evolving role of natural products in drug discovery.*Nat. Rev. Drug Discov.* 2005; 4(3):206-220

30. Weller M G. A Unifying Review of Bioassay-Guided Fractionation, Effect-Directed Analysis and Related Techniques. *Sensors*, 2012; 12(7): 9181-9209.
31. Nothias L F, Nothias-Esposito M, Da Silva R, Wang M, Protsyuk I, Zhang Z, et.al. Bioactivity-Based Molecular Networking for the Discovery of Drug Leads in Natural Product Bioassay-Guided Fractionation. *J. Nat. Prod.* 2018; 81(4):758–767.
32. Bucar F, Wube A, Schmid M. Natural product isolation – how to get from biological material to pure compounds. *Nat. Prod. Rep.* 2013; 30(4):525.
33. Newman D J, & Cragg G M. Natural Products as Sources of New Drugs from 1981 to 2014. *J. Nat. Prod.* 2016; 79(3): 629–661
34. Li J W-H, & Vederas J C. Drug Discovery and Natural Products: End of an Era or an Endless Frontier? *Science*. 2009; 325(5937): 161–165.
35. Ory L, Nazih E H, Daoud S, Mocquard J, Bourjot M et.al., Targeting bioactive compounds in natural extracts - Development of a comprehensive workflow combining chemical and biological data. *Anal Chim Acta.* 2019; 1070:29-42.
36. Srivastava M. An Overview of HPTLC: A Modern Analytical Technique with Excellent Potential for Automation, Optimization, Hyphenation, and Multidimensional Applications *In High-Performance Thin-Layer Chromatography* Srivastava M (ed). Springer, Berlin, Heidelberg. 2010; pp 3-24.
37. Attimarad M, Ahmed K K, Aldhubaib B E, Harsha S. High-performance thin layer chromatography: A powerful analytical technique in pharmaceutical drug discovery. *Pharm. Methods.* 2011; 2:71-5.
38. Ravisankar P, Lokapavani Ch, Devadasu Ch, Rao D G. HPTLC: A versatile method for rapid analysis of pharmaceutical formulations and comparison with other chromatographic techniques and its applications. *IJRPB.* 2020; 2(3):1209-1219
39. Ivanova S, Todorova V, Dyankov S, Ivanov K. High-Performance Thin-Layer Chromatography (HPTLC) method for Identification of Meloxicam and Piroxicam. *Process.* 2022; 10(2):394.
40. Charaka Samhita, Shri Gulabkunverba Ayurvedic Society, Jamnagar, Ayurvedic Mundranalaya, Jamnagar 1949; 4:1952.

41. Government of India, Ministry of Health and Family Welfare, Department of ISM & H, The Ayurvedic Pharmacopoeia of India, 1(3); pp 55.
42. Kirtikar K R, Basu B D. Indian Medicinal Plants, 2nd ed., International book distributors 1999; 3: pp 1699
43. Nadkarni K M. Indian Materia Medica, 3rd ed., Popular Prakashan Pvt. Ltd. 2002;1: pp 871.
44. Chopra R N, Nayar S L, Chopra I C. Glossary of the Indian Medicinal Plants (Including the Supplement), 1986; pp 240.
45. Chatterjee A, Pakrashi S. The Treatise on Indian Medicinal Plants, Vol. I (Revised), National Institute of Science and Communication and Information Resources, CSIR, New Delhi, 2005; pp 34-35
46. Sharma, O P. Taxonomical classification of plants, India, McGraw Hill Education Publication, 2017; pp171.
47. N.S. Chauhan, Medicinal and Aromatic Plants of Himachal Pradesh, Indus Publishing, 1999; pp. 1-632
48. Khare, C. P. Indian Medicinal Plants: An Illustrated Dictionary. Indian Medicinal Plants (2007); pp 448-449
49. Government of India Ministry of Health & Family Welfare Department of Ayurveda, Yoga & Naturopathy, Unani, Siddha And Homoeopathy (Ayush) New Delhi. The Unani Pharmacopoeia of India.1(5): pp 27-28
50. Patel, Vandana, Patel, Kalpana, Patel, Kirti, Tejal, Gandhi. Pharmacognostical, Physicochemical and Preliminary Phytochemical Standardization of Aerial Parts of *Onosmabraceatum* Wall. International Journal of Pharmacognosy and Phytochemical Research. 2017; 9(6): pp 766-771
51. P.V. Sharma, Dravyaguna-Vijnana, Vol II, Chaukhambhabharati academy, Varanasi, 12th edition, 1991; pp 256-258.
52. Bhavaprakash Nighantu. Commentary by Dr. K.C.Chunekar, A.M.S.Edited By Dr. G.S. Pandey, A.M.S.Chaukhambha Bharti Academy Publisher Varanasi. Pp 472.
53. Kaiyadev Nighantu. Edited And Translated By Prof. Priyavrata Sharma And Dr. Guru Prasad. Sharma. Chaukhambha Orientalia Varanasi. pp13.

Chapter 2

Review of Literature

REVIEW OF LITERATURE**2.1 Pharmacognostic review of *Onosma bracteatum*:**

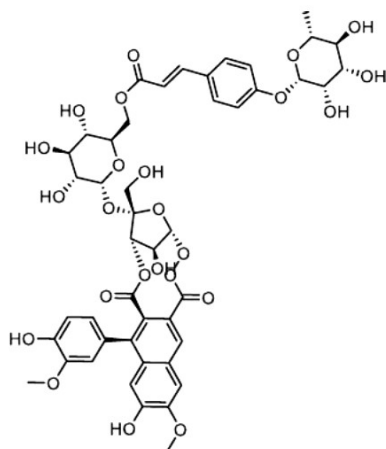
- Patel VG et al., 2017 studied powder characteristics of aerial parts of *O. bracteatum*.¹
- Dhikale et al., 2022 studied macroscopy, microscopy, powder microscopy, and quantitative microscopy of leaves of *O. bracteatum*.²

2.2 Phytochemical review of *Onosma bracteatum*:

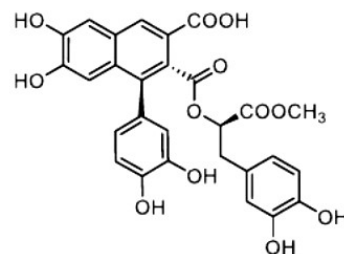
Phytochemical work on the genus *Onosma* L. reported naphthoquinones, alkaloids, and phenolic compounds. Pyrrolizidine alkaloids are key phytoconstituents from the Boraginaceae family.³

- Patel VG et al., 2017 studied for preliminary phytochemical analysis of aerial parts of *O. bracteatum* and reported to possess saponins, flavonoids, phenolic compounds, and mucilage.¹
- Farooq U et al., 2019 reported two known benzoquinones; allomicrophyllone, and ehretiquinone and three novel benzoquinones; ehretiquinones B, ehretiquinones C, and ehretiquinones D from methanolic extract of *O. bracteatum*.⁴
- Kumar A et al., 2020 reported catechin, kaempferol, epicatechin, rutin, and onosmin A by HPLC analysis of an ethanolic extract of aerial parts (leaves and stem) of *O. bracteatum*.⁵
- Sun B et al., 2021 reported pulmonarioside C, 9'-methoxyl salvianolic acid R, (-)-4-O-(E)-p-coumaroyl-L-threonic acid methyl ester along with thirty four known compounds (coumarin, 3-hydroxycoumarin, umbelliferone, scopoletin, 5,7-dimethoxycoumarin, esculetin, p-hydroxycinnamic acid, caffeic acid, caffeic acid methyl ester, Ferulic acid methyl ester, 1-O-caffeoyl glycerol, latifolicinin C, oresbiusin A, ethyl 3-(3,4-dihydroxyphenyl)lactate, p-hydroxybenzoic acid, vanillic acid, 4,5-dihydroxy-3-methoxybenzoic acid, protocatechuic acid, 5-hydroxymethyl-furoic acid, 3,4-dihydroxybenzyl alcohol, 3-(3',4'-dihydroxyphenyl)-(2R)-lactic acid, rosmarinic acid, rosmarinic acid methyl ester, salviaflasidemethylester, 9'-(2,3-dihydroxypropyl)-rosmarinic acid, p-coumarinic acid ester of trigonotin A, echiumin A, ternifoliuslignan A, ternifoliuslignan D, eritrichin, (1-R),(2-S)-

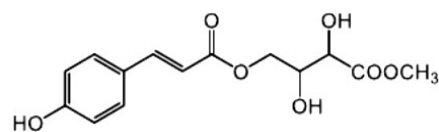
2,3-dicarboxy-6,7-dihydroxy-1-(3',4'-dihydroxy)-phenyl-1,2-dihydronaphthalene, kaempferol 3-O-[α -L-rhamnopyranosyl-(1 \rightarrow 6)- β -D-glucopyranoside]) in the ethanolic extract of aerial parts of *O. bracteatum*.⁶



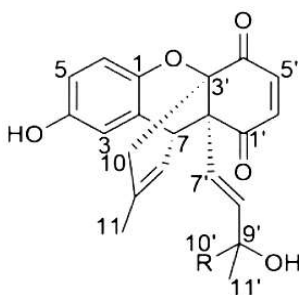
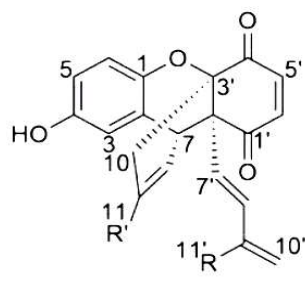
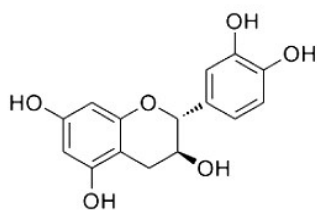
Pulmarioside C



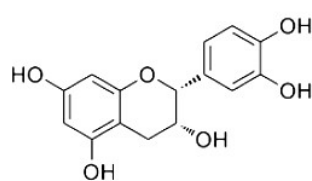
9'-methoxyl salvianolic acid R



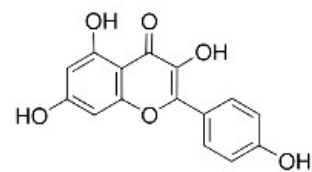
(-)-4-O-(E)-p-coumaroyl-L-threonic acid methyl ester

Allomicrophyllone R=CH₃Ehretiquinones D R=CH₂OHEhretiquinones R=CH₃ R'=CH₃Ehretiquinones B R=CH₂OH R'=CH₃Ehretiquinones C R=CH₃ R'=CH₂OH

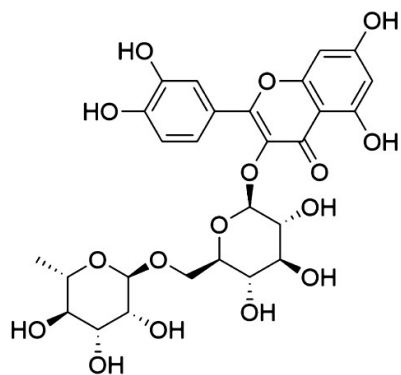
(+) Catechin



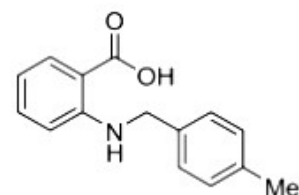
(-) Epicatechin



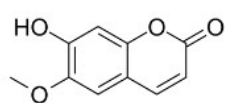
kaempferol



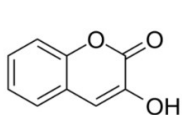
Rutin



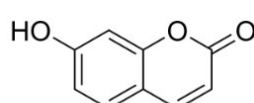
Onosmin A



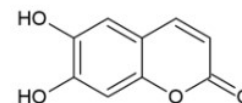
Scopoletin



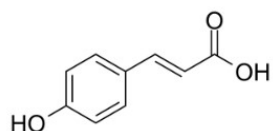
3-hydroxycoumarin



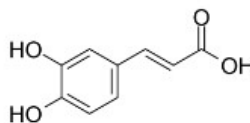
Umbelliferone



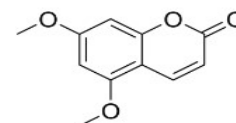
Esculetin



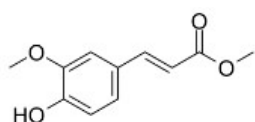
p-hydroxycinnamic acid



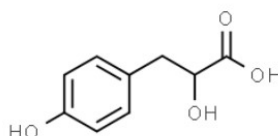
Caffeic acid



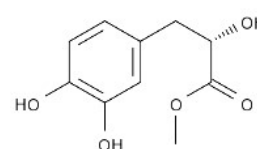
5,7-dimethoxycoumarin



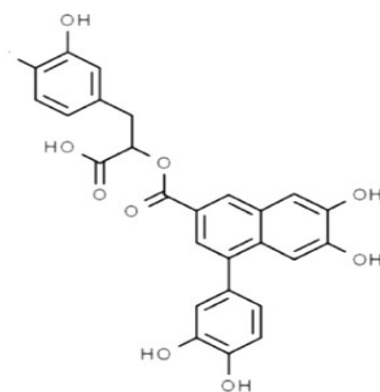
Ferulic acid methyl ester



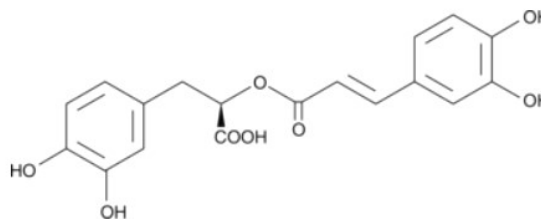
Latifolicin C



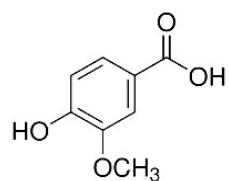
Oresbiusin A



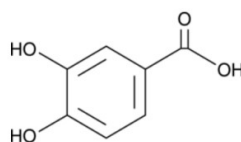
Eritrichin



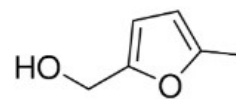
Rosmarinic acid



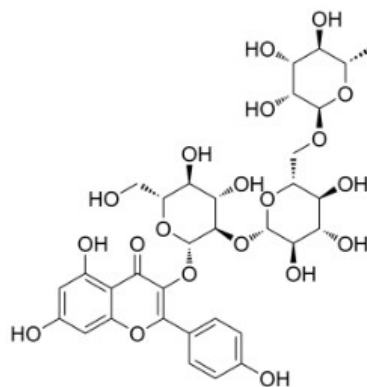
Vanillic acid



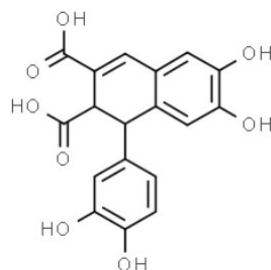
Protocatechuic acid



5-hydroxymethyl-furoic acid



Kaempferol 3-O-[\alpha-L-rhamnopyranosyl-(1→6)-\beta-D-glucopyranoside]



2,3-dicarboxy-6,7-dihydroxy-1-(3',4'-dihydroxy)-phenyl-1,2-dihydronaphthalene

Fig. 2.1 Chemical Structure of compounds from *Onosma Bracteatum*

2.3 Pharmacological Review of *Onosma bracteatum*

- Dandiya PC and Arora RB, 1957 reported that dealcoholized detannated extract of aerial parts of *O.bracteatum* in the dose of 0.1mL/kg, 0.25mL/kg, 0.5mL/kg of dose applied on 5 to 10kg weight of dog lowered the blood pressure, depressed the heart muscles. Also, the same extract in doses of 0.25mL/kg, 0.5mL/kg, 0.75mL/kg and 1mL/kg applied on 1 to 2kg weight of rabbit relaxed the small intestine and inhibited the stimulating effect of acetylcholine on the intestine hence it was concluded that it possessed spasmolytic activity compared to atropine (0.1µg/mL).⁷
- Ashraf M et al. 2011 reported AChE inhibitory activities of methanolic extract of *O.bracteatum* at a concentration of 250µg. AChE catalyzes the hydrolysis of the neurotransmitter acetylcholine and termination of the nerve impulse in cholinergic synapses, hence cholinesterase inhibitory action of *O.bracteatum* could be used in the treatment of Alzheimer's disease.⁸
- Menghani E et al., 2011 studied the antioxidant activity of methanolic extract of *O.bracteatum* for its reducing power, hydrogen peroxide scavenging activity, and DPPH scavenging capacity. Methanolic extract showed antioxidant activity potential which was equivalent to ascorbic acid.⁹
- Patel KG et al. 2011 reported antiallergic and anti-inflammatory activities of ethanolic extract of aerial parts of *O.bracteatum* using doses of 5 and 10mg/kg in vascular permeability induced by acetic acid, carrageenan-induced hind paw edema, passive paw anaphylaxis, passive cutaneous anaphylaxis, and allergic pleurisy. All these activities were proposed to be mediated by inhibiting plasma exudation, decreasing the release of mediators such as histamine, inhibiting of mast cell degranulation, and inhibiting of eosinophil accumulation by preventing the release of cytokines and chemokines.¹⁰
- Choudhary GP 2012(a) evaluated antidiarrhoeal effect of ethanolic extract of aerial parts of *O.bracteatum* at a dose of 250 and 500mg/kg using castor oil and magnesium sulfate induced-diarrhoea models in mice and showed that the extract reduced the extent of diarrhoea in both the model, while in

gastrointestinal motility test it retarded the intestinal transit of charcoal meal in mice as compared to standard loperamide at 3mg/kg of dose.¹¹

- Choudhary GP 2012(b) reported that the ethanolic extract of aerial parts of *O.bracteatum* exerted wound healing activity of on excision and incision model in albino rates in two concentrations of 5% and 10% in the form of ointment. Both the concentrations of the ethanolic extract showed wound healing activity in both the models when compared with standard control nitrofurazone ointment (2%w/w).¹²
- Badruddeen et al. 2012 studied the psychoimmunomodulatory effect of hydroalcoholic extract of *O.bracteatum* by assessing the changes in the behavior and immunity of rats and assessing biochemical changes using 5, 10, and 15mg/kg doses. The extract was shown to increase the number of T cells, antibody production, the size of the spleen and liver and a decrease total paw edema, the size of the kidney. It showed an inhibitory effect on brain cholinesterase and showed a regulatory effect on the circulating glucose levels.¹³
- Zeb MA et al. 2015 reported the antimicrobial activity of the hot and cold-water extract of *O.bracteatum* against *Staphylococcus aureus*, *Escherichia Coli*, *Proteus mirabilis*, and *Bacillus subtilis* compared to standard imipenem using streaking methods.¹⁴
- Gautam SS et al. 2015 studied the antimicrobial activity of petroleum ether, acetone, methanol, and water extract of fruits of *O.bracteatum* using five bacteria and one fungus causing respiratory tract infection. All extracts showed inhibitory activity against *H. influenza*, *P. aeruginosa*, *S. aureus*, *S. pneumonia*, *S. pyogenes*, and *Aspergillus niger* at the concentration of 200mg/mL for bacteria and 250mg/mL for fungi compared with erythromycin as a reference drug. The methanolic extract was found most active followed by water extract, acetone extract, and petroleum ether extract.¹⁵
- Imran H et al. 2018 showed dose dependent central and peripheral analgesic activity of hydro alcoholic extract of aerial parts of *O.bracteatum* by tail-flick test and acetic acid-induced writhing test models at the doses of 50, 100, 250, and 500mg/kg body weight using diclofenac sodium as reference standard.¹⁶

- Albaqami H et al. 2018 evaluated antiproliferative and caspase enzyme activation and lipid peroxidation assay of *O.bracteatum* methanolic extract of leaves on the A549 lung cancer cell line, BT549 Breast cancer cell line, and PC3 prostate cancer cell line. Extracts showed reduced cell viability in all cell lines, decreased lipid peroxides, and caused activation of caspase-3 in prostate, breast, and lung cancer cells at a concentration of 1.76µg/mL.¹⁷
- Asif MH et al. 2019 reported anxiolytic and antidepressant activity of hydroalcoholic extract of *O.bracteatum* at a dose of 50, 100, and 200mg/kg. Activity was evaluated by open field, elevated plus maze, force swimming, and tail suspension test. Open field test showed an increase in number of line crossing as well as number of rearing in dosage-dependent manner; In elevated plus maze test it showed antianxiety effect by increasing the time spent in open arms along with decreasing the time spent in closed arms in dose-dependent manner; it diminished the immobility time and expanded mobility time in force swim model in dosage-dependent way showed antidepressant effect; it expanded time span of mobility along with diminished immobility time in tail suspension method in dose-dependent way. At higher dose it showed all the effects compared with diazepam and fluoxetine as reference standards.¹⁸
- Farooq et al. 2019 reported the anti-aging activity of benzoquinones (allomicrophyllone, ehretiquinone, ehretiquinones B, ehretiquinones C, ehretiquinones D) isolated from the methanolic extract of *O.bracteatum* using yeast lifespan assay. Except for ehretiquinones B, all the benzoquinones extended the replicative lifespan of K6001 yeast compared to resveratrol as a reference standard.⁴
- Vegad UG and Pandya DJ 2022 reported Diuretic potential of methanolic and aqueous extract at dose of 200mg/kg, where as mild constipative potential was reported in aqueous extract from whole plant of *O.bracteatum*.¹⁹
- Vegad U G 2023 reported that higher binding potential of Pulmonarioside C against spike, RdRp and M^{Pro} as compared to antiviral SARS CoV-2 inhibitors in In Silico screening of eleven compounds of *Onosma bracteata* Wall.²⁰

REFERENCES

1. Patel V, Patel K, Patel K, Gandhi T. Pharmacognostical, physicochemical and preliminary phytochemical standardization of aerial parts of *Onosma bracteatum* Wall. Int. J. Pharmacogn. Phytochem. Res. 2017; 9(6):766-771
2. Dhikale R S, Gulecha V S, Zalte A G. Pharmacognostic and phytochemical evaluation of leaves of *Onosma bracteatum*. Int. j. botany stud. 2022; 7(1): 299-304
3. Huizing H J, &Malingre T M. A Chemotaxonomical Study of Some Boraginaceae: Pyrrolizidine Alkaloids and Phenolic Compounds.Plant Syst. Evol. vol. 1981; 137(1/2):127-134.
4. Farooq U, Yanjun P, Disasa D and Qi J. Novel Anti-Aging Benzoquinone Derivatives from *Onosma bracteatum*Wall. Molecules. 2019; 24: 1-9.
5. Kumar A, Kaur V, Pandit K, Tuli H S, Sak K, Jain K S et al., Antioxidant Phytoconstituents from *Onosma bracteata* Wall. (Boraginaceae) Ameliorate the CCl₄ Induced Hepatic Damage: *In vivo* Study in Male Wistar Rats. Front. Pharmacol. 2020; 11:1301
6. Sun B, Jiang H, Wang Z N, Luo H Z, Jia A Q. Phytochemical constituents of *Onosma bracteatum* Wall.Phytochem. Lett. 2021; 45:1-5
7. Dandiya, P C, & Arora R B. A Phytochemical and Pharmacological Study of *Onosma bracteatum* Wall. J Am Pharm Assoc. 1957; 46(2):111–114
8. Ashraf M, Ahmad K, Ahmad I, Ahmad S, Arshad S, Shah S M A, Nasim F H. Acetylcholinesterase and NADH oxidase inhibitory activity of some medicinal plants. J. Med. Plant Res. 2011; 5(10):2086-2089.
9. Menghani E, Sudhanshu, Rao N, Mittal S. Free radical scavenging capacity and antioxidant activity of *Onosma bracteatum*. Int. j. pharm. res. dev.2011;4(04):16-20
10. Patel K G, Detroja J R, Shah T A, Patel K V, Gandhi T R. Evaluation of the Effect of *Onosma bracteatum*, Wall (Boraginaceae) Using Experimental Allergic and Inflammatory Models.Glob. J. Pharmacol. 2011; 5 (1):40-49.
11. Choudhary G P.Antidiarrhoeal Activity of Ethanolic Extract of *Onosma bracteatum* wall. Int. j. adv. pharm. biol. chem.2012a; 1(3):402-405.
12. Choudhary G P. Wound Healing Activity of the Ethanolic Extract *Onosma bracteatum* Wall.Int. j. pharm. chem. sci.2012b;1(3):1384-1386.

13. Badruddeen, Fareed S, Siddiqui H H, Haque S E, Khalid M, Akhtar J. Psychoimmunomodulatory effects of *Onosma bracteatum* Wall. (Gaozaban) on Stress Model in Sprague Dawley Rats. *J. Clin. Diagnostic Res.* 2012;6(7):1356-1360.
14. Zeb M A, Sajid M, Rahman T R, Khattak K F, Halim A, Ullah S, Pandey S, Salahuddin M, Begum Z. Phytochemical Screening and Antibacterial Activity of *Opuntia dillenii* and *Onosma bracteatum*. *J Microbiol Exp.* 2015;2(7):1-4.
15. Gautam S S, & Kumar N S, Appraisal of antimicrobial properties of *Onosma bracteatum* Wall. fruit extracts against respiratory tract pathogens. *J. med. herbs ethnomed.* 2015; 1:108-112.
16. Imran H, Rahman A, Sohail T, Taqvi S I H, Yaqeen Z. *Onosma bracteatum* wall: A Potent analgesic agent. *Bangladesh J. Medical Sci.* 2018;17:36-41
17. Albaqami H, Myles L, Tiriveedhi V, Boadi W, Driggins N. The Effect of *Onosma bracteatum* in cancer cells. *MOJ Bioequiv Availab.* 2018;5(6):321–325.
18. Asif M H, Hayee A, Aslam M R, Ahmad K, and Hashmi A S, Dose-dependent, antidepressant, and anxiolytic effects of a traditional medicinal plant for the management of behavioural dysfunctions in animal models. *Dose response.* 2019;17(4):1-6
19. Vegad U G, Pandya D J, Evaluation of Diuretic and Laxative Potential of *Onosma bracteata* Wall.: A Species of the Controversial Drug ‘Gojihva’. *Int. J. Pharm. Investigation.* 2022;12(3):358-62.
20. Vegad U G et al, “In silico screening, ADMET analysis and MD simulations of phytochemicals of *Onosma bracteata* Wall. as SARS CoV-2 inhibitors.” *3 Biotech.* 2023;13(7):221.

Chapter 3

Material & Methods

MATERIAL & METHODS

3.1 Identification, Collection and Authentication of the Plant Material

Onosmabracteatum was collected from Uttarakhand. Authentication of the plant was done by Dr. V. P. Bhatt, Taxonomist, Herbal Research and Development Institute (HRDI), Gopeshwar, Uttarakhand, with Specimen voucher number: PCOG/2016/5. Plant material was washed to remove soil, mud, and other adhering material and dried at room temperature and 60# powder was prepared from dried sample and stored properly in airtight containers.

3.2 Assessment of quality of plant materials

The plant material was assessed as per WHO guidelines^(1,2)

3.2.1 Determination of foreign matter

The plant was subjected to determining any contamination by mold or insects and other animal contaminants.

3.2.2 Macroscopic evaluation

Dried plant parts of *O.bracteatum* was subjected to color, odor, and taste, determination of shape, size, surface characteristics, and appearance, etc.

3.2.3 Microscopical Evaluation

The powdered material of the stem, root, and flower were subjected to microscopical study.

3.2.4 Proximate analysis:

Proximate analysis of powdered plant material was carried out using reported methods.^(1,2)

3.2.4.1 Loss on drying:

In a previously tarred flat weighing vial, 2gm of air-dried plant material was accurately weighed, followed by heating the sample in an oven at 100-105°C for 5hr. Dried until two consecutive weighing did not deviate by more than 5mg. The weight loss in mg/gm of the air-dried material is then calculated.

3.2.4.2 Determination of Ash Values:

Three separate methods were used to determine the quantity of ash remaining after the powder plant material was ignited. Total ash, acid-insoluble ash, and water-soluble ash were measured.

3.2.4.2.1 Determination of Total Ash

In a muffle furnace, 2gm of accurately weighed powder plant was burnt in a silica crucible at a temperature not exceeding 450°C until white ash, demonstrating the absence of carbon is obtained. It was then cooled, weighed, and the percentage of ash was estimated using the air-dried powdered medication as a reference.

3.2.4.2.2 Determination of Acid Insoluble Ash

The ash from the plant was heated in 25mL of weak hydrochloric acid for 5min. The ash-free filter paper was used to collect the insoluble materials. The ash was cleaned with hot water before being burned to a consistent weight in a muffle furnace at 450°C. The proportion of acid-insoluble ash was estimated using the air dried medication as a reference.

3.2.4.2.3 Determination of Water-Soluble Ash

The total ash from the plant was cooked in 25mL of water for 5min. The ash-free filter paper was used to collect the insoluble materials. The ash was cleaned in hot water for 15min at a temperature of not more than 450°C. The ash's weight was removed from the weight of the insoluble substance. The water-soluble ash was represented by the weight difference. The proportion of water-soluble ash was estimated using the air-dried powdered medication as a reference.

3.2.4.3 Determination of Extractive Values

3.2.4.3.1 Determination of Alcohol Soluble Extractive Value

4gm of air-dried powdered material from the plant was macerated in 100mL of water for 6hr in a closed flask with regular shaking. It was then let to stand for 18hr before being filtered quickly to prevent any evaporation loss. In a porcelain dish, 25mL of the filtrate was evaporated to dryness and dried at 105°C to a constant weight. With reference to the air-dried powdered medication, the proportion of alcohol-soluble extractives was estimated.

3.2.4.3.2 Determination of Water-Soluble Extractive Value

4gm powdered material from the plant was soaked in 100mL water for 1hr in a covered flask with regular shaking. The weight was then readjusted after it was gently cooked for 1hr in a water bath. In a porcelain dish, 25mL of the filtrate was evaporated to dryness and dried at 105°C to a constant weight. The proportion of water-soluble extractives was estimated using air-dried powdered medication as a reference.

3.3 Phytochemical Studies^{3,4}

3.3.1 Preliminary Profile

100gm of the dried powdered drug was extracted with 300mL of methanol using a continuous Soxhlet extraction method. The sticky extract was obtained after evaporation of the solvent (TME-Total methanolic extract). The TME was subjected to qualitative and quantitative phytochemical chemical tests to determine the presence of various phytoconstituents like alkaloids, glycosides, flavonoids, phenolics, coumarins, quinones, tannins, amino acids, saponins, phytosterols and fixed oil and fats using a reported method in Harborne (1998)³.

3.3.1.1 Qualitative Phytochemical study

1. Test for alkaloids:

a. Dragendorff's test: 0.5mL of plant extract was treated with Dragendorff's reagent; reddish brown precipitate indicated the presence of alkaloids.

- b. Mayer's test: 0.5mL of plant extract was treated with Mayer's reagent; cream colored precipitate indicated the presence of alkaloids.
- c. Wagner's test: 0.5mL of plant extract was treated with Wager's reagent; reddish brown precipitate indicated the presence of alkaloids.
- d. Hager's test: 0.5mL of plant extract was treated with Hager's reagent; yellow precipitate indicated presence of alkaloids
- e. Test for Pyrrolizidine alkaloids: on the TLC plate spot of the plant extract showed a magenta color with Ehrlich's reagent.

2. Test for glycosides:

General test:

Test A: Extract 200mg of the drug with 5mL of dilute sulphuric acid by warming on a water bath and filter after neutralizing the acid extract with 5% solution of sodium hydroxide, add 0.1mL of Fehling's solution A and B until it becomes alkaline (test with pH paper) and heat on a water bath for 2min. Red precipitate formed

Test B: Extract 200mg of the drug using 5 mL water instead of sulphuric acid. After boiling add an equal amount of water as used for sodium hydroxide in the above test. Add 0.1mL Fehling's A and B until alkaline (test with pH paper) and heat in a water bath for 2min. A red precipitate formed.

Compare the quantity of precipitate formed in Test B with that formed in Test A. precipitate in Test B is the same as in Test A hence only free reducing may be present. Since Test B represents the amount of free reducing sugar already present in the crude drug, whereas Test A represents free reducing sugar plus those related-on acid hydrolysis of any glycoside in the crude drug.

3. Test for coumarins:

Place a small amount of sample in test tube and cover the test tube with a filter paper moistened with dilute sodium hydroxide solution. Place the covered test tube on water bath for several minutes. Remove the paper and expose it with ultraviolet (UV) light, the paper showed green fluorescence.

4. Test for saponins

- a. Froth formation test: About 0.5gm of the powdered drug was boiled gently for 2min with 20mL of water and filtered while hot and allowed to cool. 5mL of the filtrate was then diluted with water and shaken vigorously. A frothing indicated the presence of saponins.
- b. Hemolysis: put a drop of human blood on the slide add a few drops of extract, showed ruptured red blood cells, it indicated presence of saponins.

5. Test for Steroids and Triterpenoids:

- a. Libermann-Burchard test: Treat the extract with few drops of acetic anhydride, boil and cool. Then add concentrated sulphuric acid from the side of test tube, brown ring is formed at the junction. The layer turns green which shows presence of steroids and formation of deep red color indicated presence of triterpenoids.
- b. Salkowski test: Treat the extract with few drops of concentrated sulphuric acid red color at lower layer indicates the presence of steroids and formation of yellow colored lower layer indicated presence of triterpenoids.

6. Test for Flavonoids

- a. Shinoda test: A little of the powdered drug was heated with alcohol and filtered. To the test solution add pieces of metallic magnesium and a few drops of concentrated hydrochloric acid and Boiled for five minutes. A red color indicated the presence of flavonoids.
- b. Alkali Test: To the small quantity of extract 10% aqueous sodium hydroxide solution was added. A yellow orange color indicated the presence of flavonoids.
- c. Acid Test: To a small quantity of extract, few drops of concentrated sulphuric acid were added. A yellow orange color indicated the presence of flavonols.

7. Phenolic compounds (Tannins):

- a. Gelatin test: To the extract add 1% gelatin solution containing 10% sodium chloride white bulky precipitate was formed.

b. Phenazone test: Add about 0.5gm of sodium acid phosphate to 5mL of extract warm it and filter. To the filtrate add 2% phenazone solution, colored bulky precipitate were formed.

c. Ferric chloride test: Treat the extract with ferric chloride solution, blue color appears if hydrolyzable tannins are present and green color appeared because of condensed tannins.

8. Test for Quinones

a. Plant extract treated with 10% potassium hydroxide; produced pink color.

9. Test for Proteins and free amino acids

a. Biuret Test: To the extract powdered drug, 1ml of dilute sodium hydroxide(10%) solution was added followed by one drop of very dilute copper sulfate solution was added. A violet color indicated the presence of proteins.

b. Millon's Test: A small quantity of acidulous-methanolic extract of the powdered drug was heated with Millon's reagent. A white precipitate turning red on heating indicated the presence of proteins.

10. Test for Fixed oil and Fat:

The extract is rubbed between the folds of filter paper. The appearance of a translucent spot confirmed the presence of fats and fixed oil.

3.3.1.2 Quantitative Phytochemical study

1. Total Phenolic content⁵

The total phenolics content was determined by using the Folin-Ciocalteu assay. 1mL of Folin-Ciocalteu phenol reagent was added to the TME and shaken, the above mixture was kept for 5min, and then 4mL of 20% sodium carbonate solution, this mixture was kept for 30min and absorbance against the reagent blank was determined at 760nm. A calibration curve was prepared, using a standard solution of gallic acid (0.12, 0.36, 0.6, 0.84, 1.08, 1.2 μ g)

2. Total Flavonoids⁶

Total flavonoid content was measured by the Aluminium chloride colorimetric assay. TME was mixed with 0.1mL of 10% AlCl₃, and 0.1mL of 1M potassium acetate and 2.8mL of distilled water. This mixture was incubated at room temperature for 30min. The absorbance of the color developed was measured at 415nm. A calibration curve was prepared, using a standard solution of rutin (1, 3, 5, 7, 9, 11µg)

3. Total Alkaloids⁷

Total alkaloids content was measured by the Dragendorff's precipitation method.

10gm powdered drug was extracted with 25mL 2% ethanolic acetic acid at 100°C for 10min. repeat it with 2 times. Above extract was diluted to 30mL with 2% ethanolic acetic acid. Take 5mL above extract and adjust pH 2-2.5 with dilute HCl, add 2mL dragendorff's reagent. After centrifugation, the precipitate was washed with alcohol, and treated with 2mL sodium sulphide solution. Brownish black precipitate formed was centrifuged and completion of precipitation was checked by sodium sulphide solution. The residue was dissolved in 2mL conc. Nitric acid, with warming and diluted to 10mL with distilled water. 1mL of above solution was mixed with 5mL 3% thiourea and absorbance was measured at 435nm against blank containing nitric acid and thiourea. Alkaloid content was estimated using calibration curve of quinine sulphate (10, 20, 30, 40, 50µg).

Total methanolic extract was subjected to antioxidant activity, brine shrimp lethality test and preliminary cytotoxicity on lung cancer cell lines (A549 and NCI-H23)

3.4 Antioxidant activity of TME

Antioxidant activity of TME can be evaluated by DPPH scavenging assay, phosphomolybdenum assay and nitric oxide scavenging assay.

3.4.1 DPPH scavenging assay⁷

Antiradical activity was measured terms of the extract mediated decrease in absorbance of the methanol. The solution of DPPH (1, 1-diphenyl-2-picryl hydrazyl), a stable free radical, at 516nm. A stock solution of DPPH (4.3mg/3.3mL methanol)

was prepared such that, 75µL of it in 3mL methanol gave an initial absorbance of 0.9. BHT was used as a reference standard with concentration of 20, 40, 60, 80 and 100µg/mL and TME was prepared in methanol and used in concentration of 100, 200, 300, 400, 600 and 800µg/mL and 75µL of stock solution of DPPH in 3mL methanol as a control. The activity was expressed as median inhibitory concentration (IC₅₀), deduced from mean % inhibition.

3.4.2 Phosphomolybdenum assay⁸

0.3mL of TME extract was combined with 3mL of reagent solution (1mL each of 0.6M sulphuric acid, 28mM sodium phosphate and 4mM ammonium molybdate) and the solution containing vial was capped and incubated in a water bath at 95°C for 90min. after incubation samples were cooled to room temperature the absorbance of solutions were measured at 765nm against blank.

3.4.3 Nitric oxide scavenging assay⁷

Scavengers of nitric oxide compete with oxygen leading to reduce the production of nitrite ions. In an aqueous medium, sodium nitroprusside (in PBS) generates NO and nitrite ions on reacting with oxygen subsequently, which is estimated using the Griess reagent. The reaction mixture contained 0.3mL sodium nitroprusside (10mM) in phosphate buffer saline and TME at different concentrations (50-350µg/mL) incubated at room temperature for 150min. The same reaction mixture without the tested samples but with an equivalent amount of solvent served as control. After the incubation of 1mL, Griess reagent (1% sulphanilamide, 2% H₃PO₄, and 0.1% naphthalene diamine dihydrochloride) was added. The absorbance of the reaction mixture was measured at 546nm.

3.5 Preliminary cytotoxicity study of TME

3.5.1 Brine shrimp lethality assay^{9,10}

Brine shrimp lethality bioassay is a simple, high throughput preliminary cytotoxicity test of bioactive chemicals. It is based on the killing ability of the test component on a simple zoological organism-brine shrimp (*Artemia salina*).

Briefly, the cysts of *Artemia salina* were hatched in an illuminated, aerator aided separating funnel containing 0.33% sea salt medium (Natural Sea salt mix, Oceanic Systems, Texas, U.S.A.) under conditions specified earlier, with some minor modifications. After incubation for 24hr, 10 nauplii were harvested and used for the assay. The extract (TME) was tested in triplicates up to a total volume of 5mL, and 10 nauplii were added. TME was administered at 1000, 500, 100, 10, and 1 μ g/mL, with control. Mortality was evaluated after incubation of 24hr. The % mortality and median lethal concentration (LC₅₀) were calculated as mentioned earlier.

$$\% \text{ Mortality} = [\text{number of dead nauplii} / \text{total number of nauplii}] \times 100$$

3.5.2 Cell line study (A549 and NCI-H23 cell line)

The usefulness of cell lines acquired from tumors allows the study of tumor cells in a simplified and controlled environment. Non-small cell lung cancer (NSCLC) is a common and aggressive form of lung cancer that accounts for approximately 85% of all lung cancer cases. Researchers often select NSCLC for study due to its prevalence and the urgent need for improved treatments. Among the various NSCLC cell lines available, A549 and NCI-H23 are frequently chosen for research purposes for several reasons. NCI-H23 cell line is derived from human lung adenocarcinoma cells from a 51-year-old black male prior to any therapy. NCI-H23 cells are epithelial cells with adherent and monolayer when growing in cell culture. They exhibit characteristics similar to A549 cells but may possess distinct genetic or phenotypic features, offering researchers the opportunity to compare responses and investigate heterogeneity within NSCLC.¹¹ A549 cells are adenocarcinomic human alveolar basal epithelial cells, making them a representative model for studying NSCLC. The A549 cell line was first developed in 1972 by D. J. Giard, et al. through the removal and culturing of cancerous lung tissue in the explanted tumor of a 58-year-old Caucasian male. A549 cells have been extensively characterized and are widely used in lung cancer research due to their stable phenotype and responsiveness to various stimuli.¹²

Molecular Characteristics of A549 and NCI-H23 cells^{13,14}:

EGFR Mutation Status: Both A549 and NCI-H23 cells are known to have mutations in the epidermal growth factor receptor (EGFR) gene, a common molecular alteration found in NSCLC. EGFR mutations can lead to dysregulated cell growth and survival pathways, contributing to tumor development and progression.

TP53 Status: The tumor suppressor gene TP53 is frequently mutated in NSCLC, including A549 and NCI-H23 cells. TP53 mutations can disrupt cell cycle regulation and promote genomic instability, facilitating cancer progression and resistance to therapy.

KRAS Mutation Status: KRAS mutations are prevalent in NSCLC and are associated with aggressive tumor behavior and resistance to targeted therapies. A549 cells harbor KRAS mutations, which contribute to their tumorigenic phenotype.

Expression of Drug Resistance Markers: Both A549 and NCI-H23 cells may exhibit altered expression of drug resistance markers, such as multidrug resistance protein 1 (MDR1) or ATP-binding cassette (ABC) transporters, which can impact the response to chemotherapy and targeted therapies.

Sample Preparation

Sterilization of extract was done by autoclaving (120psi, 15min) or by filter sterilization. Sterile extract was validated by adding 10 μ L of extract in sterile media (RPMI 1640) and incubated at 37°C for 24hr. After 24hr if no contamination in terms of cloudy appearance in media was found only later extract was subjected to cell culture. On the day of the treatment, required quantities of the test item was used.

Method

Growth Medium for NCI-H23 : RPMI 1640 + FBS 10%+ Pen-Strep 1%

Growth Medium for A549 : Ham's F12K + 10% Fetal bovine serum + 1% pen-strep

Receipt of Frozen Cells and Starting Cell Culture

Frozen cells were kept immediately in liquid nitrogen freezer storage until ready to culture. On disappearing of ice crystals, the ampoule's outer surface was swabbed with 70% ethanol, content was dispensed into a T25 flask with 2mL of warm growth media. Cells were allowed to recover overnight in 37°C, 5% CO₂ humidified incubator.

Sub-culture

Cells were propagated until density reached 60-70% confluence. Medium was aspirated. Cells were washed at room temperature (or warm) 1XPBS. 1mL of Trypsin was added and cells were monitored for detachments. To the culture 3mL of complete medium was added and aspirated by gentle pipetting. Complete content with medium was transferred to sterile centrifuge tube and cells pelleted. Supernatant media was aspirated and discarded, subjecting cells to 1mL of media and further cell count. After count, cells were split. Approx. 1X10⁴ to 2X10⁴ cells/well is seeded in 96 well plate

(for MTT). Inoculants were further cultured at 37°C, 5% CO₂ humidified incubator. Culture medium was changed every alternative day till the cells reached 80% confluence. Extracts were exposed to the cells for 24hr duration in different concentration as per experimental design.

Exposure of Test extract

Media was replaced with fresh media and test extract (TME) in various dose concentrations, and the time was noted as T₀. Plate was again incubated in incubator for further 24hr. After completion of the exposure duration, cells were subjected to parametric analysis.

MTT assay¹⁵

Principle

The MTT (3-[4,5-dimethylthiazol-2-yl]-2,5 diphenyl tetrazolium bromide) assay is based on the conversion of MTT into formazan crystals by living cells, which determines mitochondrial activity. For most cell populations the total mitochondrial activity is related to the number of viable cells. This assay is broadly used to measure the *in vitro* cytotoxic effects of drugs on cell lines

Protocol

Media containing test compounds was removed from the culture wells and fresh 100µL 1XPBS buffer was added. Two washes were given to the culture to remove traces of the test compound from the culture. Further 100µL media was added to the culture. 20µL of MTT (5mg/mL) solution in PBS was added. The culture was incubated at 37°C for 3hr for reaction. After the incubation, media with unbound MTT was aspirated out and two washes of 1XPBS were given to cells to remove traces of unbound MTT compound. After washes 100µL of DMSO was added to cells, to dissolve water insoluble compounds and a reading was taken at 570nm.

3.6 Successive solvent extraction

500gm of plant material was subjected to successive solvent extraction using petroleum ether, chloroform, ethyl acetate, n-butanol and water. After evaporation of solvents under vacuum the dried extracts obtained were labelled as pet. ether (A1),

chloroform (A2), ethyl acetate (A3), *n*-butanol (A4) and Water (A5) and were kept in refrigerator till required for further analyses.

3.7 Antioxidant activity of A1 to A5 extract

A1 to A5 extracts were subjected to antioxidant activity as per the method mentioned in 3.4

3.8 Brine shrimp lethality test of A1 to A5 extract

A1 to A5 extract was subjected to a brine shrimp lethality test as per the method mention in 3.5.2

3.9 Preliminary cytotoxicity assay of A1, A2 and A4

From the results of the brine shrimp assay A1, A2, and A4 were selected for further preliminary cytotoxicity on lung cancer cell lines (A549 and NCI-H23) by MTT assay as method mention in 3.5.2

3.10 Apoptosis Profile of mixture of A1 and A2

From the results of the MTT assay A1 and A2 was mixed in equal quantity and subjected to the below assays for detecting apoptosis profile on A549 and NCI-H23 cell line

MTT assay

Wound healing assay

Annexin V assay

Caspase 3/7 assay

Comet assay

3.10.1 MTT assay: as mention in 3.5.2

3.10.2 Scratch or wound healing assay¹⁶

Principle

The scratch or wound healing assay is the method of choice for studying cell migration due to the low cost and simplicity of its experimental design. A scratch assay involves growing a cell monolayer to confluence in a multiwell assay plate; creating a ‘wound’ a cell-free zone in the monolayer into which cells can migrate; and monitoring the recolonization of the scratched region to quantify cell migration. This experimental technique is commonly used to understand the molecular mechanisms that affect cell migration and to identify pharmaceutical compounds that can modulate cell migration and consequently drive treatment therapies

Protocol

Cells were cultured in 12 well plates and allowed to reach 80% confluency. Media was replaced with fresh media and the test compound (500µL of extract) was exposed and the time was noted as T0. The plate was again incubated in an incubator for a further 24hr. Seed your cells in multi-well plates and culture until confluent. We normally use 6 or 12 well plates, but a plate with a larger number of wells is possible. It is important that all the cultures are confluent at the start of the experiment. Using a pipette tip make a straight scratch, simulating a wound. Often we make a scratch by keeping the pipette tip under an angle of around 30 degrees to keep the scratch width limited. This allowed imaging of both wound edges using the 10x objective. Take images at 0hr and rest as per the experimental requirements.

3.10.3 Annexin V assay¹⁷

Principle

The Annexin V-PE Apoptosis Detection Kit is based on the observation that soon after initiating apoptosis, most cell types translocate the membrane phospholipid phosphatidylserine (PS) from the inner face of the plasma membrane to the cell surface. Once on the cell surface, PS can be easily detected by staining with a fluorescent conjugate of Annexin V, a protein that has a strong natural affinity for PS. The one-step staining procedure takes only 10min. In addition, the assay can be

directly performed on live cells, without the need for fixation. The Annexin V-PE Apoptosis detection kit contained the bright orange-red PE fluorescent probe that can be easily detected by flow cytometry or fluorescence microscopy.

Annexin V-PE assay protocol

- A. Incubation of cells with Annexin V-PE
 1. Apoptosis was induced by test samples
 2. Collect $1-5 \times 10^5$ cells by centrifugation.
 3. Resuspend cells in 500 μ L of 1X Binding Buffer.
 4. Add 5 μ L of Annexin V-PE.
 5. Incubate at room temperature for 5min in the dark.
- B. Quantification by Flow Cytometry
 - Analyze Annexin V-PE binding by flow cytometry (Ex = 488nm; Em = 578nm) using the phycoerythrin emission signal detector (usually FL2).
 - For analyzing adherent cells, gently trypsinize and wash cells once with serum containing media before incubation with Annexin V-PE (A 2-5).

3.10.4 Caspase 3/7 assay¹⁸

Principle

The Caspase-Glo® 3/7 Assay is a homogeneous, luminescent assay that measures caspase-3 and -7 activities. The assay provides a luminogenic caspase-3/7 substrate, which contains the tetrapeptide sequence DEVD, in a reagent optimized for caspase activity, luciferase activity, and cell lysis. Adding a single Caspase-Glo® 3/7 Reagent in an “add-mix-measure” format results in cell lysis, followed by caspase cleavage of the substrate and generation of a “glow-type” luminescent signal, produced by luciferase. Luminescence is proportional to the amount of caspase activity present. The Caspase-Glo® 3/7 Reagent relies on the properties of a proprietary thermostable luciferase (Ultra-Glo™ Recombinant Luciferase), which is formulated to generate a stable “glow-type” luminescent signal and improved performance across a wide range of assay conditions.

Reagent preparation and storage

Equilibrate the Caspase-Glo® 3/7 Buffer and lyophilized Caspase-Glo® 3/7 Substrate to room temperature before use.

Transfer the contents of the Caspase-Glo® 3/7 Buffer bottle into the amber bottle containing Caspase-Glo® 3/7 Substrate. Mix by swirling or inverting the contents until the substrate is thoroughly dissolved to form the Caspase-Glo® 3/7 Reagent.

The reconstituted Caspase-Glo® 3/7 Reagent may be stored at 4°C for up to 3 days with no loss of activity compared to that of freshly prepared reagent.

Prepare the following reactions to detect caspase-3 and -7 activities in cell culture.

- Blank reaction: Caspase-Glo® 3/7 Reagent, vehicle, and cell culture medium without cells
- Negative control: Caspase-Glo® 3/7 Reagent and vehicle-treated cells in medium
- Assays: Caspase-Glo® 3/7 Reagent and treated cells in medium

The blank reaction is used to measure background luminescence associated with the cell culture system and Caspase-Glo® 3/7 Reagent. Subtract the value for the blank reaction from experimental values. Negative control reactions are important for determining the basal caspase activity of the cell culture system.

Standard Protocol for Cells Cultured in a 96-Well Plate

- Remove 96-well plates containing treated cells from the incubator and allow plates to equilibrate to room temperature.
- Add 100µL of Caspase-Glo® 3/7 Reagent to each well of a white-walled 96-well plate containing 100µL of blank, negative control cells or treated cells in culture medium. Because of the sensitivity of this assay, be careful not to touch pipet tips to the wells containing samples to avoid cross-contamination. Cover the plate with a plate sealer or lid. (If you are reusing pipet tips, do not touch pipet tips to the wells containing samples to avoid cross contamination).

- Gently mix contents of wells using a plate shaker at 300–500rpm for 30sec. Incubate at room temperature for 30min to 3hr, depending upon the cell culture system. The optimal incubation period should be determined empirically.
- Temperature fluctuations will affect the luminescence reading. If the room temperature fluctuates, use a constant-temperature incubator.
- Measure the luminescence of each sample in a plate-reading luminometer.

3.10.5 Comet assay¹⁹

Principle

Cell Biolabs' OxiSelect™ 96-Well Comet Assay is a single cell gel electrophoresis assay (SCGE) for simple evaluation of cellular DNA damage. First, individual cells are mixed with molten agarose before application to the OxiSelect™ 96-Well Comet Slide. These embedded cells are then treated with a lysis buffer and alkaline solution, which relaxes and denatures the DNA. Finally, the samples are electrophoresed in a horizontal chamber to separate intact DNA from damaged fragments. Following electrophoresis, the samples are dried, stained with a DNA dye, and visualized by epifluorescence microscopy. Under these conditions, the damaged DNA (containing cleavage and strand breaks) will migrate further than intact DNA and produce a “comet tail” shape.

Reagent preparation

OxiSelect™ Comet Agarose: Heat the Comet Agarose bottle at 90-95°C in a water bath for 20min, or until agarose liquefies. Transfer the bottle to a 37°C water bath for 20min and maintain until needed.

Vista Green DNA Dye: Prepare a 1X Vista Green DNA Staining Solution by diluting the provided stock 1:10000 in TE Buffer (10 mM Tris, pH 7.5, 1 mM EDTA). The solution can be stored at 4°C for up to 3 weeks, protected from light.

Lysis Buffer: To prepare 100 mL of 1X Lysis Buffer

NaCl 14.6gm

EDTA Solution (provided) 20mL

10X Lysis Solution (provided) 10mL

DMSO 10mL (optional for heme containing samples)

DI H₂O Adjust volume to 90mL

Mix thoroughly to dissolve NaCl. Slowly adjust the Lysis Buffer to pH 10.0 with 10 NNaOH, then QS to 100 mL with DI H₂O. Chill Lysis Buffer to 4°C before use.

(Note: Buffer will appear cloudy at room temperature, but will clear at 4°C. pH will also remain ~10.0.)

Electrophoresis Running Solution: To prepare 1L of Electrophoresis Solution (Alkaline Electrophoresis Solution 300mM NaOH, pH >13, 1mM EDTA)

NaOH 12gm

EDTA Solution (provided) 2mL

DI H₂O Adjust volume to 1L

Mix thoroughly to dissolve NaOH. Chill Alkaline Running Solution to 4°C before use.

(To avoid ultraviolet light damage to cell samples, perform the assay under low/dim light conditions.)

Preparation of samples and slides

1. Prepare Lysis Buffer, Alkaline Solution, and Electrophoresis Running Solution (see Preparation of Reagents) prior to performing the assay. Chill all solutions to 4°C thoroughly.
2. Heat OxiSelect™ Comet Agarose to 90-95°C in a water bath for 20min, or until agarose liquefies. Cool the agarose by transferring the bottle to a 37°C water bath for 20min.
3. Add 20µL of Comet Agarose per well onto the OxiSelect™ 96-Well Comet Slide to create a Base Layer. Ensure complete well coverage by spreading the solution over the well with the pipette tip. Maintaining the slide horizontally, transfer the slide to 4°C for 15min.
4. Prepare cell samples, including controls, as follows:
 - Suspension Cells: Centrifuge cells at 700 x g for 2min and discard supernatant. Wash cell pellet once with ice-cold PBS (without Mg²⁺ and Ca²⁺), centrifuge, and discard the supernatant. Finally, resuspend the cells at 1 x 10⁵ cells/mL in ice-cold PBS (without Mg²⁺ and Ca²⁺).
 - Adherent Cells: Gently remove cells from flask/dish by scraping with a rubber policeman. Transfer cell suspension to a conical tube and centrifuge at 700 x g for 2min, discarding the supernatant. Wash cell pellet once with ice-cold PBS (without Mg²⁺ and Ca²⁺), centrifuge,

and discard the supernatant. Finally, resuspend the cells at 1×10^5 cells/mL in ice-cold PBS (without Mg^{2+} and Ca^{2+}).

- Test sample preparation: 10mg of test extract in 1-2mL of ice cold PBS containing 20mM EDTA (without Mg^{2+} and Ca^{2+}). Allow the tissue/cell suspension to stand for 5min before transferring the supernatant to a centrifuge tube; avoid transferring debris. Centrifuge, discarding the supernatant, and then resuspend the cells at 1×10^5 cells/mL in ice-cold PBS (without Mg^{2+} and Ca^{2+}).

5. Combine cell samples with Comet Agarose (step 2) at 1:10 ratio (v/v). Mix well by pipetting, and immediately transfer 20 μ L/well onto the top of the Comet Agarose Base Layer using a multichannel micropipette. If necessary, ensure complete well coverage by spreading the suspension very gently and carefully with the pipette tip, without disturbing the Base Layer.

Note: For multiple samples, maintain suspensions at 37°C to avoid gelation. Titrate samples again just prior to slide addition.

6. Maintaining the slide horizontally, transfer the slide to 4°C in the dark for 15min.

7. Carefully, transfer the slide to a small basin/container containing pre-chilled Lysis Buffer (~50-100 mL/slide). Immerse the slide in the buffer for 30-60min at 4°C in the dark.

8. Carefully, aspirate the Lysis Buffer from the container and replace with pre-chilled Alkaline Solution (~50-100mL/slide). Immerse the slide in the solution for 30min at 4°C in the dark.

Assay Protocol

Alkaline Electrophoresis

1. Maintaining the slide horizontally, carefully transfer the slide from the Alkaline Solution to a horizontal electrophoresis chamber. Fill the chamber with cold Alkaline Electrophoresis Solution until the buffer level covers the slide.

2. Apply voltage to the chamber for 15-30min at 1volt/cm (e.g. if the chamber electrodes are 35cm apart, you would then apply 35volts to the slide). Additionally, adjust the volume of Alkaline Electrophoresis Solution to produce a current setting of 300mA.

3. Maintaining the slide horizontally carefully transfer the slide from the electrophoresis chamber to a clean, small basin/container containing pre-chilled DI

H₂O (~50-100mL/slide). Immerse the slide for 2min, aspirate, and then repeat twice more.

4. Aspirate the final water rinse and replace with cold 70% Ethanol for 5min.
5. Maintaining the slide horizontally, remove the slide from the 70% Ethanol and allow to air dry.
6. Once the agarose and slide is completely dry, add 50 μ L/well of diluted Vista Green DNA Dye (see Preparation of Reagents). Incubate at room temperature for 15min.
7. View slides by epifluorescence microscopy using a FITC filter.

3.11 Preparation of Fractions

A cylinder-shaped glass column holding a stationary phase (silica gel) is slowly approached from the top by a liquid solvent (mobile phase) that flows down the column with the assistance of gravity or external pressure. Purification of compounds from a mixture is accomplished using this method. The sample is loaded into the top of the column once the column is ready. After that, the mobile solvent is allowed to flow down the column. Because the compounds in the mixture interact differently with the stationary phase (silica gel) and the mobile phase, they will flow along the mobile phase according to their polarity. The separation of compounds from the mixture is accomplished in this manner, which is then studied further for structure elucidation.²⁰

Here A1+A2 were tried for further isolation process but was not able to isolate a compound from the mixture. Various fractions were prepared by column chromatography of the A1 extract. A1 (0.500gm) was subjected to silica gel column chromatography for the isolation of phytoconstituents. The column was packed with silica gel (60-120#) as the stationary phase, the extract was loaded on the column, and gradient elution was performed using n-hexane: ethyl acetate. A total of 141 fractions, each of 10mL were collected and simultaneously studied on TLC. Fractions with similar patterns on TLC were pooled, concentrated, and then allowed to evaporate to dryness. Fractions collected as below PF1: 43-45, PF2: 53-70, PF3: 74-84, PF4: 85-102, PF5: 113-123, PF6: 124-141. (Fig 3.1)

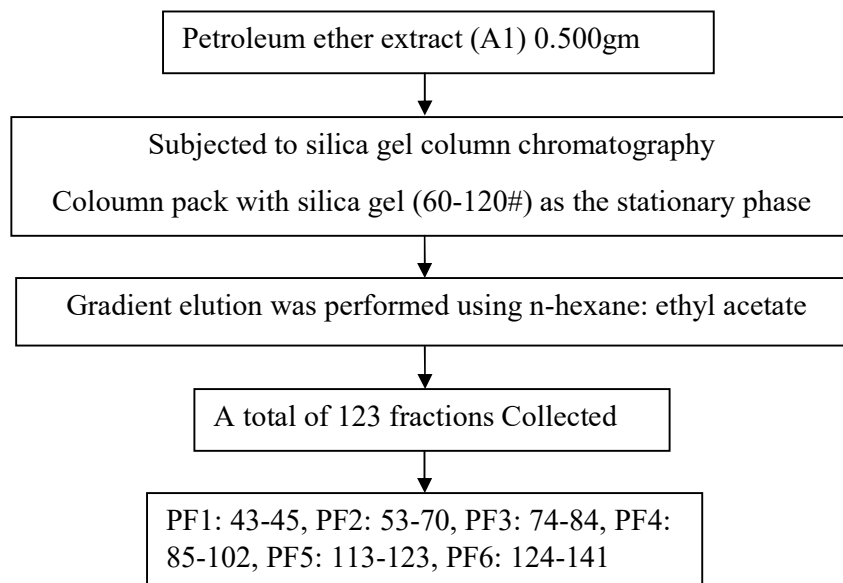


Fig.3.1 Flow chart of preparation of Fractions

Column condition:

Column length: 52cm

Column diameter: 1.8cm (inner), 2.3cm (outer)

Stationary phase: Silica gel 60-120#

Mobile phase: n-Hexane: Ethyl acetate

Type of elution: Gradient

Number of fractions collected: 123 (10 each mL)

3.12 Apoptosis profile and Isolation compound from active fractions

Fractions PF1 to PF6 & Lupeol were studied for Preliminary cytotoxicity assay and apoptosis profile on both the cell line A549 and NCI-H23 cell line. The apoptosis profile includes wound healing assay, Annexin V assay, Caspase 3/7 assay, and Comet assay. The method was used the same as 3.5.2 for MTT assay 3.10.2, 3.10.3, 3.10.4, and 3.10.5 for wound healing assay, annexin V assay, caspase 3/7 assay, and comet assay respectively. Active fractions from the Apoptosis profile study were subjected to purification. PF5, PF6, and Lupeol were found most active from all the samples. Then PF5 and PF6 were subjected to TLC and it showed minor impurities on the TLC plate separately. After repeated wash of PF5 fraction with solvents and recrystallization with methanol it showed single spot-on TLC. PF6 showed a single spot-on TLC plate after repeated washing with hexane. The primary schematic

diagram of the apoptosis profile and isolation of compounds are described in Figure 3.2. Both the compounds were subjected to TLC for identification and IR, mass, and NMR for characterization.

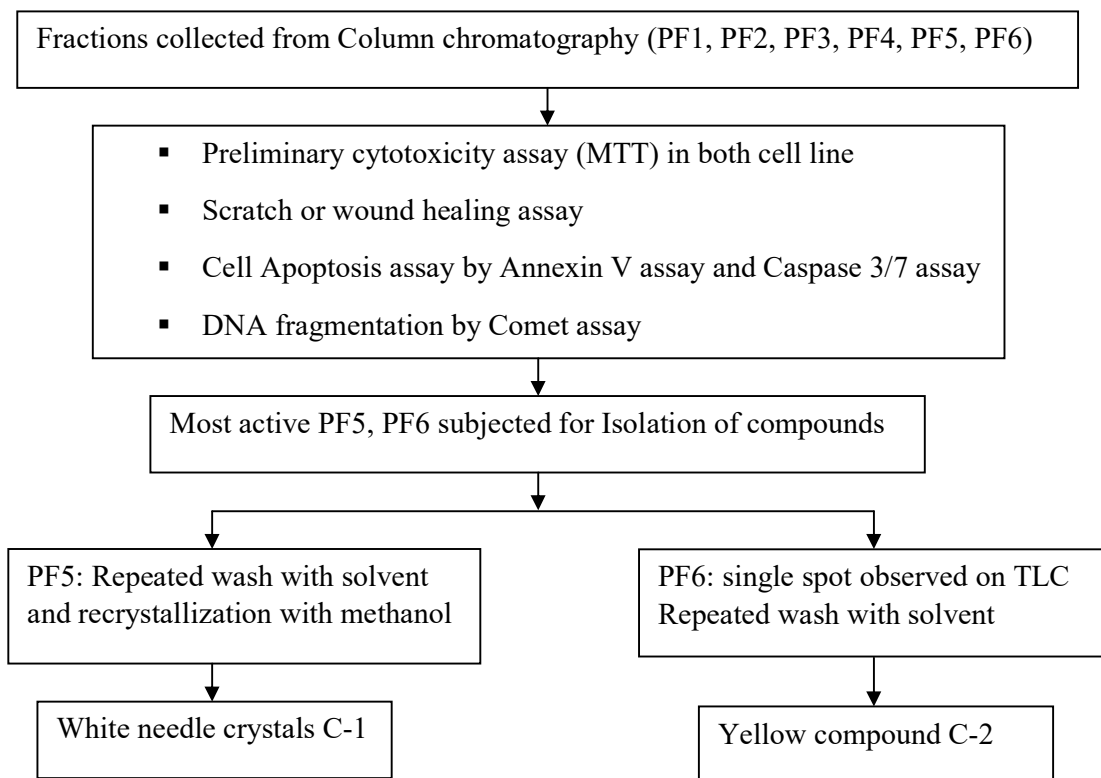


Figure 3.2 Scheme for Apoptosis profile and Isolation of compounds from active fractions

3.13 Identification and characterization of compounds

Identification of C-1

Test solution : Fraction PF5
 Stationary phase : Silica gel G60 F₂₅₄
 Mobile phase : Toluene : methanol (9.6:0.4)
 Visualization : Under UV light at 254nm
 Spraying reagent : Anisaldehyde sulphuric acid

Identification of C-2

Test solution : Fraction PF6
 Stationary phase : Silica gel G60 F₂₅₄
 Mobile phase : n-Hexane : ethyl acetate : methanol (9.8:0.2:0.1)

Visualization : Under UV light at 366nm (Yellow-orange fluorescence)

Spraying reagent : 10% Methanolic KOH

Infrared spectroscopy²¹: IR spectroscopy is useful in the identification of functional groups present in a compound. This technique is based on the absorption of electromagnetic radiation at wavelength ranging between 4000 and 400 cm^{-1} . At this range of wavelength, specific functional groups give characteristic vibration, bending and stretching vibrations at characteristic wavelengths. This is recorded in a spectrum by the IR instrument and gives basic information on the structure.

NMR spectroscopy²²: Nuclear magnetic resonance (NMR) spectroscopy is the study of compounds by measuring the interaction of radiofrequency electromagnetic radiations with the nuclei of molecules placed in a strong magnetic field. Transmission of energy is possible from base energy to higher energy levels when an external magnetic field is applied and at a wavelength that coincides with the radio frequency. The energy is emitted at the same frequency when the spin comes back to its base level. Therefore, by measuring the signal which matches this transfer the processing of the NMR spectrum for the concerned nucleus is yield. Protons in the molecule will behave differently depending on the surrounding chemical environment, making it possible to elucidate their structure.

Mass spectroscopy²³: A chemical is ionized at high energy at a certain voltage in mass spectroscopy. In a magnetic or electric field, the resulting ions are sorted based on their mass to charge ratio (m/z). A plot of the measured m/z ratios against their relative abundance is recorded in the spectra of the separated ions. The parent compound's molecular weight and fragmentation patterns are revealed by analyzing the mass spectrum. The fragmentation patterns are combined to form the compound's molecular skeleton.

3.14 HPTLC method development for quantification of C-2

3.14.1 Preparation of standard stock Solution of C-2

Compound-2 (2mg) was weighed accurately and transferred into 5mL vial and dissolved using dichloromethane and make up volume up to 4mL (S1=0.5mg/mL of Compound-I)

3.14.2 Preparation of Test solution

20mg of fraction PF-6 was dissolved in 1.5mL dichloromethane (T1=13.33mg/mL)

3.14.3 Chromatography

HPTLC has been performed on 10cm × 10cm precoated silica gel 60 F254 plates (E. Merck, Darmstadt, Germany). The plates were prewashed with methanol and activated at 60°C for 5min. The samples were applied to the plates as bands 6mm wide and 10mm apart using a CAMAG Linomat V applicator (CAMAG, Muttenz, Switzerland) fitted with a 100µL syringe (CAMAG, Muttenz, Switzerland). The plate was developed using *n*-hexane: ethyl acetate: methanol (9.8:0.2:0.1v/v/v) as the mobile phase. After drying, the plates were derivatized using 10% methanolic KOH followed by heating at 105°C for 10min and scanned in a CAMAG TLC Scanner using win- CATS software at 254nm with slit dimensions 4 × 0.1mm. The scanning speed was 20mm s⁻¹, and the source of radiation was a tungsten lamp.

3.14.4 Calibration curve of C-2

The graded concentration of standard solutions (0.5mg/mL) in 0.6, 1.0, 1.4, 1.8, and 2.2µL volumes were applied on a plate. The concentration of C-2 was 300, 500, 700, 900, and 1100ng/band. The plate was developed in mobile phase *n*-hexane: ethyl acetate: methanol (9.8:0.2:0.1v/v/v) and scanned at 254nm. Data on the peak area of each C-2 was recorded. The calibration curve was obtained by plotting the curve area vs. concentration of each peak corresponding to the respective band.

3.14.5 Estimation of C-2 in sample of *O.bracteatum*

2µL of test solution was spotted along with a working standard solution of 0.6, 1.0, 1.4, 1.8, and 2.2µL on a plate. The plate was developed in mobile phase *n*-hexane: ethyl acetate: methanol (9.8:0.2:0.1v/v/v) and scanned at 254nm. The peak areas were noted, and quantification was performed using linear regression equations.

3.15 HRLC-MS study of A1+A2 and PF1 to PF6

After lots of trials, we are able to isolate 2 compounds only, so for more phytochemical profiling mixture of A1 and A2 & all the fractions PF1 to PF6 were subjected to HRLC-MS.

phytochemical profile of the A1+A2 and Fractions PF1 to PF6 were analyzed using a Q-Exactive Plus Biopharma, High Resolution Orbitrap Thermo Scientific. The data Acquisition Software used was Thermo Scientific Xcalibur, Version 4.2.28.14 and Data Processing Software was Compound Discoverer 2.1 SP1. The column used for the study was Hypersil Gold C18 (100 x 2.1MM 3µ) (Thermo Scientific), with mobile phase A: 0.1% formic acid in the water, Solvent B: Methanol.

Compounds were identified via their mass spectra and their unique mass fragmentation patterns. Compound Discoverer 2.1, ChemSpider, and PubChem were used as the main tools for the identification of the phytochemical constituents.

3.16 Separation and Identification and estimation of compounds from A1 extract

A1 extract was subjected to triphasic system, three phases was separated in which upper phase is followed by wax removal process by adding excess of acetonitrile. Chloroform soluble fraction is subjected TLC with toluene: methanol (9.6:0.4, v/v) as mobile phase. (Fig 3.3)

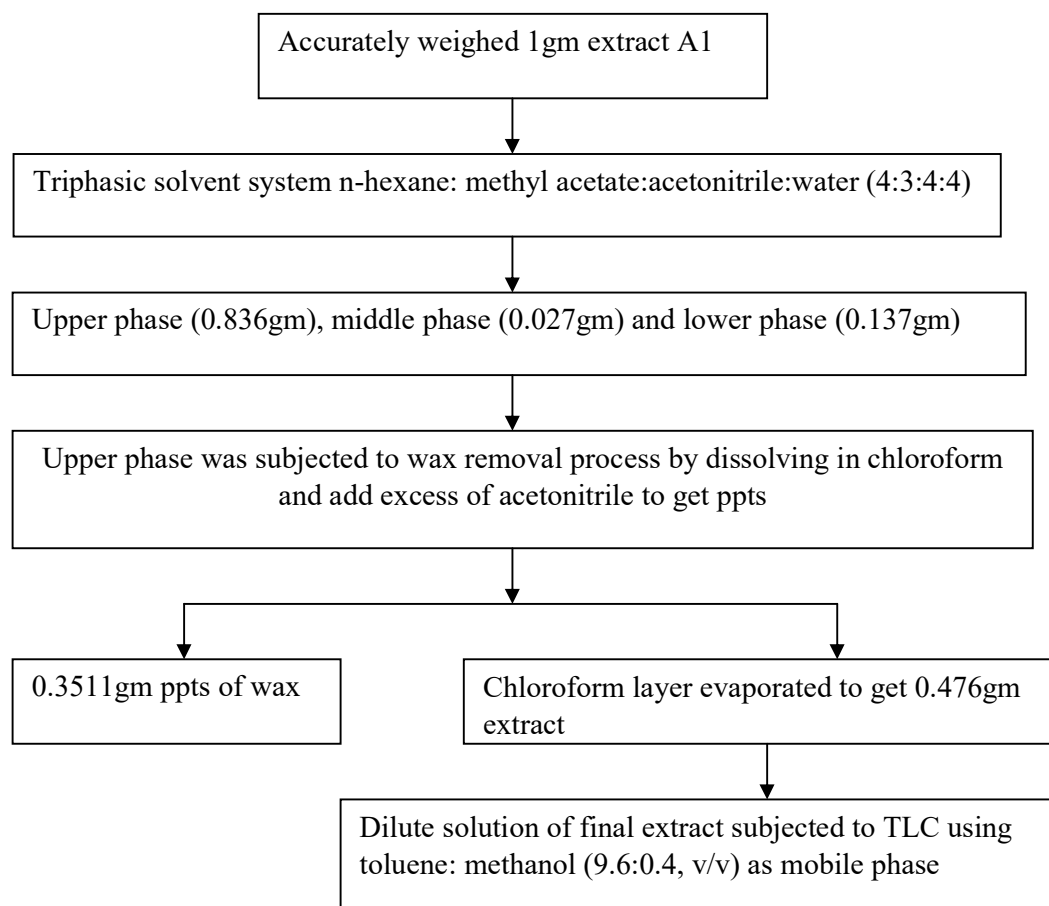


Figure 3.3 Scheme for separation of compounds on TLC from A1 extract

3.16.1 Identification of compounds by co-TLC

Test solution	Chloroform extract
Reference solution 1	β -sitosterol
Reference solution 2	Lupeol
Stationary phase	Silica gel G60 F254
Mobile phase	Toluene: methanol (9.6:0.4 v/v)
Visualization	Spraying with Anisaldehyde sulphuric acid

3.16.2 Estimation of β -sitosterol and lupeol in *Onosma bracteatum* by HPTLC method

3.16.2.1 Preparation of test sample

10mg of extract obtained in the above method was dissolved in 10mL methanol to get a concentration of 1mg/mL.

3.16.2.2 Preparation of reference sample

Stock solutions of β -sitosterol (1mg/mL), and Lupeol (1mg/mL) were separately prepared by dissolving the standards in methanol.

3.16.2.3 Instruments

CAMAG Linomat V applicator (CAMAG, Muttenz, Switzerland)

Hamilton 100 μ L HPTLC syringe

Camag twin trough chambers (20X10cm)

CAMAG TLC Scanner 4 with visionCATS software, version 2.5.18262.1

3.16.2.4 Material

Stationary phase : Methanol washed precoated silica gel 60 F 254 plates (E. Merck, Darmstadt, Germany). 10X10

Reagents used : Distilled toluene and methanol

Reference standard : β -sitosterol and lupeol

Test samples: Fraction of extract A1

3.16.2.5 Chromatographic condition

Mobile phase: Toluene: methanol (9.6:0.4)

Spotting volume: 1, 3, 5, 7 and 9 μ L

Amount/band: 1000 to 9000ng (for calibration curve)

Separation technique: ascending

Chamber saturation time: 30min

Migration distance: 8cm

Derivatisation with anisaldehyde sulphuric acid

3.16.2.6 Spotting parameter

Start position: 14mm from bottom edge

Band width: 6mm

Space between two bands: 12mm

Application speed: 150nLs⁻¹

3.16.2.7 Densitometric scanning

Mode: UV light

Wavelength: 525nm

Lamp used: tungsten lamp

Slit dimension: 5X0.45

Detection : Purple violet coloured spot

3.16.2.8 Calibration curve of β -sitosterol and lupeol

Graded concentrations of standard solution (1mg/mL) of β -sitosterol and lupeol in 1, 3, 5, 7 and 9 μ L volume were applied on a pre-coated TLC silica gel 60 F254 plate (E. Merck) using CAMAG Linomat V applicator. The plate was developed in a mobile phase Toluene: Methanol (9.6:0.4) and scanned at 525nm. Data of peak area of each

standard spot was recorded. The calibration curve was obtained by plotting area vs. concentration of each peak corresponding to the respective spot.

3.16.2.9 Quantification of β -sitosterol and lupeol

Test solution of 10 μ L of 1mg/mL was spotted along with 1, 3, 5, 7 and 9 μ L of standard β -sitosterol and lupeol solution on the HPTLC plate. The peak areas were noted and quantification of β -sitosterol and lupeol were performed using linear regression equations of the respective compounds.

3.16.2.10 Validation of HPTLC method²⁴

Linearity: The capacity of an analytical method to elicit test results that are directly or mathematically proportionate to the concentration of analyte in a sample throughout a specific range is known as linearity. Linearity is measured by the linear regression analysis' correlation coefficient. The interval between the upper and lower level of analyte measured with precision and accuracy using the method is known as the analytical method's range.

The linear response was determined by analyzing the calibration curve of β -sitosterol and lupeol in the concentration range **1000-9000ng/spot** of linear regression analysis.

Precision: The degree of reproducibility or repeatability of an analytical method is measured by precision. The standard deviation (SD) or relative standard deviation (RSD) is used to express it (RSD). It indicates a random error, with the findings reported as RSD or co-efficient of variation.

Repeatability (Precision or Replication): It is the precision involved in analyzing the same sample under the same condition, same analyte, same apparatus, a short interval of time and identical reagents.

Repeatability of measurement of peak area: (RSD<1%, n=7)

The 5 μ L of working standard solution of β -sitosterol and Lupeol were applied on pre-coated TLC plate. The plate was developed, dried, derivatized and analyzed as described previously. The peak area and height of spot was measured 7 times without changing the position of plate. %RSD was calculated.

Repeatability of measurement of peak area was measured by seven times measurement of the same spot without changing plate's position (RSD < 1 %).

Repeatability of sample application: (RSD< 2%, n=7)

The 5 μ L working standard solution of β -sitosterol and Lupeol were applied on a pre-coated TLC plate seven times. The plate was developed, dried, derivatized, and analyzed. The areas of seven spots were measured and % RSD was calculated.

Reproducibility: Variations of a result within the same day and amongst days are called reproducibility. It includes the following parameters.

Intra-Day Reproducibility (n=3): A variation in results within the same day is called intraday variation. It was determined by repeating the calibration curve 3 times on the same day at 3 different concentrations.

Inter-Day Reproducibility (n=3): A variation in results across days is called interday variation. It was determined by repeating the calibration curve daily for 3 different days at 3 different concentrations.

Limit of detection (LOD): Under specified conditions, it is the lowest concentration of analyte in a sample that can be identified but not necessarily quantified. LOD proves that the concentration of an analyte is above or below a specific threshold. The regression analysis feature in Excel is used to determine this.

Limit of quantification (LOQ): It refers to an analytical method's ability to detect analyte quantitatively in the presence of other substances. A signal to noise ratio of 10:1 defines it. Different amounts of standards were employed, and the minimum quantifiable limit for acceptable precision and accuracy was identified. The regression analysis feature in Excel is used to determine this.

Accuracy: The accuracy of an analytical method is the degree to which the actual (true) value and the analytical value agree; it is determined by repeating the test process. It is calculated by calculating standard recovery by addition at three different standard concentration levels.

Specificity: The capacity of an analytical method to measure the analyte properly in the presence of other components in the sample, such as synthetic precursors, excipients, degradants, or matrix components, is known as specificity. The purity of spectra was measured at three levels: beginning, middle, and end. The correlation between them was taken into account when determining peak purity. It was determined by spotting a working standard solution on a pre-coated TLC plate, developing, drying, and analyzing the plate.

Robustness: Robustness is a measure of a technique's ability to remain unaffected by modest but deliberate changes in the method conditions, and it is an indicator of the method's reliability.

Ruggedness: It is a measure of the reproducibility of test results under normal, expected operating conditions from instrument to instrument and from analyst to analyst.

3.17 Separation and Identification and estimation of compounds from TME extract

10 gm of powdered whole plant were extracted continuously by methanol using soxhlet and the extract obtained (1.8%w/w) was hydrolyzed with 2N HCL under reflux condition for 3-4hr and partitioned with toluene (3×25mL) first to yield 0.86gm extract, then partition with ethyl acetate (3×25mL) to yield 0.15gm extract.

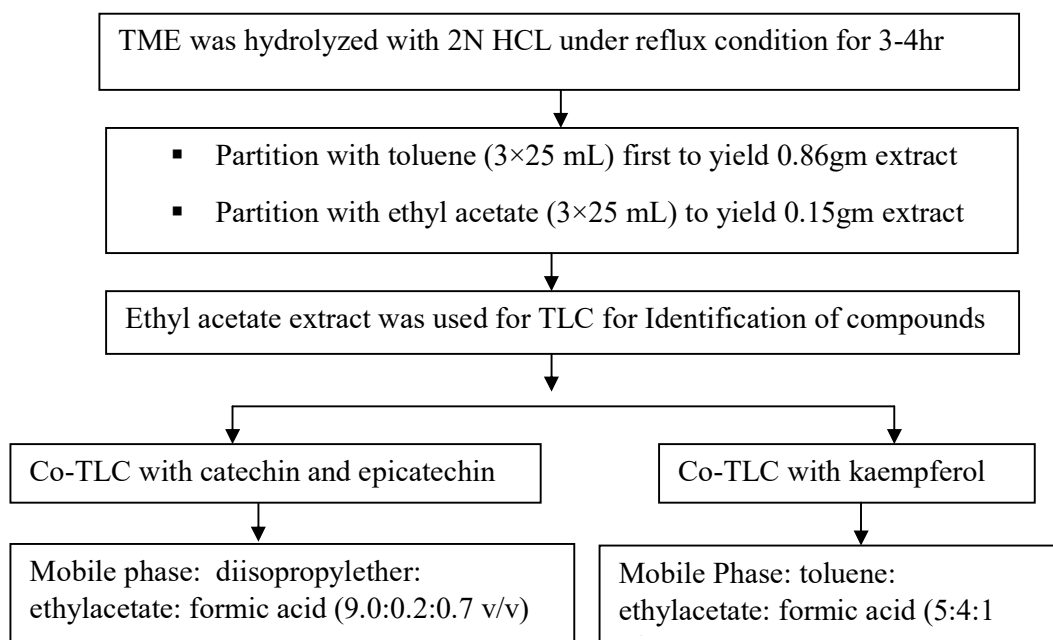


Figure 3.4 Scheme for separation of compounds on TLC from TME

This ethyl acetate extract was used for spotting for identification of catechin and epicatechin using diisopropylether: ethylacetate: formic acid (9.0:0.2:0.7v/v) as mobile phase and Kaempferol using toluene:ethylacetate: formic acid (5:4:1 v/v) as mobile phase (Fig.3.4)

3.17.1 Identification of compounds by co-TLC

Test solution Ethyl acetate extract

Reference solution 1 Catechin

Reference solution 2	Epicatechin
Stationary phase	Silica gel G60 F254
Mobile phase	diisopropylether: ethylacetate:formic acid (9.0:0.2:0.7 v/v)
Visualization	280nm

3.17.2 Identification of compounds by co-TLC

Test solution	Ethyl acetate extract
Reference solution	Kaempferol
Stationary phase	Silica gel G60 F254
Mobile phase	toluene: ethylacetate: formic acid (5:4:1 v/v)
Visualization	254nm

Spots of catechin, epicatechin and kaempferol identified in test sample were scraped from TLC plate and were used for further identification by mass spectra.

3.17.3 Estimation of catechin and epicatechin in *Onosma bracteatum* by HPTLC method

3.17.3.1 Preparation of test sample

5mg of ethyl acetate extract obtained from TME dissolved in 1mL methanol to get a concentration 5mg/mL.

3.17.3.2 Preparation of reference sample

Stock solutions of catechin (1mg/mL) and epicatechin (1mg/mL) were separately prepared by dissolving the standards in methanol.

3.17.3.3 Instruments

CAMAG Linomat V applicator (CAMAG, Muttenz, Switzerland)

Hamilton 100 μ L HPTLC syringe

Camag twin trough chambers (20X10cm)

CAMAG TLC Scanner 4 with visionCATS software, version 2.5.18262.1

3.17.3.4 Material

Stationary phase : Methanol washed precoated silica gel 60 F 254 plates (E. Merck, Darmstadt, Germany). 20X10

Reagents used : diisopropyl ether, ethyl acetate, formic acid

Reference standard : catechin and epicatechin

Test samples : fraction of TME

3.17.3.5 Chromatographic condition

Mobile phase: diisopropylether: ethylacetate: formic acid(9.0:0.2:0.7 v/v)

Spotting volume: 1, 2, 3, 4 and 5 μ L

Amount/band : 1000 to 5000ng (for calibration curve)

Separation technique: ascending

Chamber saturation time: 30min

Migration distance : 9cm

3.17.3.6 Spotting parameter

Start position: 14mm from bottom edge

Band width: 6mm

Space between two bands: 12mm

Application speed: 150nLs⁻¹

3.17.3.7 Densitometric scanning

Mode: UV light

Wavelength : 280nm

Lamp used: deuterium lamp

Slit dimension: 5X0.45

3.17.3.8 Calibration curve of catechin and epicatechin

Graded concentrations of standard solution (1mg/mL) of catechin and epicatechin in 1, 2, 3, 4 and 5 μ L volume were applied on a pre-coated TLC silica gel 60 F254 plate (E. Merck) using CAMAG Linomat V applicator. The plate was developed in a mobile phase diisopropylether:ethylacetate:formic acid (9.0:0.2:0.7 v/v) and scanned at 280nm. Data of peak area of each standard spot was recorded. The calibration curve was obtained by plotting area vs. concentration of each peak corresponding to the respective spot.

3.17.3.9 Quantification of catechin and epicatechin

A test solution of 10 μ L of 5mg/mL was spotted along with 1, 2, 3, 4, and 5 μ L of standard catechin and epicatechin solution on the HPTLC plate. The peak areas were noted and quantification of catechin and epicatechin were performed using linear regression equations of the respective compounds.

3.17.3.10 Validation of HPTLC method²⁴

Linearity: The capacity of an analytical method to elicit test results that are directly or mathematically proportionate to the concentration of analyte in a sample throughout a specific range is known as linearity. Linearity is measured by the linear regression analysis' correlation coefficient. The interval between the upper and lower level of analyte measured with precision and accuracy using the method is known as the analytical method's range.

The linear response was determined by analyzing the calibration curve of catechin and epicatechin in the concentration range of **1000-5000ng/spot** of linear regression analysis.

Precision: The degree of reproducibility or repeatability of an analytical method is measured by precision. The standard deviation (SD) or relative standard deviation (RSD) is used to express it (RSD). It indicates a random error, with the findings reported as RSD or co-efficient of variation.

Repeatability (Precision or Replication): It is the precision involved in analyzing the same sample under the same condition, same analyte, same apparatus, a short interval of time and identical reagents.

Repeatability of measurement of peak area: (RSD<1%, n=7)

The 3 μ L of working standard solution of catechin and epicatechin were applied on pre-coated TLC plate. The plate was developed, dried, derivatized and analyzed as

described previously. The peak area and height of spot was measured 7 times without changing the position of plate. %RSD was calculated.

Repeatability of measurement of peak area was measured by seven times measurement of the same spot without changing plate's position (RSD < 1 %).

Repeatability of sample application: (RSD < 2%, n=7)

The 3 μ L of working standard solution of catechin and epicatechin was applied on a pre-coated TLC plate seven times. The plate was developed, dried, derivatized and analyzed. The areas of seven spots were measured and % RSD was calculated.

Reproducibility: Variations of the result within the same day and amongst days are called reproducibility. It includes the following parameters.

Intra-Day Reproducibility (n=3): A variation in results within the same day is called intraday variation. It was determined by repeating the calibration curve 3 times on the same day at 3 different concentrations.

Inter-Day Reproducibility (n=3): A variation in results across days is called interday variation. It was determined by repeating the calibration curve daily for 3 different days at 3 different concentrations.

Limit of detection (LOD): Under specified conditions, it is the lowest concentration of analyte in a sample that can be identified but not necessarily quantified. LOD proves that the concentration of an analyte is above or below a specific threshold. The regression analysis feature in Excel is used to determine this.

Limit of quantification (LOQ): It refers to an analytical method's ability to detect analyte quantitatively in the presence of other substances. A signal to noise ratio of 10:1 defines it. Different amounts of standards were employed, and the minimum quantifiable limit for acceptable precision and accuracy was identified. The regression analysis feature in Excel is used to determine this.

Accuracy: The accuracy of an analytical method is the degree to which the actual (true) value and the analytical value agree; it is determined by repeating the test process. It is calculated by calculating standard recovery by addition at three different standard concentration levels.

Specificity: The capacity of an analytical method to measure the analyte properly in the presence of other components in the sample, such as synthetic precursors, excipients, degradants, or matrix components, is known as specificity. The purity of spectra was measured at three levels: beginning, middle, and end. The correlation between them was taken into account when determining peak purity. It was

determined by spotting a working standard solution on a pre-coated TLC plate, developing, drying, and analyzing the plate.

Robustness: Robustness is a measure of a technique's ability to remain unaffected by modest but deliberate changes in the method conditions, and it is an indicator of the method's reliability.

Ruggedness: It is a measure of the reproducibility of test results under normal, expected operating conditions from instrument to instrument and from analyst to analyst.

3.17.4 Estimation of kaempferol in *Onosma bracteatum* by HPTLC method

3.17.4.1 Preparation of test sample

5mg of ethyl acetate extract obtained from TME dissolved in 1mL methanol to get a concentration of 5mg/mL.

3.17.4.2 Preparation of reference sample

A stock solution of Kaempferol (1mg/mL) was prepared by dissolving the standards in methanol.

3.17.4.3 Instruments

CAMAG Linomat V applicator (CAMAG, Muttenz, Switzerland)

Hamilton 100 μ L HPTLC syringe

Camag twin trough chambers (10X10cm)

CAMAG TLC Scanner 4 with visionCATS software, version 2.5.18262.1

3.17.4.4 Material

Stationary phase : Methanol washed precoated silica gel 60 F 254 plates (E. Merck, Darmstadt, Germany). 10X10

Reagents used : toluene, ethyl acetate, formic acid

Reference standard : kaempferol

Test samples : fraction of TME

3.17.4.5 Chromatographic condition

Mobile phase: toluene:ethylacetate:formic acid (5:4:1 v/v)

Spotting volume: 0.5, 1, 1.5, 2 and 2.5 μ L

Amount/band : 500 to 2500ng (for calibration curve)

Separation technique: ascending

Chamber saturation time: 30min

Migration distance : 8cm

3.17.4.6 Spotting parameter

Start position: 14mm from bottom edge

Band width: 6mm

Space between two bands: 12mm

Application speed: 150nLs⁻¹

3.17.4.7 Densitometric scanning

Mode: UV light

Wavelength : 254nm

Lamp used: deuterium lamp

Slit dimension: 5X0.45

3.17.4.8 Calibration curve of kaempferol

Graded concentrations of standard solution (1mg/mL) of kaempferol in 0.5, 1, 1.5, 2, and 2.5 μ L volumes were applied on a pre-coated TLC silica gel 60 F254 plate (E. Merck) using CAMAG Linomat V applicator. The plate was developed in a mobile phase toluene: ethylacetate: formic acid (5:4:1 v/v) and scanned at 254nm. Data on the peak area of each standard spot was recorded. The calibration curve was obtained by plotting the area vs. concentration of each peak corresponding to the respective spot.

3.17.4.9 Quantification of kaempferol

A test solution of 10 μ L of 5mg/mL was spotted along with 0.5, 1, 1.5, 2, and 2.5 μ L of standard kaempferol solution on the HPTLC plate. The peak areas were noted and quantification of kaempferol was performed using linear regression equations of the respective compounds.

3.17.4.10 Validation of HPTLC method²⁴

Linearity: The capacity of an analytical method to elicit test results that are directly or mathematically proportionate to the concentration of analyte in a sample throughout a specific range is known as linearity. Linearity is measured by the linear regression analysis correlation coefficient. The interval between the upper and lower level of analyte measured with precision and accuracy using the method is known as the analytical methods range.

The linear response was determined by analyzing the calibration curve of kaempferol in the concentration range **500-2500ng/spot** of linear regression analysis.

Precision: The degree of reproducibility or repeatability of an analytical method is measured by precision. The standard deviation (SD) or relative standard deviation (RSD) is used to express it (RSD). It indicates a random error, with the findings reported as RSD or co-efficient of variation.

Repeatability (Precision or Replication): It is the precision involved in analyzing the same sample under the same condition, same analyte, same apparatus, a short interval of time and identical reagents.

Repeatability of measurement of peak area: (RSD<1%, n=7)

The 1.5 μ L of working standard solution of kaempferol was applied on a pre-coated TLC plate. The plate was developed, dried, and analyzed as described previously. The peak area and height of the spot were measured 7 times without changing the position of the plate. %RSD was calculated.

Repeatability of measurement of peak area was measured by seven times measurement of the same spot without changing the plate's position (RSD < 1 %).

Repeatability of sample application: (RSD< 2%, n=7)

The 1.5 μ L of working standard solution of kaempferol was applied on a pre-coated TLC plate seven times. The plate was developed, dried, and analyzed. The areas of seven spots were measured and % RSD was calculated.

Reproducibility: Variations of the result within the same day and amongst days are called reproducibility. It includes the following parameters.

Intra-Day Reproducibility (n=3): A variation in results within the same day is called intraday variation. It was determined by repeating the calibration curve 3 times on the same day at 3 different concentrations.

Inter-Day Reproducibility (n=3): A variation in results across days is called interday variation. It was determined by repeating the calibration curve daily for 3 different days at 3 different concentrations.

Limit of detection (LOD): Under specified conditions, it is the lowest concentration of analyte in a sample that can be identified but not necessarily quantified. LOD proves that the concentration of an analyte is above or below a specific threshold. The regression analysis feature in Excel is used to determine this.

Limit of quantification (LOQ): It refers to an analytical method's ability to detect analyte quantitatively in the presence of other substances. A signal to noise ratio of 10:1 defines it. Different amounts of standards were employed, and the minimum quantifiable limit for acceptable precision and accuracy was identified. The regression analysis feature in Excel is used to determine this.

Accuracy: The accuracy of an analytical method is the degree to which the actual (true) value and the analytical value agree; it is determined by repeating the test process. It is calculated by calculating standard recovery by addition at three different standard concentration levels.

Specificity: The capacity of an analytical method to measure the analyte properly in the presence of other components in the sample, such as synthetic precursors, excipients, degradants, or matrix components, is known as specificity. The purity of spectra was measured at three levels: beginning, middle, and end. The correlation between them was taken into account when determining peak purity. It was determined by spotting a working standard solution on a pre-coated TLC plate, developing, drying, and analyzing the plate.

Robustness: Robustness is a measure of a technique's ability to remain unaffected by modest but deliberate changes in the method conditions, and it is an indicator of the method's reliability.

Ruggedness: It is a measure of the reproducibility of test results under normal, expected operating conditions from instrument to instrument and from analyst to analyst.

REFERENCES

1. World Health Organization. General guidelines for methodologies on research and evaluation of traditional medicine, Geneva.2000.
2. World Health Organization. Analysis of questionnarire on traditional medicine. Geneva. 1992.
3. Harborne J B. Textbook of Phytochemical Methods. A Guide to Modern Techniques of Plant Analysis. 5th Edition, Chapman and Hall Ltd, London. 1998.
4. Safety evaluation of certain food additives and contaminants: prepared by the eightieth meeting of the Joint FAO/WHO Expert Committee on Food Additives (JECFA). Supplement 2: Pyrrolizidine alkaloids. World Health Organization, Geneva, 2020
5. Singleton V L & Rossi J A, Colorimetry of total phenolics with phosphomolybdic phosphotungstic acid reagents.Amer J Enol Viticult. 1965;16:144-58.
6. Zhishen J, Mengcheng T, Jianming W, The determination of flavonoid contents in mulberry and their scavenging effect on superoxide radicals.Food Chem. 1999; 64:555-9.
7. Khan R A, Khan M R, Sahreen S, Ahmed M. Assessment of flavonoids contents and in vitro antioxidant activity of *Launaea procumbens*. Chem Cent J.2012; 6(1):43.
8. Ravishankara M N, Padh H and Rajani M.Antioxidant activity of *Cinchona officinalis* stem bark extracts.Orient Pharm Exp Med.2003; 3(4):205-211.
9. Meyer B N, Ferrigni N R, Putnam J E, Jacobsen L B, Nichols D E, McLaughlin J L. Brine shrimp: A convenient general bioassay for active plant constituents. Planta Med. 1982; 45:31-4.
10. Mentor R H, Blagica J, Tatjana K P. Toxicological evaluation of the plant products using Brine Shrimp (*Artemia salina* L.) model. Macedonian pharm. bulletin.2014;60(1):9 - 18
11. Gazdar A F, Carney D N, Russell E K, et al., Small cell carcinoma of the lung; establishment of continuous clonable cell lines having APUD properties. Cancer Res. 1980; 40:3502-3507.

12. Giard D J, Aaronson S A, Todaro G J, Arnstein P, Kersey J H, Dosik H et al., *In Vitro* Cultivation of Human Tumors: Establishment of Cell Lines Derived From a Series of Solid Tumors. *J. Natl. Cancer Inst.* 1973; 51(5):1417-1423.
13. F. C. Brusselle, "A549 cell line," in *Encyclopedia of Respiratory Medicine*, Second Edition, 2021, Pages 170–172.
14. P. J. Morin et al., "NCI-H23 cell line," in *Encyclopedia of Cancer* (Third Edition), 2019, Pages 195–196.
15. Hsu H F, Huang K H, Lu K J, Chiou S J, Yen J H, Chang C C et.al., Typhoniumblumei extract inhibits proliferation of human lung adenocarcinoma A549 cells via induction of cell cycle arrest and apoptosis. *J Ethnopharmacol.* 2011; 135(2):492-500.
16. Ritch S J, Brandhagen B N, Goyeneche A A et al., Advanced assessment of migration and invasion of cancer cells in response to mifepristone therapy using double fluorescence cytochemical labeling. *BMC Cancer.* 2019;19:376.
17. BIOVISION AnnexinV-PE Apoptosis Detection Kit, Catalogue number: K128-100.
18. PROMEGA Caspase-Glo® 3/7 Assay System, Catalogue number : G8090
19. CELL BIOLABS, INC.OxiSelect™ 96-Well Comet Assay Kit, Catalogue number : STA-355
20. Bajpai VK, Majumder R, Park J. Isolation and purification of plant secondary metabolites using column-chromatographic technique. *Bangladesh J Pharmacol.* 2016; 11:844.
21. Hasan S. *Theory of IR Spectroscopy.* 2022.
22. Marion D. An introduction to biological NMR spectroscopy. *Mol Cell Proteomics.* 2013; 12(11):3006-25
23. Murayama C, Kimura Y, Setou M. Imaging mass spectrometry: principle and application. *Biophys Rev.* 2009; 1(3):131
24. International Conference on Harmonization, Q2 (R1) Validation of Analytical Procedures, Text and Methodology, Geneva. 2005.

Chapter 4

Results & Discussion

RESULTS AND DISCUSSION

In this chapter, the various results obtained from different experiments carried out are compiled. An attempt has also been made to discuss these results to provide a convincing reason for the studies performed.

4.1 Identification, Collection, and Authentication of the Plant Material

The whole plants of *Onosma bracteatum* were collected from Uttarakhand. Authentication of the plant was done by Dr. V. P. Bhatt, Taxonomist, Herbal Research and Development Institute (HRDI), Gopeshwar, Uttarakhand.



Plant *Onosma bracteatum*

4.2 Assessment of quality of plant materials

4.2.1 Morphology of stem, root, and flower of *O. bracteatum* (Fig.4.1)

The stems are cylindrical and twisted, with a rough surface due to white, hard, hispid hairs and cicatrices. The fracture is fibrous, and the taste is bitter. The stems are odorless and available in cut pieces of 3-5cm in length and 0.9-1.5cm in diameter.

The roots are also cylindrical and twisted, with a rough surface. The fracture is fibrous, and the taste is bitter. The roots are odorless and available in cut pieces of 6-8cm in length and 0.3-0.6cm in diameter.

The inflorescence is composed of terminal glomerate clusters that are very dense, measuring 4-10cm in width in flowers. The flowers are deep blue, later turning purplish color, and are thickly actinomorphic and pedicellate. The bracts are

lanceolate and hairy. The calyx is divided to the base with 5 lobes that are linear-lanceolate and 15-18mm long. The corolla is blue or purple and usually gradually expands from the base upward. The throat is unappendaged, while the nectary is ring-like or lobed with a dentate margin.

4.2.2 Microscopical study (Powder study)

The powder of *Onosma bracteatum* appears to be yellowish brown, fibrous with a bitter taste, and revealed the following characteristics. (Fig.4.2)

Cork cell: Polygonal cork cells in surface view

Xylem vessels: Fragments with reticulate thickening

Calcium oxalate: Rosettes of calcium oxalate crystals

Trichomes: Long, unicellular, warty trichomes with acuminate apical region

Pollen: Hexagonal and star-shaped pollen

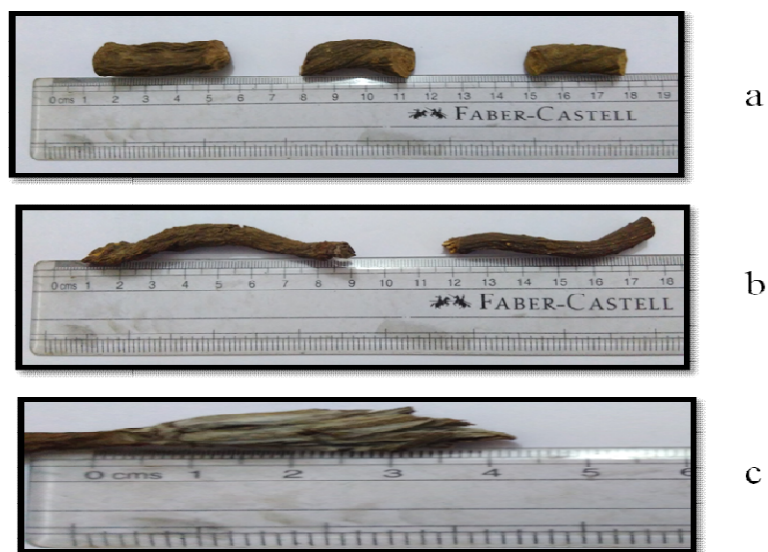
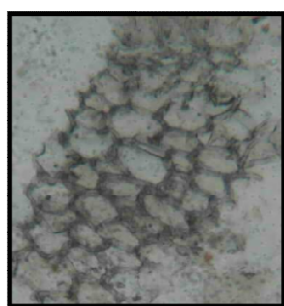
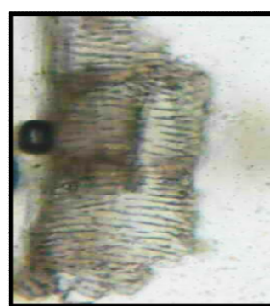


Figure 4.1 Morphology of *Onosma bracteatum*. a) Stem b) Root c) Flower



Cork cell



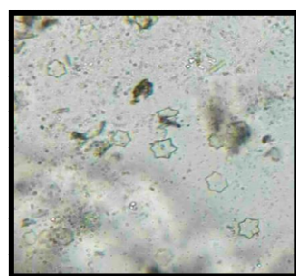
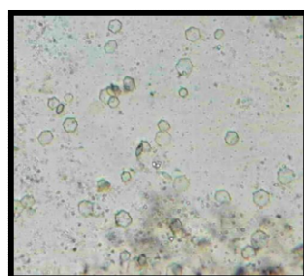
Reticulate vessels



Rosette of calcium oxalate crystals



Unicellular warty trichomes



Hexagone and star shape pollen

Figure 4.2 Powder characteristics of *O. bracteatum*

4.2.3 Proximate Analysis

The results obtained for various physicochemical parameters (Table 4.1) complied with the data mentioned in Ayurvedic pharmacopoeia¹. The values given here are expressed as percentages of air-dried material. Each value is an average of three.

The morphological, microscopical, and physicochemical parameters of *O.bracteatum* will be useful in standardization viz., sample identification, quality, and purity. It also helps to differentiate the drug from their respective other species and adulterants.

4.3 Phytochemical studies

4.3.1 Preliminary Profile

4.3.1.1 Preparation of extract and qualitative phytochemical study

Table 4.1 Physico-chemical parameters of *O.bracteatum*

Sr.No.	Parameters	<i>Onosma bracteatum</i> values (%w/w)	<i>Onosma bracteatum</i> value (%w/w) as per Ayurvedic pharmacopoeia
1	% Moisture content	5.4%	-
2	Ash value		
	Total ash	5.51%	NMT 26%
	Acid insoluble ash	0.075%	NMT 4%
	Water soluble ash	2.623%	-
3	Extractive value		
	Alcohol extractive value	6.9%	NLT 1%
	Water extractive value	10.2%	-

Table 4.2 Qualitative phytochemical screening of *Onosma bracteatum*

Sr.No.	Test	TME (Total Methanolic Extract)
1	Alkaloids	+
2	Glycosides	-
3	Coumarins	+
4	Saponins	+
5	Steroid and terpenoids	+
6	Flavonoids	+
7	Phenolic compounds	-
8	Quinones	+
9	Protein and Amino acid	+
10	Fixed oil and Fats	+
11	Sugar	-

+ : Present, - : Absent

Soxhlet extraction of *O. bracteatum* powder using methanol yielded 18.3%w/w reddish brown-coloured extract. Phytoconstituents were found to be present in the extract based on the phytochemical screening tests are mentioned in Table 4.2

Table 4.3 Quantitative phytochemical screening of *Onosma bracteatum*

Extract	TPC (%w/w)	TFC (%w/w)	TAC(%w/w)
TME	1.45±0.0047	1.12±0.0014	0.22±0.0032

Values are expressed as mean ± standard deviation (SD), n=3

4.4 *In vitro* Antioxidant assay of TME

4.4.1 Phosphomolybdenum assay

The basic principle to assess the antioxidant capacity through phosphomolybdenum assay includes the reduction of Mo (VI) to Mo (V) by the plant extract possessing antioxidant compounds². The total antioxidant capacity of TME was 37.75±1.2 µgBHTe/mg of dry extract it was suggested the presence of effective antioxidants in TME (Table 4.4).

Table 4.4 Total Antioxidant capacity of TME of *O.bracteatum*

Extract/Fractions	µgBHTe/mg of dry extract
TME	37.75±1.2

4.4.2 DPPH scavenging assay

DPPH is a stable free radical, which has been widely used in phytomedicine for the assessment of scavenging activities extracts and fractions. The scavenging activity of TME was determined using free radicals of 1, 1-diphenyl 1-2-picryl-hydrazyl (DPPH).² Results showed that TME possessed EC₅₀ 74.15 ± 1.44µg/mL. (Figure 4.3)

4.4.3 Nitric oxide scavenging assay

Sodium nitroprusside in an aqueous solution at physiological pH spontaneously produces nitric oxide, which interacts with oxygen to produce nitrite ions that can be estimated using Griess's reagent. Scavengers of nitric oxide compete with oxygen,

leading to reduced production of nitrite ions³. The TME showed EC₅₀ 215.64 ± 2.42 µg/mL.(Figure 4.3)

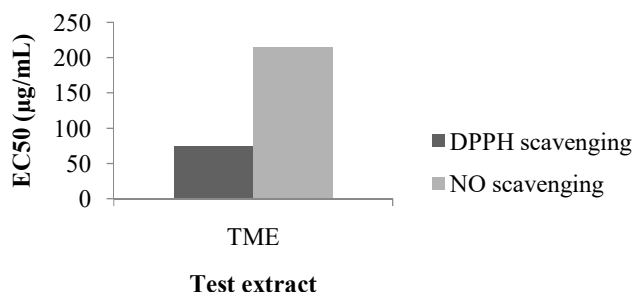


Figure 4.3 DPPH and NO scavenging activity of TME

4.5 Preliminary cytotoxicity assay of TME

4.5.1 Brine Shrimp lethality assay

The LC₅₀ value obtained from brine shrimp lethality bioassay (Figure 4.4 and Table 4.5) was 131.82 µg/mL for TME compared to positive control potassium dichromate 13.63 µg/mL. Resulting LC₅₀ values less than 250 µg/mL were considered significantly active and had the potential for further investigation⁴.

The median lethal concentration (LC₅₀) and 95% confidence intervals of the test samples were calculated using the probit analysis method described by Finney, as the measure of toxicity of the TME^{5,6}.

Table 4.5 Effect of TME and Potassium dichromate on brine shrimp

Conc (µg/mL)	1	10	100	500	1000	LC ₅₀	Inference
Log conc	0	1	2	2.69897	3	-	-
TME	0±0.00	16.66±5.77	40.66±11.01	83.33±5.77	93.33±5.77	131.82	Cytotoxic
Potassium dichromate	0±0.00	36.66±5.77	100±0.00	100±0.00	100±0.00	13.63	Potent cytotoxic

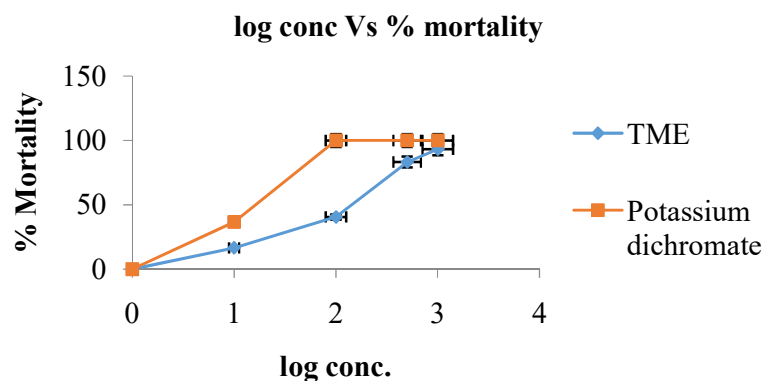


Figure 4.4 Plot of log concentration of TME versus percent shrimp mortality after 24hr of exposure

4.5.2 MTT assay on cell line (A549 and NCI-H23 cell line)

Results by MTT assays are presented in figure 4.5 showed percent inhibition values of the A549 cells incubated for 48hr with TME. Figure 4.6 showed the percent inhibition values of NCI-H23. In both the cell lines percent inhibition values were found to increase with the increase in concentration. The TME exhibited in-vitro cytotoxicity at 48hr incubation leading to decreased viability in the treated cells when compared with the untreated controls. Table 4.6 showed the IC_{50} value of TME on both cell lines.

Table 4.6 IC_{50} value of TME

Cell line	$IC_{50}(\mu\text{g/mL})$
A549	913.04 $\mu\text{g/mL}$
NCI-H23	825.42 $\mu\text{g/mL}$

The MTT assay involves the conversion of the water-soluble yellow dye MTT [3-(4,5-dimethylthiazol-2-yl)-2,5-diphenyltetrazolium bromide] to an insoluble purple formazan by the action of mitochondrial reductase. Formazan is then solubilized and the concentration determined by optical density at 570nm⁷. **Figure 4.5 and 4.6** shows % inhibition of cells with increase in concentration.

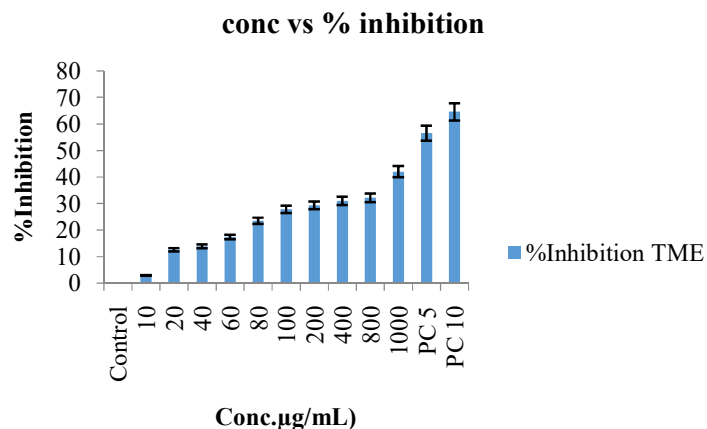


Figure 4.5 Graph of sample concentration vs % inhibition of A549 cells treatment with TME of *O. bracteatum*

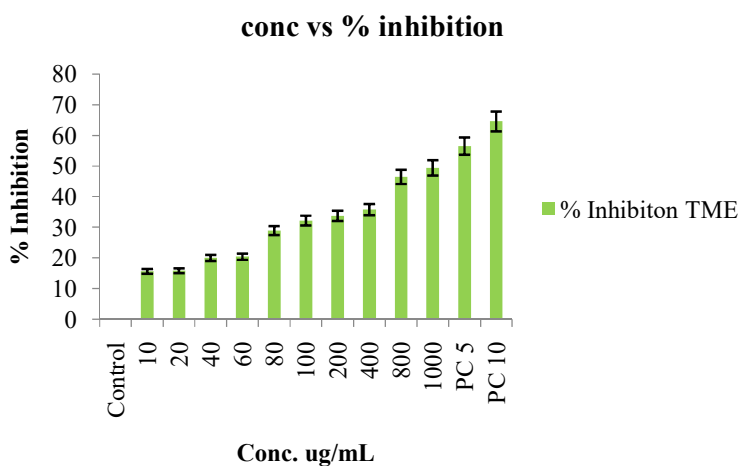


Figure 4.6 Graph of sample concentration vs % inhibition of NCI-H23 cells treatment with TME of *O. bracteatum*

4.6 Yield of extract

Yield of extract by successive solvent extraction with continuous soxhlet method is mention in table 4.7.

Table 4.7 % Yield of extracts

Extract	Colour	% Yield
Petroleum ether (A1)	Orange Red	1.4
Chloroform(A2)	Reddish Brown	2.2
Ethyl acetate(A3)	Brownish Yellow	0.82
Butanol(A4)	Brownish Black	8.6
Water(A5)	Dark brown	12.2

4.7 *In vitro* antioxidant activity of Extracts

4.7.1 Phosphomolybdenum assay

The total antioxidant capacity of the A1 to A5 extract is mentioned in Table 4.8. The highest total antioxidant capacity was found in the A4 extract and the lowest antioxidant capacity was found in the A1 extract. A4 extract activity might be due to the presence of phenolics and flavanoid compounds in the extract.

Table 4.8 Total Antioxidant capacity of A1 to A5 of *O.bracteatum*

Extract/Fractions	$\mu\text{gBHTe}/\text{mg}$ of dry extract
A1	18.25 \pm 1.5
A2	24.08 \pm 1.6
A3	37.19 \pm 1.8
A4	58.56 \pm 1.5
A5	30.5 \pm 1.2

4.7.2 DPPH scavenging assay

DPPH scavenging activity of A1 to A5 extracts is shown in Figure 4.7. The highest activity was found with A4 extract and the lowest activity was found with A2 extract (Table 4.9)

Table 4.9 EC₅₀ value of A1 to A5 in DPPH assay

Extract/Fractions	EC ₅₀ (µg/mL)
A1	570.74±1.66
A2	780.27±1.34
A3	500.05±1.21
A4	201.27±1.87
A5	400.22±1.53

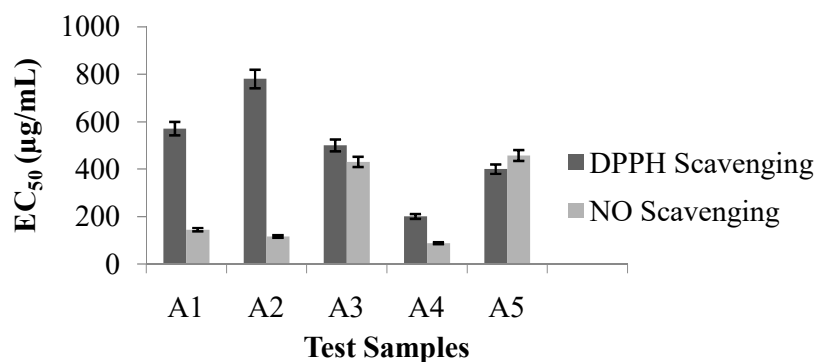


Figure 4.7 DPPH and Nitric oxide scavenging activity of A1 to A5 extract

4.7.3 Nitric oxide scavenging assay

Nitric oxide scavenging activity of A1 to A5 extracts is shown in figure 4.7. The highest activity was found with A4 extract. (Table 4.10)

Table 4.10 EC₅₀ value of A1 to A5 in nitric oxide scavenging assay

Extract/Fractions	EC ₅₀ (µg/mL)
A1	145.07±1.23
A2	116.49±1.87
A3	413.02±1.64
A4	88.46±1.93
A5	457.74 ±1.76

4.8 In vitro cytotoxicity assay of extracts

4.8.1 Brine shrimp lethality assay

The LC₅₀ value obtained from the brine shrimp lethality bioassay (Figure 4.8) was mentioned in Table 4.11. Extract A1 to A5 was studied and compared with positive control potassium dichromate. LC₅₀ value was found to be lowest with A4>A1>A2>A3>A5. The present study evaluates that the extent of lethality was directly proportional to the concentration of the extracts. The presence of alkaloids, flavonoids, phenolics, coumarins, and quinones could be accounted for its cytotoxic activity⁸. From the results only A1, A2 and A4 subjected for MTT assay on A549 and NCI-H23 cell lines.

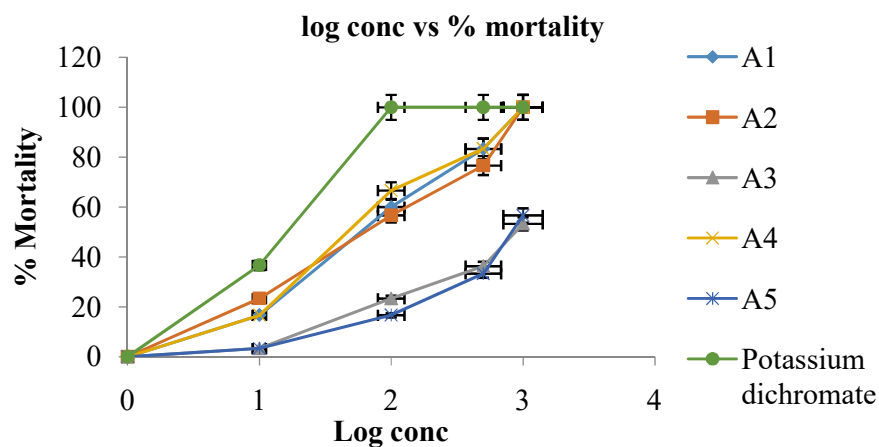


Figure 4.8 Plot of log concentration of A1, A2, A3, A4, A5 and potassium dichromate versus percent shrimp mortality after 24 h of exposure

Table 4.11 Effect of A1, A2, A3, A4, A5 and potassium dichromate on brine shrimp

Conc ($\mu\text{g/ml}$)	1	10	100	500	1000	LC ₅₀ ($\mu\text{g/mL}$)	Inference
Log conc	0	1	2	2.69897	3	-	-
A1	0 \pm 0.00	16.66 \pm 5.77	60 \pm 10.0	83.33 \pm 5.77	100 \pm 0.00	75.85	Cytotoxic
A2	0 \pm 0.00	23.33 \pm 5.77	56.66 \pm 11.54	76.66 \pm 5.77	100 \pm 0.00	79.43	Cytotoxic
A3	0 \pm 0.00	3.33 \pm 5.77	23.33 \pm 5.77	36.66 \pm 5.77	53.33 \pm 11.54	575.43	Less- cytotoxic
A4	0 \pm 0.00	16.66 \pm 5.77	66.33 \pm 11.54	83.33 \pm 5.77	100 \pm 0.00	74.13	Cytotoxic
A5	0 \pm 0.00	3.33 \pm 5.77	16.66 \pm 5.77	33.33 \pm 11.54	56.66 \pm 5.77	602.55	Less- cytotoxic
Std K ₂ Cr ₂ O ₇	0 \pm 0.00	36.66 \pm 5.77	100 \pm 0.00	100 \pm 0.00	100 \pm 0.00	13.63	Potent Cytotoxic

Data are expressed as mean \pm SD. Each sample was analyzed three times.

4.8.2 MTT assay on A549 and NCI-H23 cell lines

Active extracts from brine shrimp assay were further studied for MTT assay on A549 and NCI-H23 cell line. It was found that the highest IC₅₀ value was found with A4 extracts in both the cell line. IC₅₀ value of extract A4>A2>A1 in comparison with 5-flouro uracil taking as standard. As in the brine shrimp assay, highest % of mortality was found with A4 extract but in the MTT assay lowest activity of A4 was found compared to A1 and A2 extract, so we have selected A1 and A2 extract for the study. IC₅₀ value of all extracts is shown in Table 4.12. Literature suggested that shikonin, alkannin, quinines, and pyrrolizidine alkaloids present in plant extracts *O.bracteatum* are responsible for cytotoxicity^{8,9}. A1 and A2 extract is selected for further study apoptosis profile on A549 and NCI-H23 cell lines.

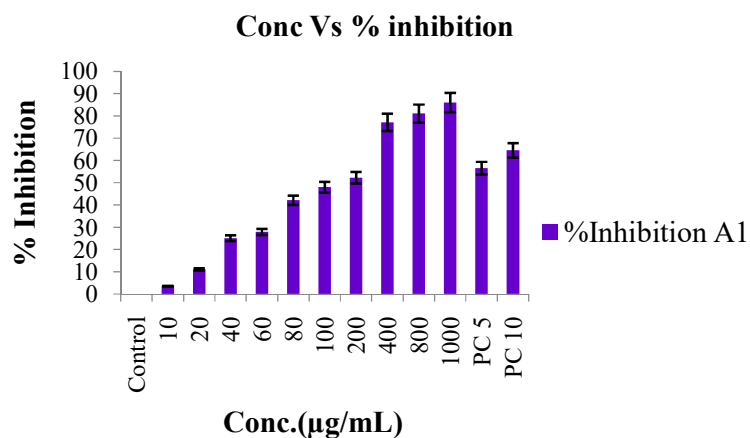


Figure 4.9 Effect of extract A1 on A549 cell

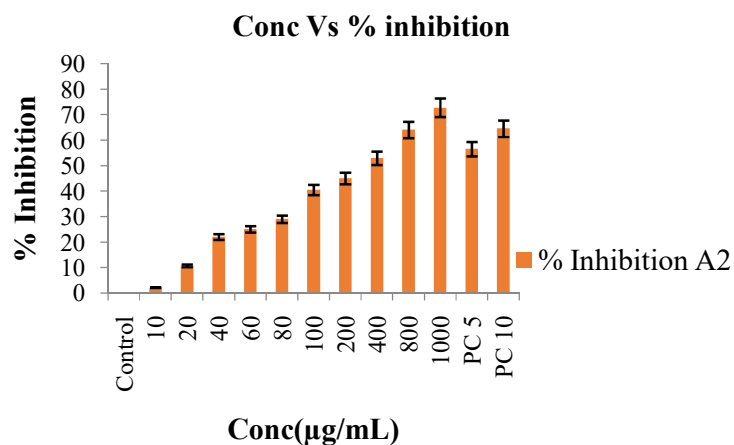


Figure 4.10 Effect of extract A2 on A549 cell

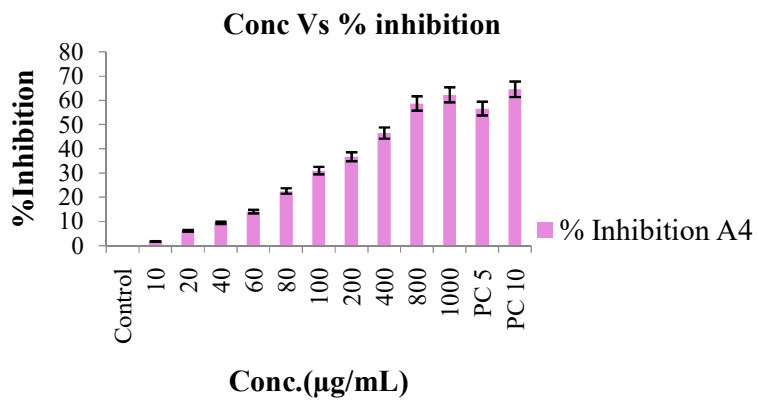


Figure 4.11 Effect of extract A4 on A549 cells

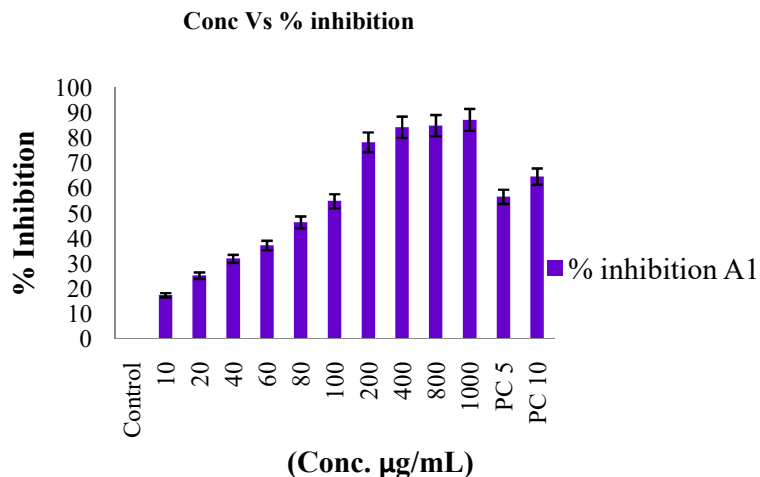


Figure 4.12 Effect of extract A1 on NCI-H23 cells

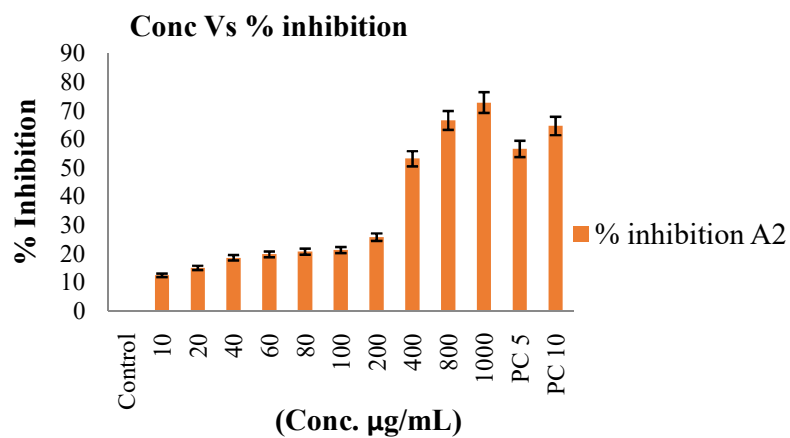


Figure 4.13 Effect of extract A2 on NCI-H23 cells

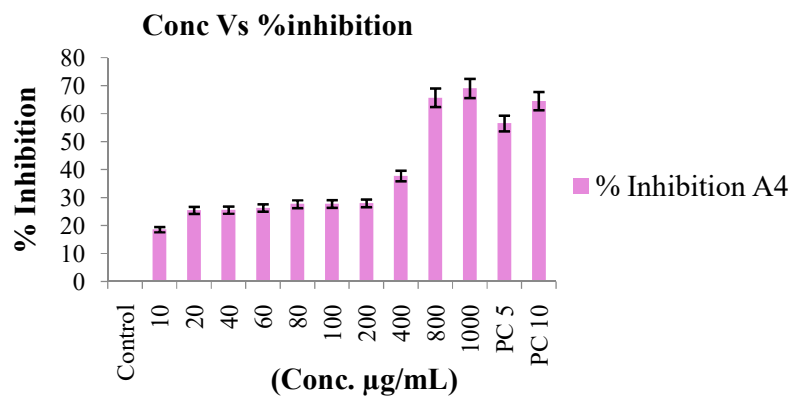


Figure 4.14 Effect of extract A4 on NCI-H23 cells

Table 4.12 IC₅₀ value of A1, A2 and A4 extracts on A549 and NCI-H23 cells

Extract	IC ₅₀ (µg/mL) A549 cells	IC ₅₀ (µg/mL) NCI-H23 cells
A1	104.16±1.56	99.65±1.27
A2	377.38±1.72	377.35±1.85
A4	681.66±1.34	572.59±1.62

4.9 Apoptosis profile of mixture of A1 and A2 on A549 and NCI-H23 cell line

4.9.1 MTT assay

The mixture of A1 and A2 shows less IC₅₀ value on both the cell lines compared to individual extracts. The mixture showed synergistic activity in the MTT assay using A549 and NCI-H23 cell lines. IC₅₀ value of the mixture of A1 and A2 was found to be 91.01µg/mL and 76.93µg/mL on A549 and NCI-H23 cell lines respectively. (Table 4.13)

Table 4.13 IC₅₀ value of mixture of A1 and A2 on A549 cells and NCI-H23 cells

Extract	IC ₅₀ (µg/mL) A549 cells	IC ₅₀ (µg/mL) NCI-H23 cells
A1+A2	76.93±1.25	91.01±1.63

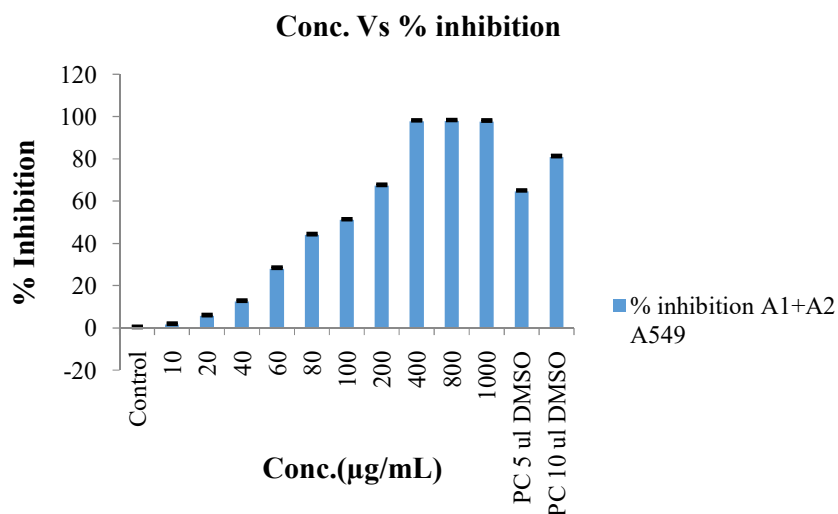


Figure 4.15 effect of mixture of A1 and A2 on A549 cell lines

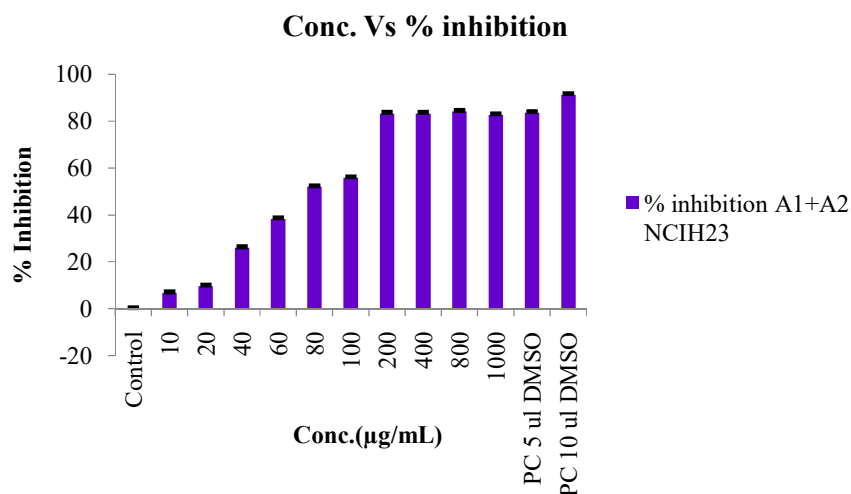


Figure 4.16 effect of mixture of A1 and A2 on NCI-H23 cell line

4.9.2 Wound healing assay or scratch assay

The ability of cells to migrate is essential for many physiological processes like embryonic development, wound repair, tumor invasion, neoangiogenesis, and metastasis¹⁰. We examined cell migration in response to the mechanical scratch wound in the absence and presence of a mixture of A1 and A2 extract in concentration of 100µg/ml. Images of a scratch area in the time line of 0hr and 24hr are illustrated in figure 4.17. The mixture of A1 and A2 inhibit cell migration compared to a control group.

4.9.3 Annexin V assay

Exposure of phosphatidylserine on the external surface of the cell membrane is generally accepted as one of the biomarkers of apoptosis. It is an important cell death mechanism that does not trigger an inflammatory response that occasions collateral destruction of normal cells in the surrounding microenvironment¹¹. Results of A549 and NCI-H23 cell lines demonstrated that a mixture of A1 and A2 at concentration of 100µg/mL showed late apoptotic rates was 80.26% and 79.54% respectively. Hence, the extract induces late apoptosis in both cell lines. (Fig. 4.18 and Fig. 4.20)

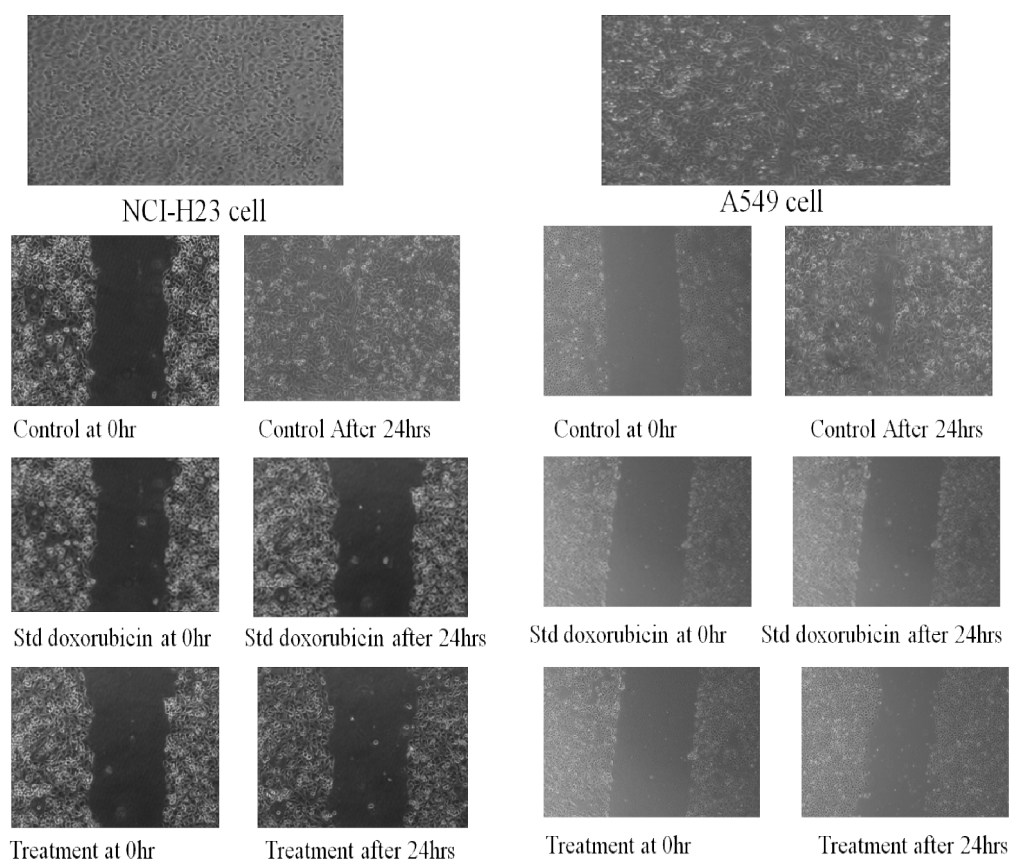


Figure 4.17 cell migration of mixture of A1 and A2 on A549 and NCI-H23 cell lines

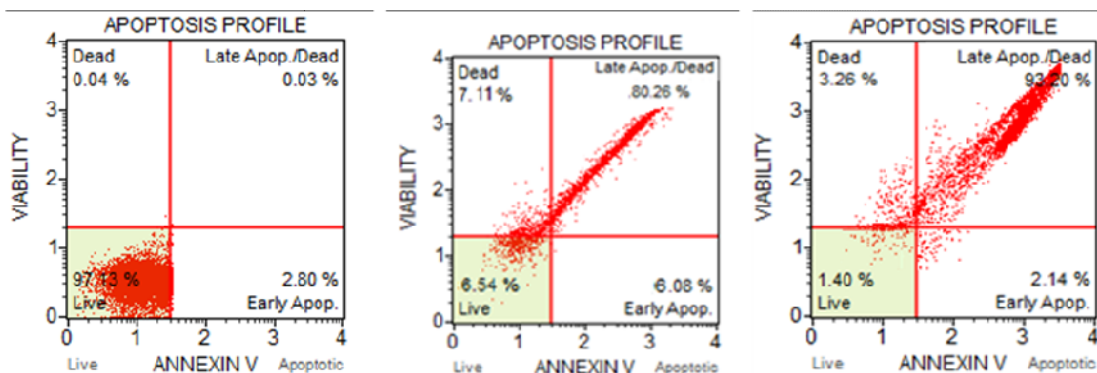


Figure 4.18 Apoptosis profile of mixture of A1 and A2 using Annexin V on A549 cell line

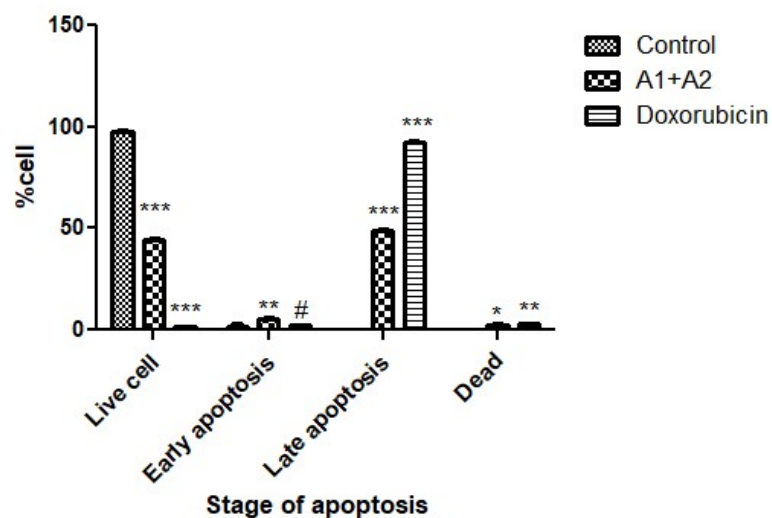


Figure 4.19 Graphical representation of stages of apoptosis (All data presented are the Mean \pm SD and are representative of three independent experiments. values < 0.05 were considered to be statistically significant, and significance was marked as * p values < 0.05 , ** values < 0.01 , and ***values < 0.001 , # represented as non-significant

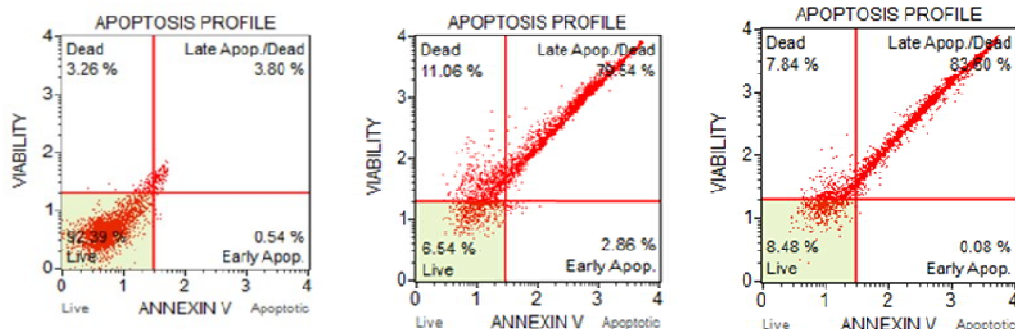


Figure 4.20 Apoptosis profile of mixture of A1 and A2 using Annexin V on NCI-H23 cell lines

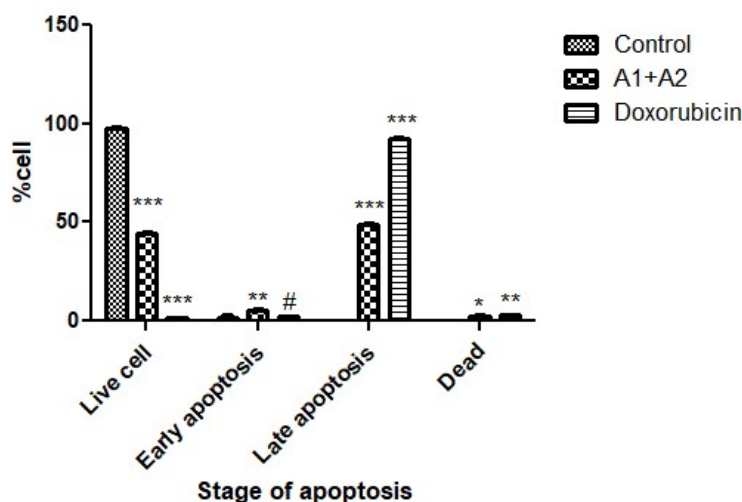


Figure 4.21 Graphical representation of stages of apoptosis (All data presented are the Mean \pm SD and are representative of three independent experiments. values < 0.05 were considered to be statistically significant, and significance was marked as * p values < 0.05 , ** values < 0.01 , and *** values < 0.001 , # represented as non-significant)

4.9.4 Caspase 3/7 activity

The activation of caspases 3/7 was evaluated in cancer cells to establish the cell death pathway induced by the extract¹¹. Figure 4.22 and 4.23 indicates that a mixture of A1 and A2 showed caspase 3/7 activation at concentration of 100 μ g/ml using doxorubicin as positive control.

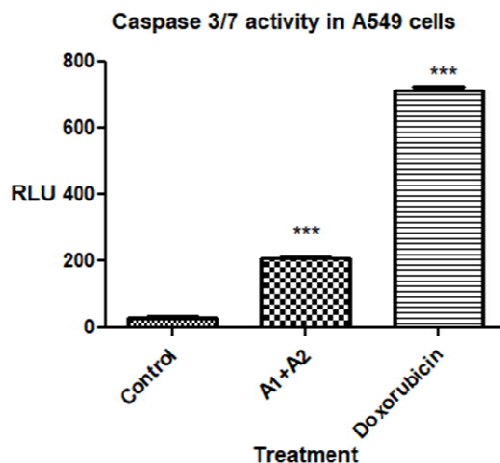


Figure 4.22 Effects of mixture of A1 and A2 extract on the caspase activation in A549 cell line. (The graph is reported as the means \pm SD of three independent experiments using GraphPad Prism 6 statistical software. *** indicate significance difference with control group $P < 0.001$)

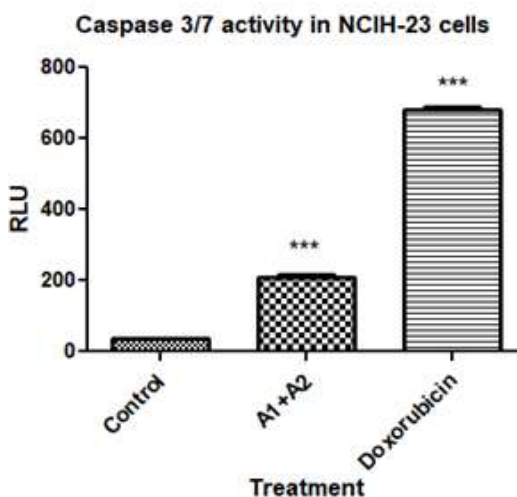


Figure 4.23 Effects of mixture of A1 and A2 extract on the caspase activation in NCI-H23 cell lines. (The graph is reported as the means \pm SD of three independent experiments using GraphPad Prism 6 statistical software. *** indicate significance difference with control group $P < 0.001$)

4.9.5 comet assay

In the comet assay, DNA strand breaks were represented by the mean tail DNA, that is, the percentage of DNA in the comet tail relative to the total amount of DNA¹². In the untreated control samples no detectable or shorter tails were as in treatment with extract and positive control cells detectable tails were observed. DNA damage is observed in the treatment group at concentration of 100µg/ml in both cell lines. (Figures 4.24, 4.25, 4.26, and 4.27) Genotoxic anticancer agents induce DNA damage, which, if severe enough, will lead to apoptosis. Rapidly dividing cells, such as cancer cells, are particularly sensitive to these agents. Therefore, Agents that induce DNA damage and activate programmed cell death in cancer cells could be valuable anti-cancer therapeutics^{12,13}

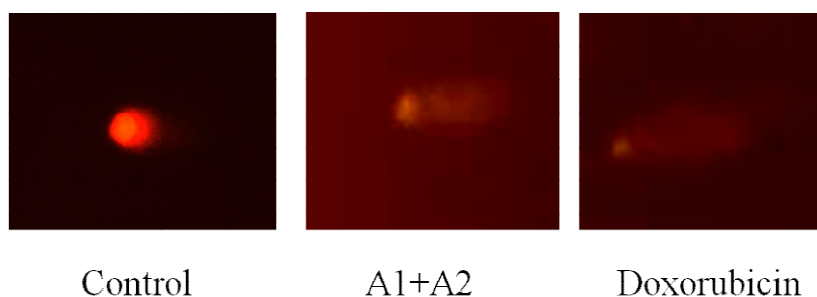


Figure 4.24 Representative images of comets showing the genotoxic effect of mixture of A1 and A2 on A549 cells analysed by comet assay

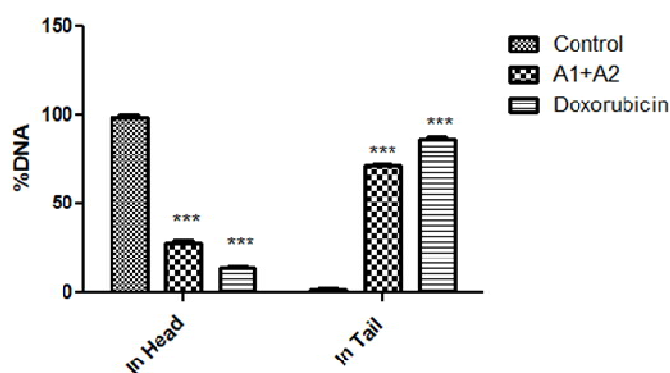


Figure 4.25 Graphical representation of genotoxic effect of mixture of A1 and A2 on A549 cells analysed by comet assay

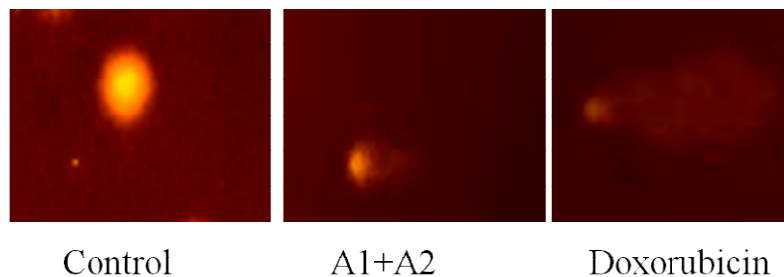


Figure 4.26 Representative images of comets showing the genotoxic effect of mixture of A1 and A2 on NCI-H23 cells analysed by comet assay

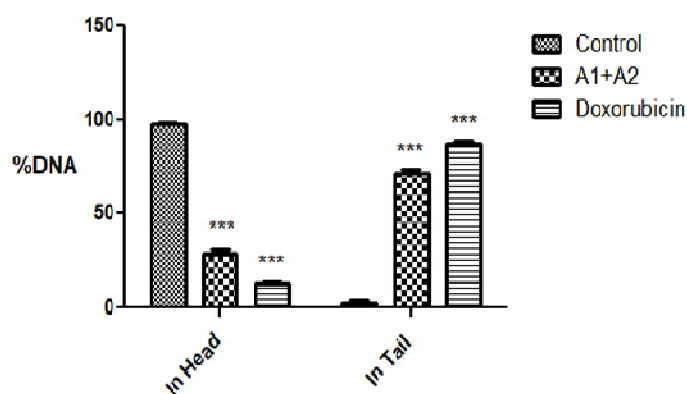


Figure 4.27 Graphical representation of genotoxic effect of mixture of A1 and A2 on NCI-H23 cells analysed by comet assay

4.10 Preparations of fractions

Fractions were prepared by column chromatography of A1 extract. Fractions were collected from PF1 to PF6 and their description and yield were mentioned in Table 4.14

Table 4.14 % Yield of Fractions

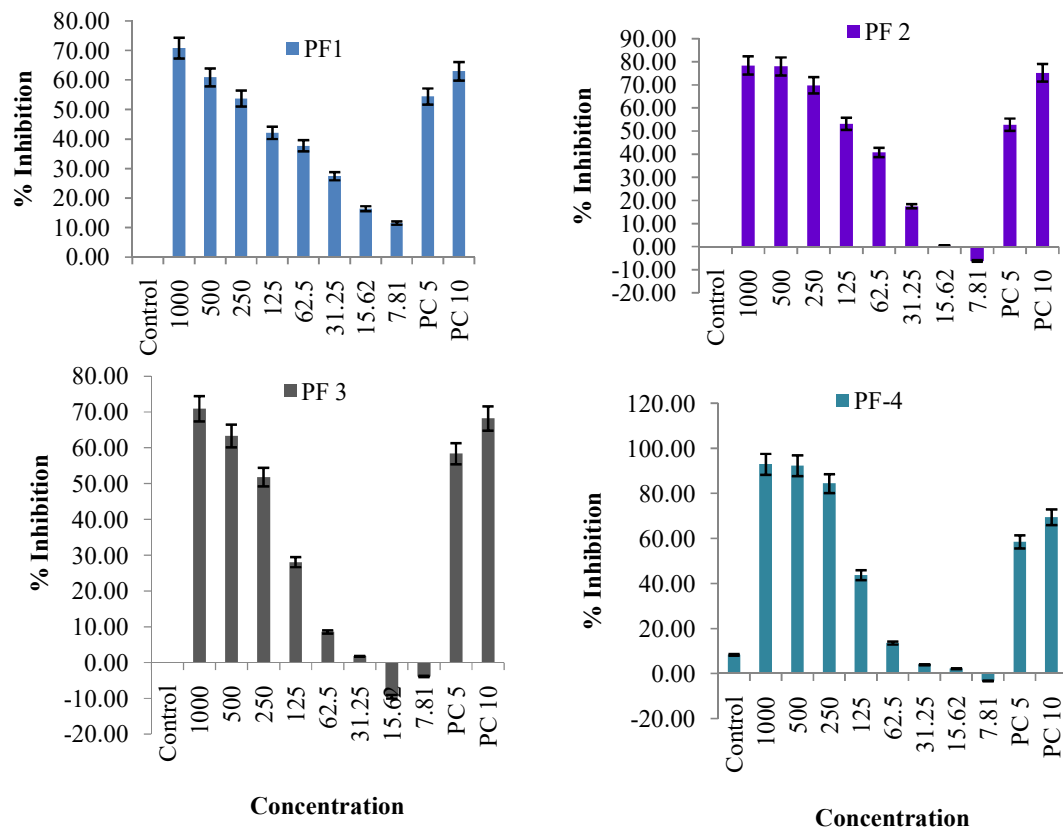
Fractions	Colour	% Yield (w/w)
PF1	Reddish brown	0.106
PF2	Orange Red	0.08
PF3	Reddish Brown	0.14
PF4	Yellowish orange	0.308
PF5	Yellowish orange	0.271
PF6	Yellowish brown	0.235

4.11 Apoptosis profile of Fractions on A549 and NCI-H23 cell line

4.11.1 Cytotoxicity of Fractions by MTT assay

MTT assay was performed for preliminary screening of fractions against A549 and NCI-H23 cell lines. Figure 4.28 and 4.29 shows data on % inhibition of all fractions.

The effect of fractions was concentration dependant.



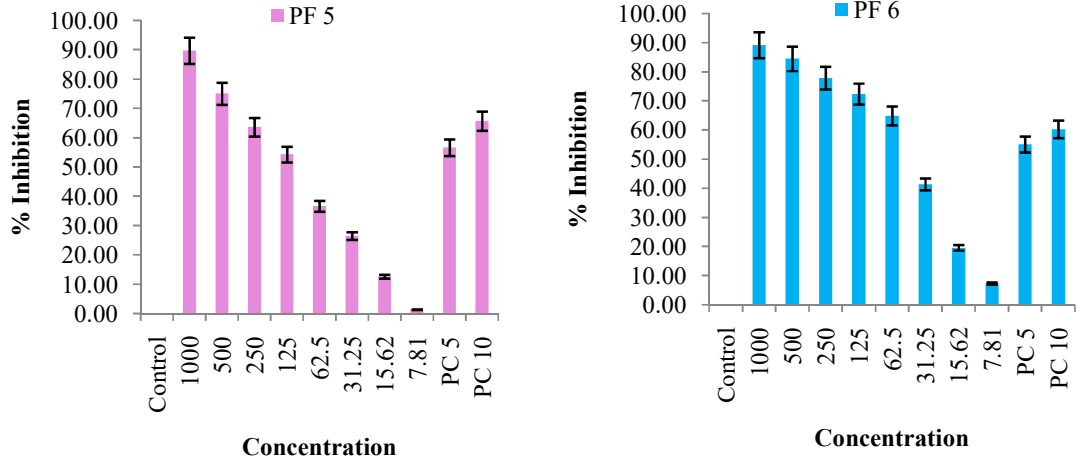
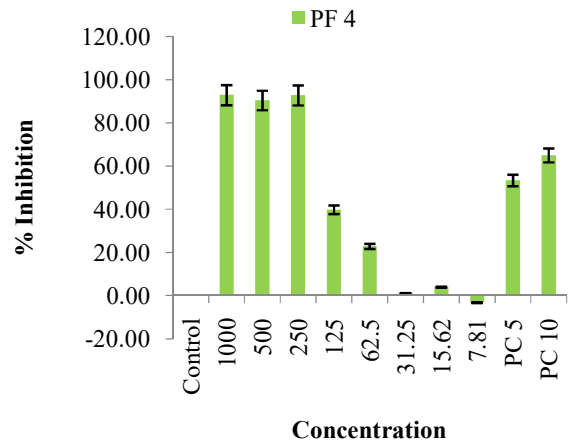
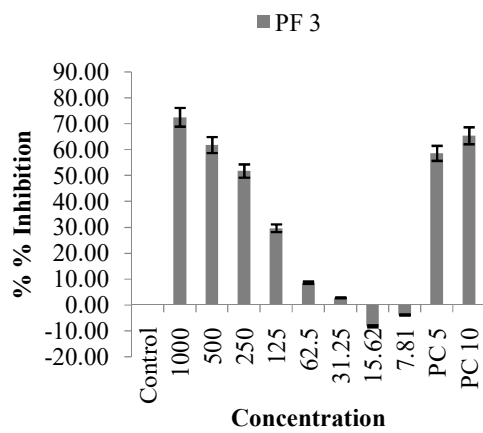
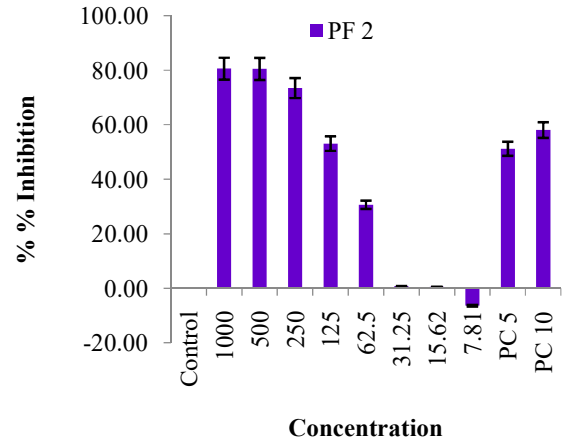
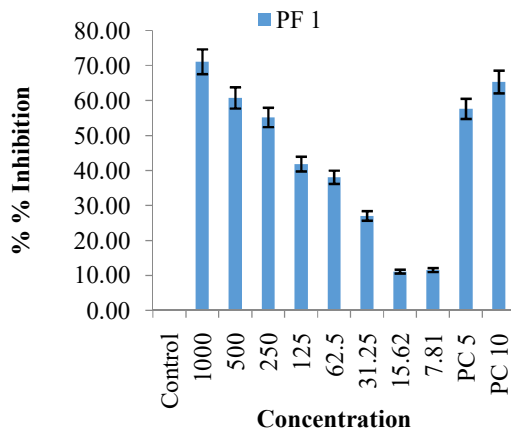


Figure 4.28 % Inhibition of fractions on A549 cell line



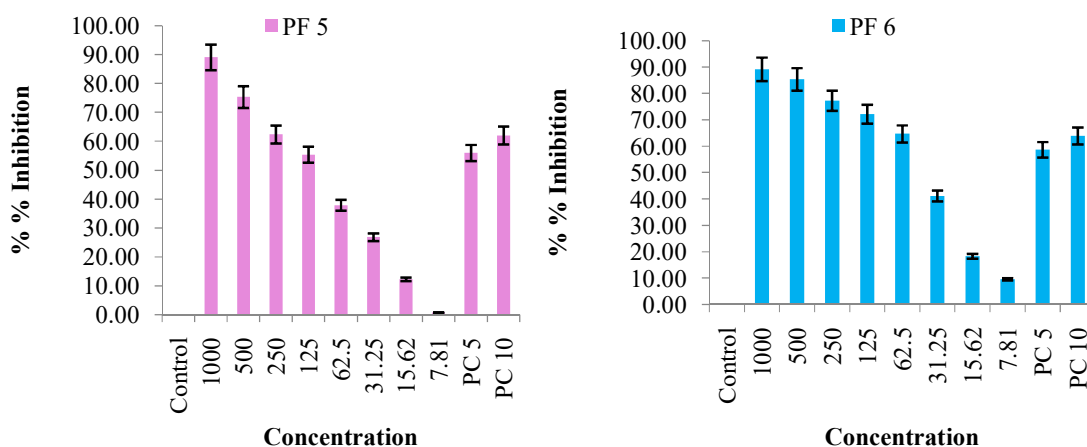


Figure 4.29 % Inhibition of fractions on NCI-H23 cell lines

Tablet 4.15 shows lowest IC_{50} was found with PF6 extract $49.96\mu\text{g/mL}$ and $50.06\mu\text{g/mL}$ in A549 and NCI-H23 cells respectively and the highest IC_{50} was found with PF3 extract $312.9\mu\text{g/mL}$ and $310.6\mu\text{g/mL}$ in A549 and NCI-H23 cell respectively.

Table 4.15 IC_{50} values of Fraction on A549 and NCI-H23 cells

Fraction	IC_{50} ($\mu\text{g/mL}$) A549 cells	IC_{50} ($\mu\text{g/mL}$) NCI-H23 cells
PF1	202.6 \pm 1.82	203.2 \pm 2.23
PF2	125.4 \pm 2.01	133.9 \pm 1.98
PF3	312.9 \pm 1.76	310.6 \pm 1.62
PF4	135.6 \pm 1.21	128.7 \pm 1.51
PF5	118.6 \pm 1.39	117.5 \pm 1.85
PF6	49.96 \pm 1.56	50.06 \pm 1.29

4.11.2 Wound healing assay or scratch assay

The wound healing method was carried out to ascertain and determine the interference in cell migration by fractions of A1 extract. In scratch assay there was great inhibitory action of cell migration in the fraction treated group, lupeol, and doxorubicin treated group was found compared to vehicle-treated group. (Fig. 4.30 and Fig. 4.31)

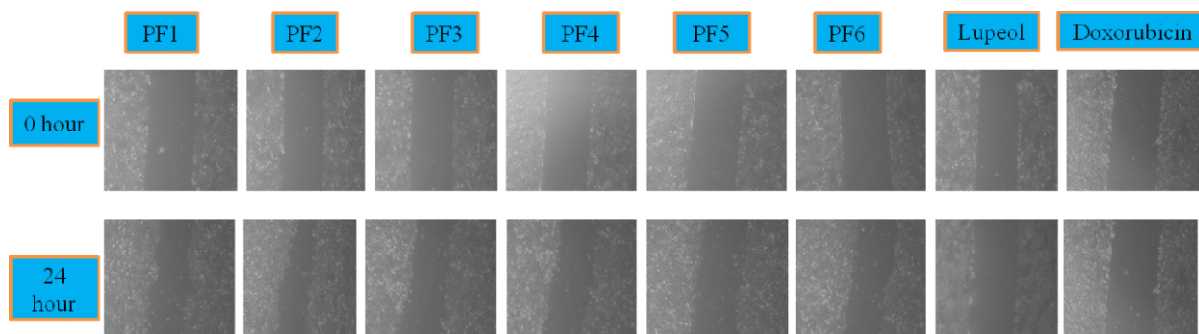


Figure 4.30 Cell migration effects of fractions with positive standard on A549 cell

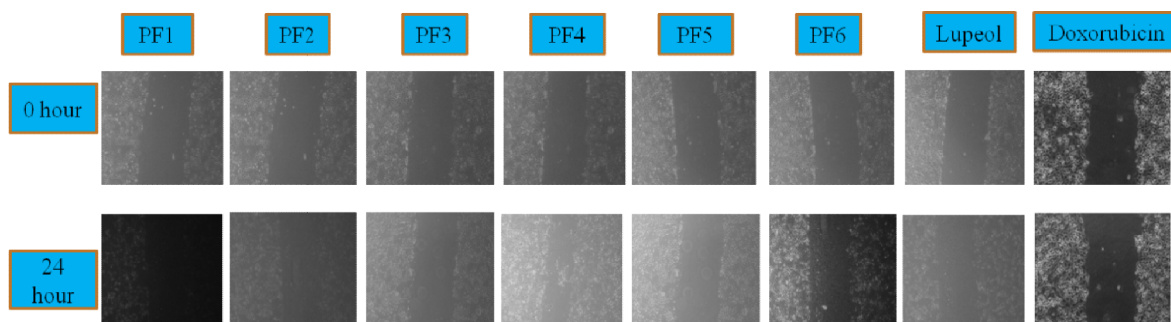


Figure 4.31 Cell migration effects of fractions with positive standard on NCI-H23 cell

4.11.3 Annexin V assay

Apoptosis profiles are displayed in a quadratic format showing various stages of apoptosis after treatment of A549 lung cancer cells with fractions and positive control. Figure 4.32 shows PF1 induces early apoptosis 21.55% and late apoptosis 18.80%, PF2 induces early apoptosis 38.45% and late apoptosis 22.89%, PF3 induces early apoptosis 50.06% and late apoptosis 26.00%, PF4 induces early apoptosis 29.74% and late apoptosis 27.97%, PF5 induces early apoptosis 50.95% and late apoptosis 44.80%

and PF6 induces early apoptosis 17.80% and late apoptosis 68.40% compared to control group using lupeol and doxorubicin as positive control.

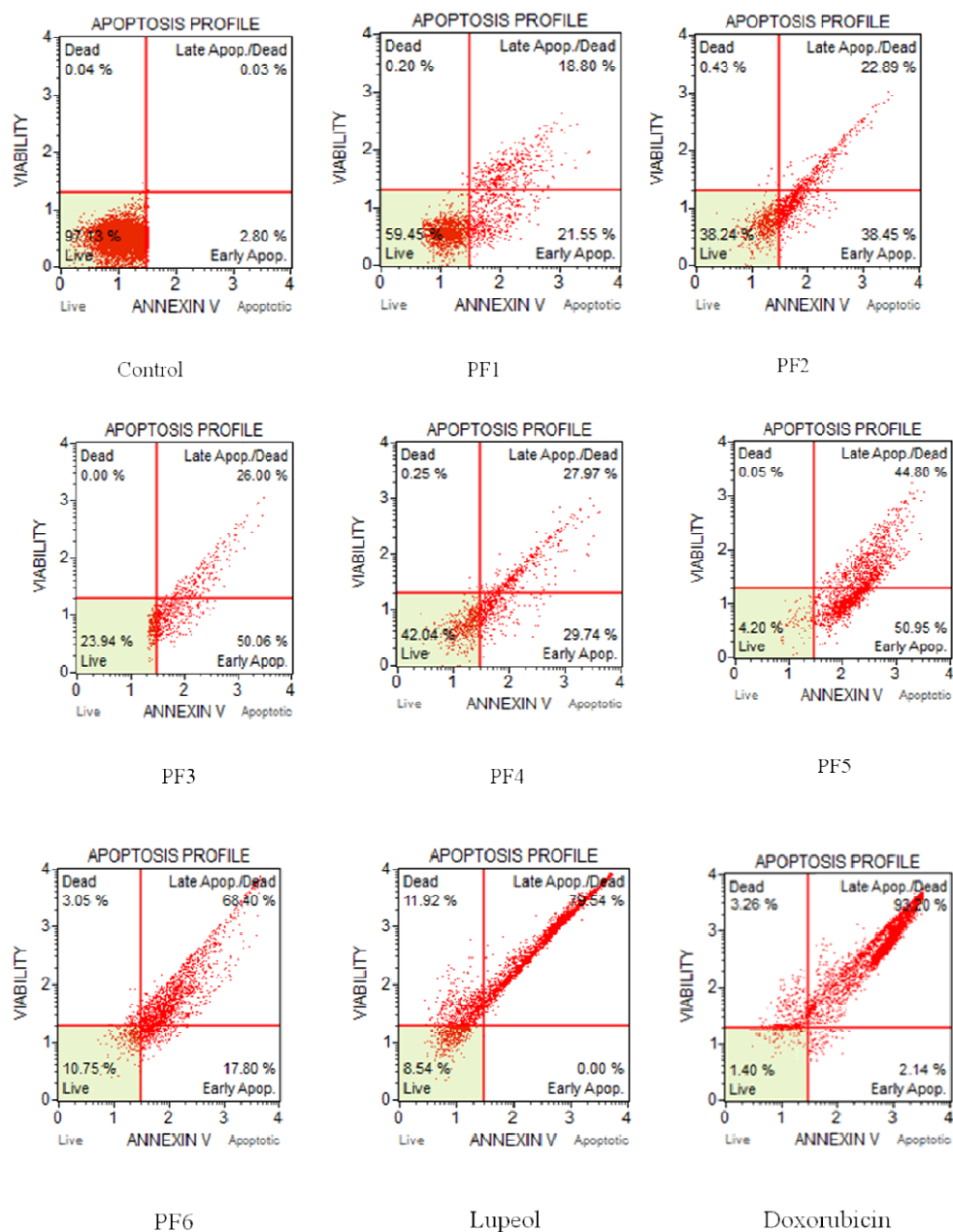


Figure 4.32 Apoptosis profile of fractions on A549 cell line

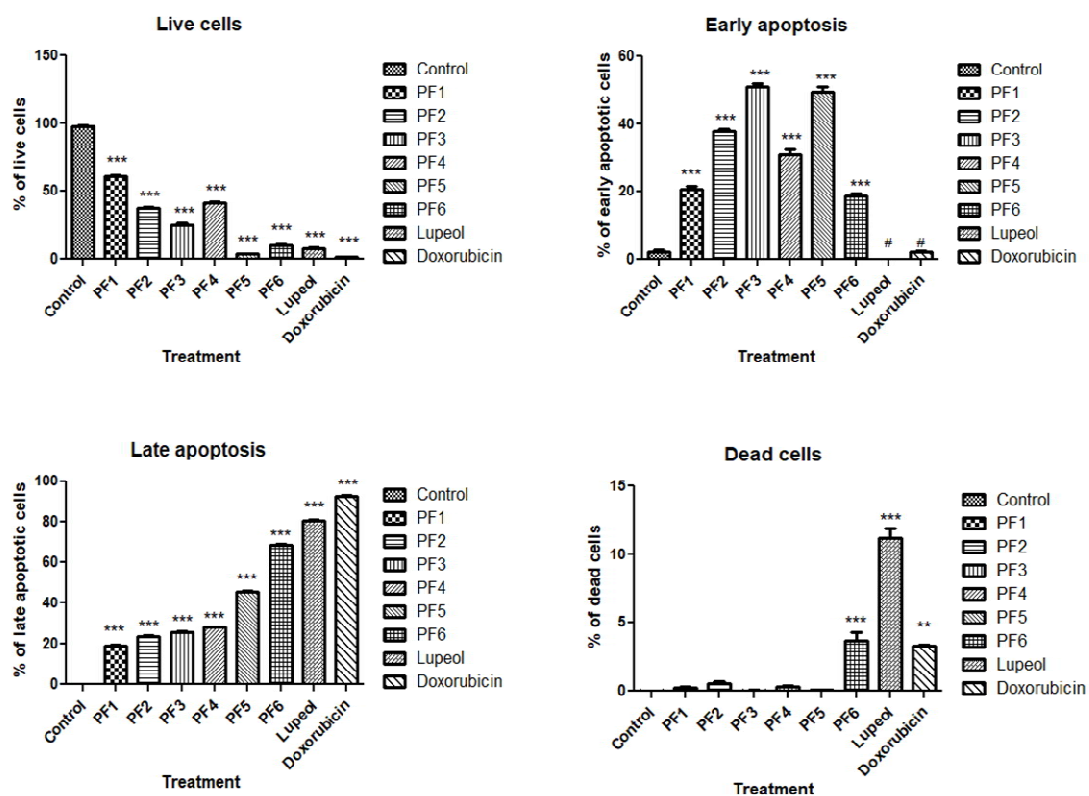


Figure 4.33 Graphical representation of stages of apoptosis (All data presented are the Mean \pm SD and are representative of three independent experiments. values < 0.05 were considered to be statistically significant, and significance was marked as *** p values <0.001 , # represented as non significant)

Apoptosis profiles are displayed in a quadratic format showing various stages of apoptosis after treatment of NCI-H23 lung cancer cells with fractions and positive control. Figure 4.34 shows PF1 induces early apoptosis 60.80% and late apoptosis 4.10%, PF2 induces early apoptosis 0.54% and late apoptosis 81.86%, PF3 induces early apoptosis 54.07% and late apoptosis 0.77%, PF4 induces early apoptosis 71.70% and late apoptosis 6.00%, PF5 induces early apoptosis 62.19% and late apoptosis 0.83% and PF6 induces early apoptosis 0.45% and late apoptosis 93.20% compared to control group using lupeol and doxorubicin as positive control.

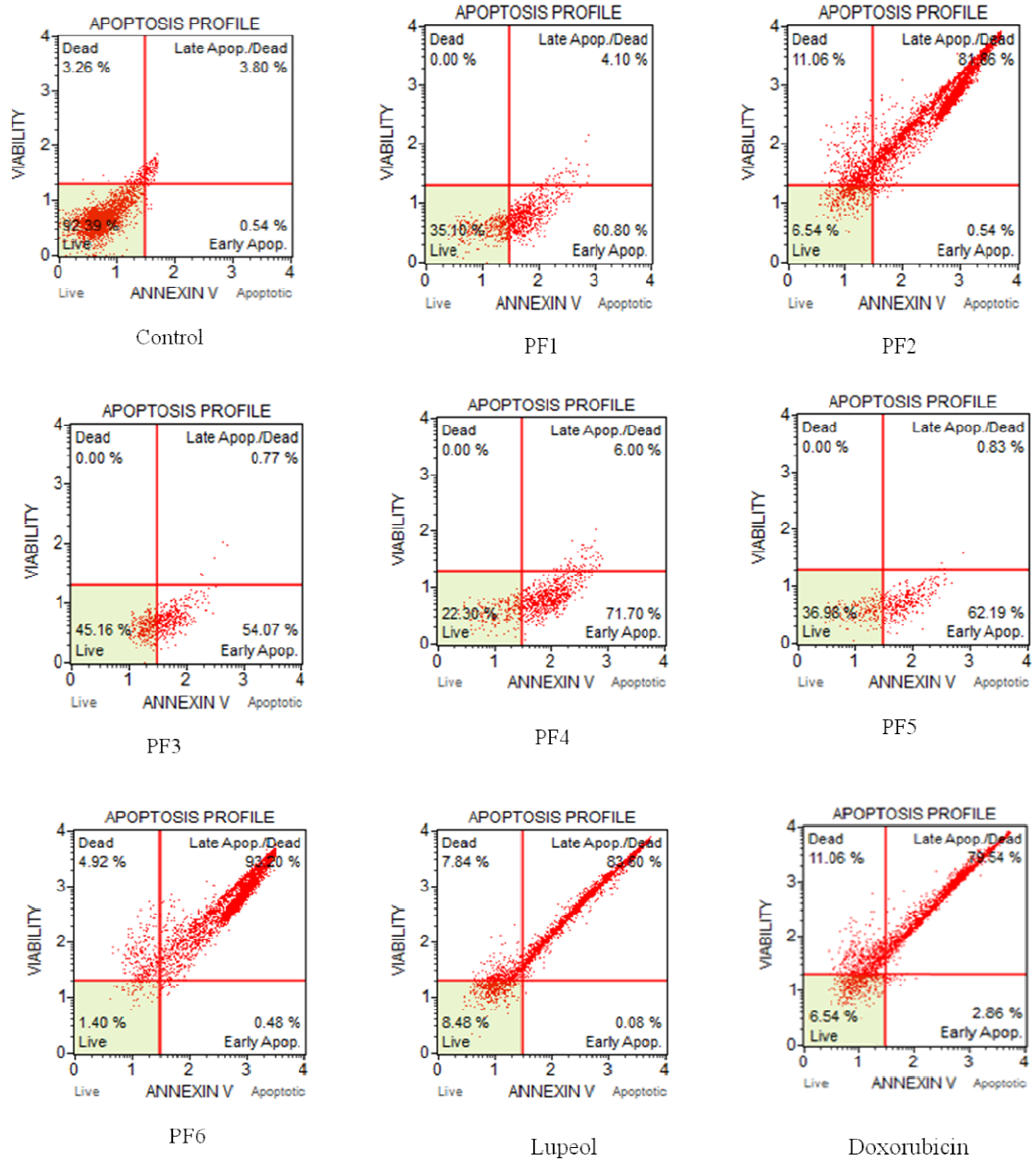


Figure 4.34 Apoptosis profile of fractions on NCI-H23 cell line

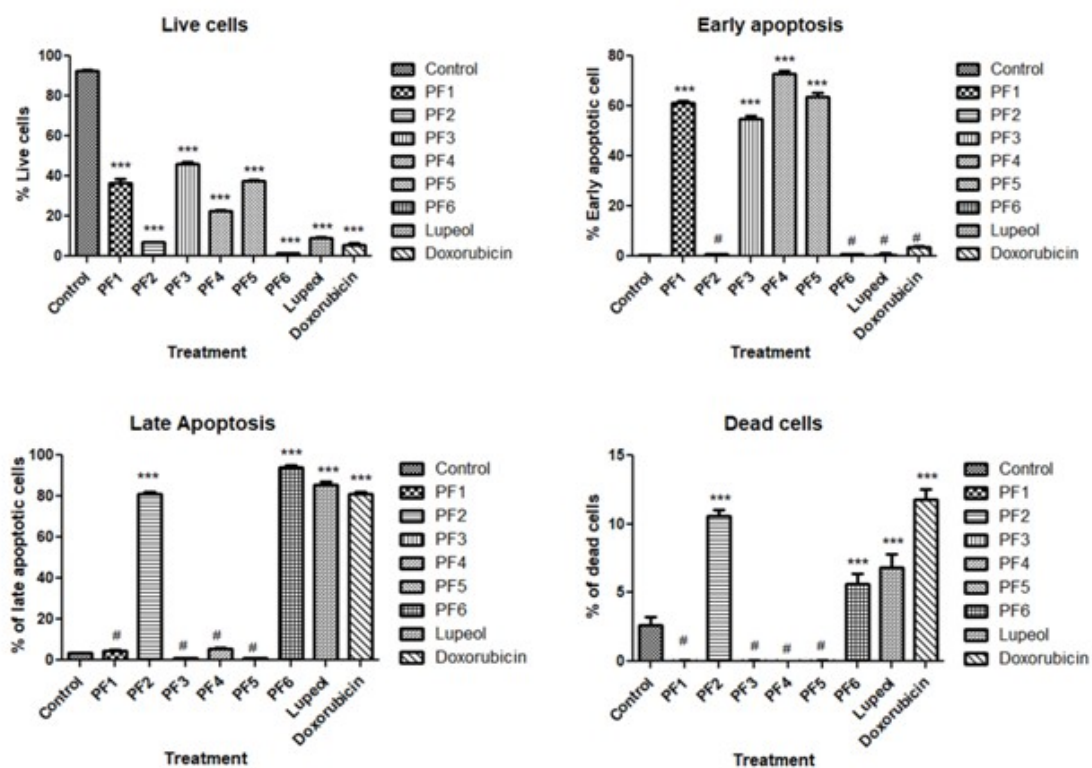


Figure 4.35 Graphical representation of stages of apoptosis (All data presented are the Mean \pm SD and are representative of three independent experiments. values < 0.05 were considered to be statistically significant, and significance was marked as * p values<0.001, # represented as non significant**

4.11.4 Caspase 3/7 Assay

One of the important parameters that play essential roles in necrosis, apoptosis, and inflammation is caspase enzymes which are a family of cysteine proteases, cause cleavage of cellular proteins¹¹. To check whether the apoptosis is induced by the fractions of A1 is depend upon the caspase's activation. The caspase 3/7 activity was evaluated on A549 and NCI-H23 cells treated with the fractions of A1 extract for 24 hrs. caspase 3/7 activity of fractions was recorded as PF6>PF5>PF3>PF4>PF2>PF1 on both the cell line. The positive control used here is lupeol and doxorubicin. Graphical representation of caspase 3/7 activity on both cell lines is shown in Figure 4.36.

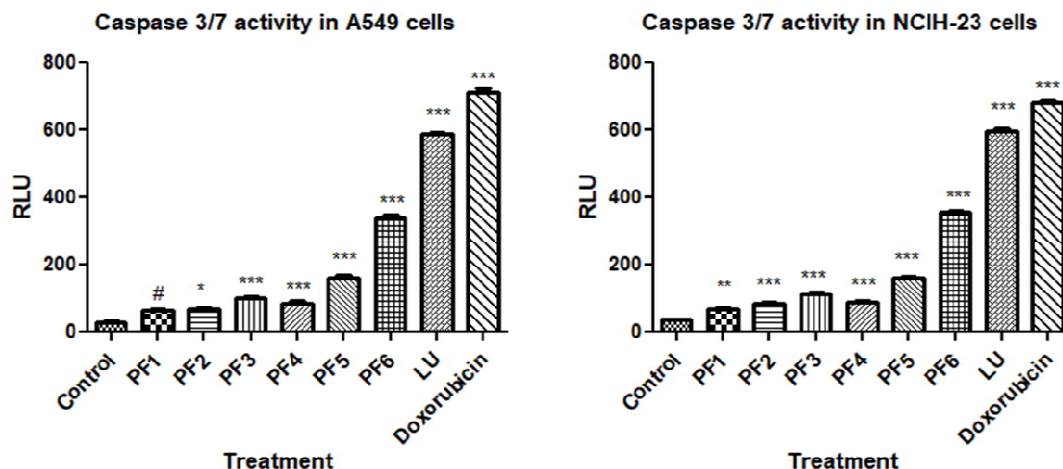


Figure 4.36 Graphical representation of caspase 3/7 activity (All data presented are the Mean \pm SD and are representative of three independent experiments. Values < 0.05 were considered to be statistically significant, and significance was marked as * p values < 0.05 , ** values < 0.01 , and ***values < 0.001 , # represented as non significant)

4.11.5 Comet assay

The comet assay was used to examine the influence of fractions of A1 extracts on DNA damage in A549 and NCI-H23 cells. Figure 4.37 represent the typical image of comets exposed to fractions of A1 extract in the A549 cell line. A high % of DNA in the tail indicated that DNA has fragmented and is responsible for apoptosis. Figure 4.38 presents the distribution of A549 cells based on the percentage of damaged DNA in the comet tail. Figure 4.39 represent a typical image of comets exposed to fractions of A1 extract in the NCI-H23 cell line. Among all the fractions genotoxicity were detected in PF5 and PF6 fractions in both the cell line. Figure 4.40 presents the distribution of NCI-H23 cells based on the percentage of damaged DNA in the comet tail.

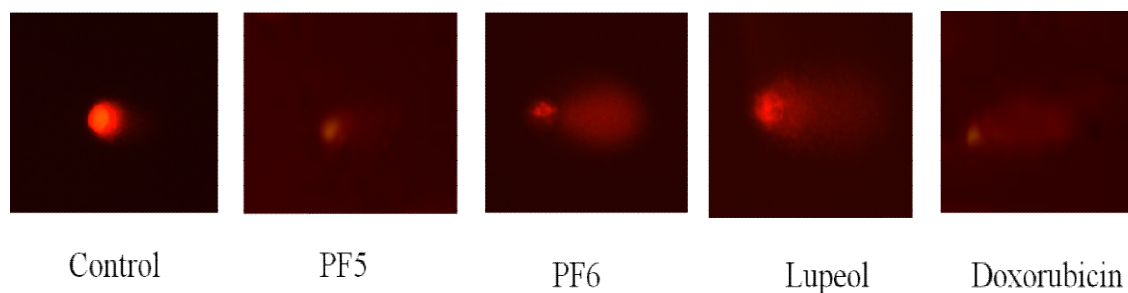


Figure 4.37 Representative images of comets showing the genotoxic effect of Fractions on A549 cells analysed by comet assay

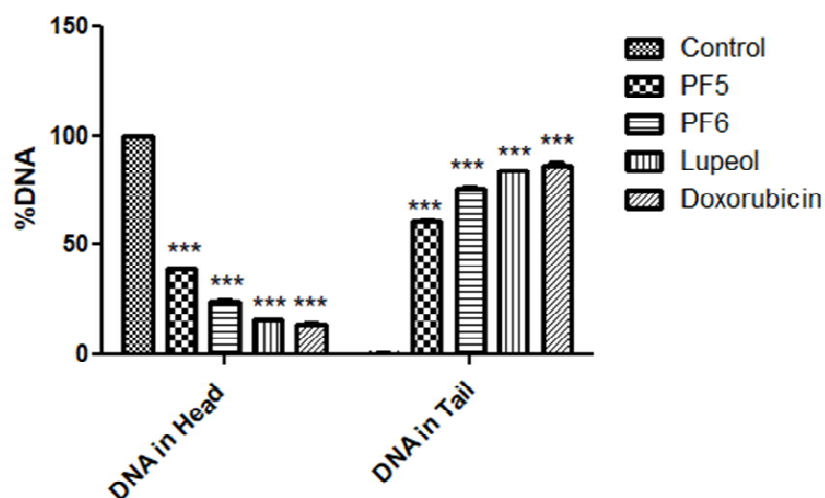


Figure 4.38 Graphical representation of DNA fragmentation activity in A549 cell line (All data presented are the Mean \pm SD and are representative of three independent experiments. Values < 0.05 were considered to be statistically significant, and significance was marked as *** p values < 0.001)

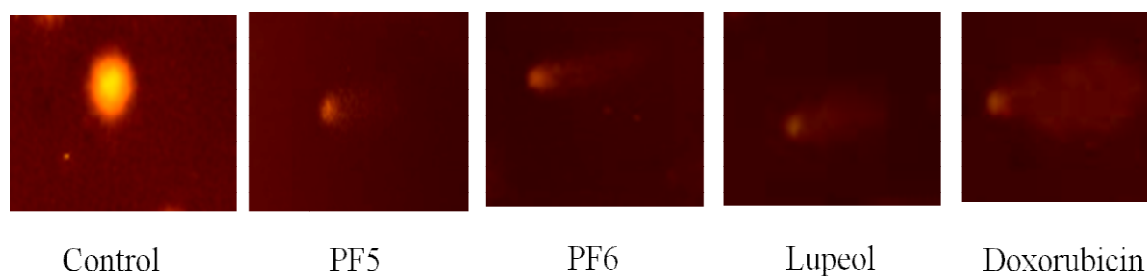


Figure 4.39 Representative images of comets showing the genotoxic effect of Fractions on NCI-H23 cells analysed by comet assay

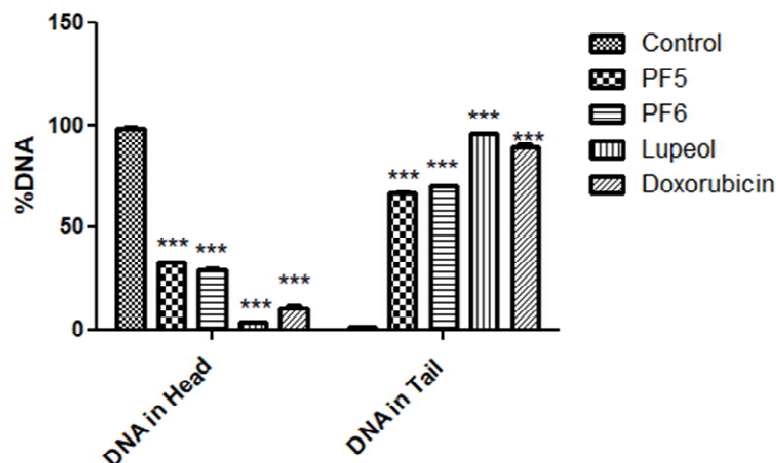


Figure 4.40 Graphical representation of DNA fragmentation activity in NCI-H23 cell line (All data presented are the Mean \pm SD and are representative of three independent experiments. Values < 0.05 were considered to be statistically significant, and significance was marked as *** p values < 0.001)

O.bracteatum is an important source of drugs used in traditional medicine to cure different diseases such as Leprosy, Urinary disorder, Fever, Dyspnea, Cough, As a tonic in building the body's immune resistance, Asthma, Bronchitis, Spasmolytic, Rheumatism, Syphilis, Wound and skin disease¹⁴⁻¹⁷. The present study evaluated the cytotoxicity of the extracts and fractions of *O.bracteatum* in lung cancer cells (A549 and NCI-H23). The results of this study show that the extracts and fractions exhibited cytotoxic effects towards both the cancer cell lines in a dose-dependent manner. The IC₅₀ values obtained for the various treatment protocols demonstrate that both cells are sensitive to the cytotoxic activity of the plant. Furthermore, the wound healing assay was performed to detect the inhibition of cell migration by the extract and fractions. To further elucidate the pathways of the cell death induced by the extracts and fractions, phosphatidylserine flipping was evaluated using the Annexin/PI flow cytometric assays. Exposure of phosphatidylserine on the external surface of the cell membrane is generally accepted as one of the biomarkers of apoptosis¹⁸. Results demonstrate that the extracts and fractions induce early and late apoptosis. Apoptosis is a protective mechanism that maintains tissue homeostasis by removing ailing cells. Two main pathways involved in apoptosis are intrinsic pathway (mitochondrial) and extrinsic (death receptor) pathways¹⁹. Caspase-3/7 is one of the effector caspases that is involved in the final execution of dying cells. The results showed that the extracts

and fractions increase the caspase-3/7 activity in both the cell line. However, comet assay is developed for detecting DNA damage; results demonstrated that a mixture of extract A1 and A2, PF5 and PF6 showed genotoxicity against cancer cells.

4.12 Identification and characterization of compound C-1 isolated from fraction PF5

4.12.1 Physical characteristic of compound C-1

State: Solid crystalline

Color: White

4.12.2 Chemical characteristic of compound C-1

In the TLC study, compound C-1 from fraction PF5 shows R_f 0.65 in the mobile phase Toluene: methanol (9.6:0.4), spraying with anisaldehyde sulphuric acid shows the violet color spot. (Fig. 4.41)



C-1

Figure 4.41 TLC of compound C-1

4.12.3 Spectroscopic analysis of compound C-1²⁰

4.12.3.1 IR Spectra of C-1

The IR Spectrum of proposed compound C-1 Showed Absorption at $2850\text{-}2958\text{cm}^{-1}$ was assigned to Asymmetric aliphatic -CH stretching of -CH_2 and -CH_3 groups. A band Observed at 1548cm^{-1} was Assigned to $\text{C}=\text{C}$ Stretching.

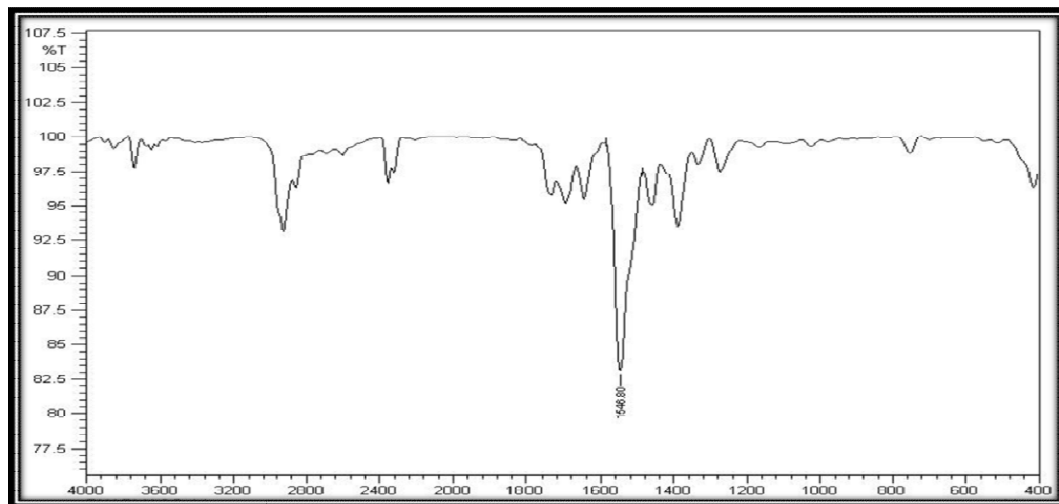


Figure 4.42 IR spectra of Compound C-1

4.12.3.2 Mass spectra of C-1

The Mass spectrum presents Molecular ion at M/Z 376 in Accordance with the Formula $\text{C}_{28}\text{H}_{40}$.

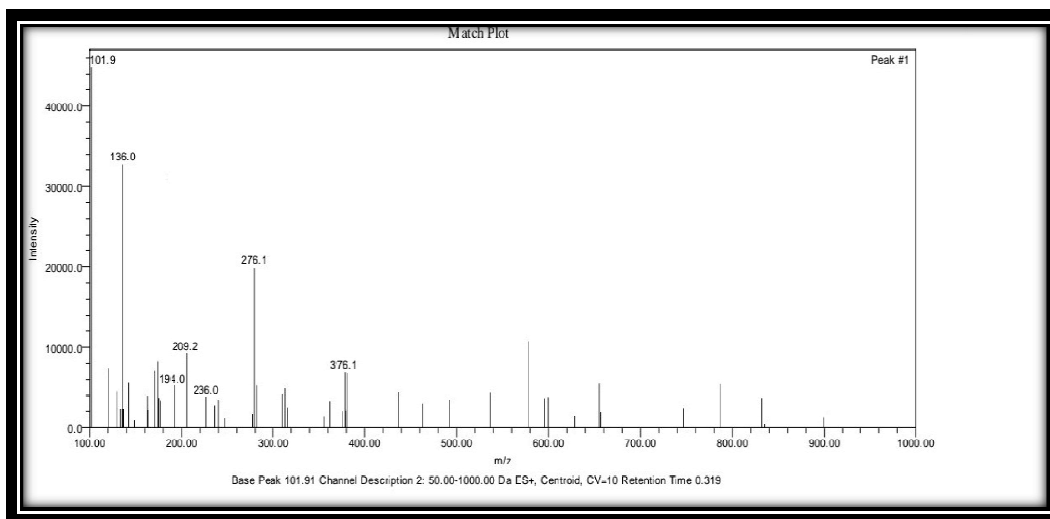


Figure 4.43 Mass spectra of compound C-1

4.12.3.3 NMR spectra of C-1

The H1 NMR showed a downfield 1H intensity at δ 5.34 ppm indicative of olefinic proton (H-6). It also showed olefinic proton at δ 5.14 ppm and at δ 5.04 ppm (H-21 and H-23). The Spectrum showed presence of six methyl proton at δ 0.69 (H-18), 0.84 (H-26), 0.82 (H-27), 0.86 (H-22), 1.00 (H-19) and 0.82 (H-28) respectively.

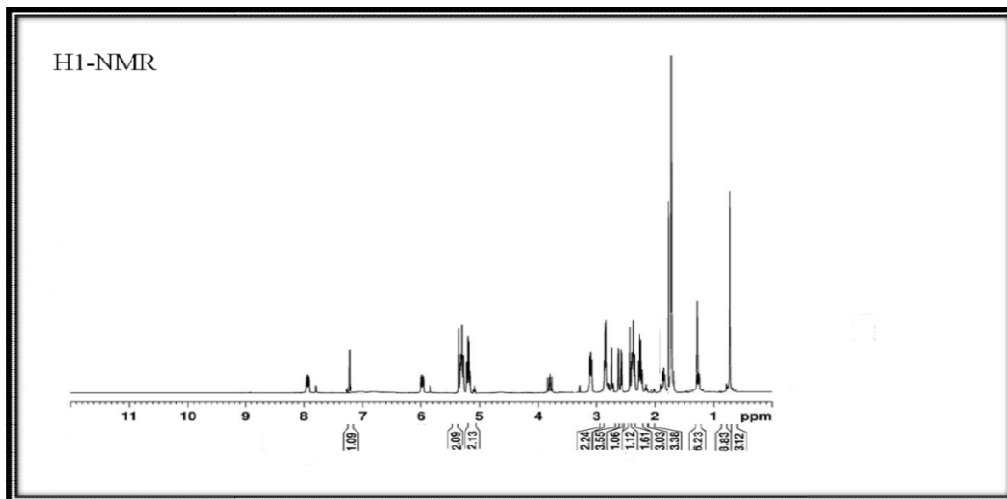


Figure 4.44 H1-NMR Spectra of compound C-1

¹³C NMR Spectrum revealed the presence of 28 carbons suggestive of a steroidal structure. The signals at δ C(141.01) C-5, 42.41 (C-12) and 36.17 (C-10) were assigned to three Quaternary carbons. Two Olefinic carbon signals at δ C 141.0 and 121.73 ppm were for (C-4 and C-7) and Signals at δ C 138.0 and 128.95 ppm for (C-21 and C-23).

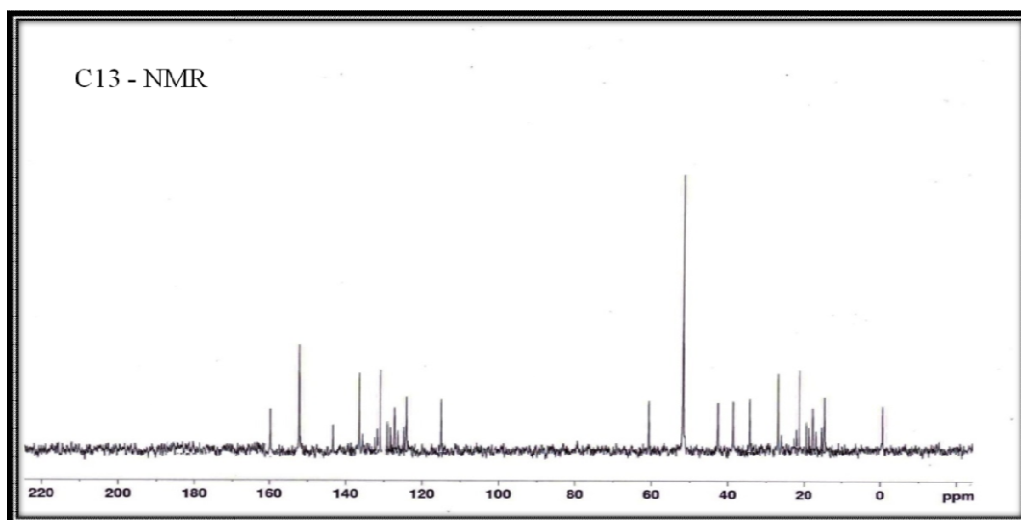


Figure 4.45 C13-NMR spectra of compound C-1

4.12.4 Probable structure of compound C-1

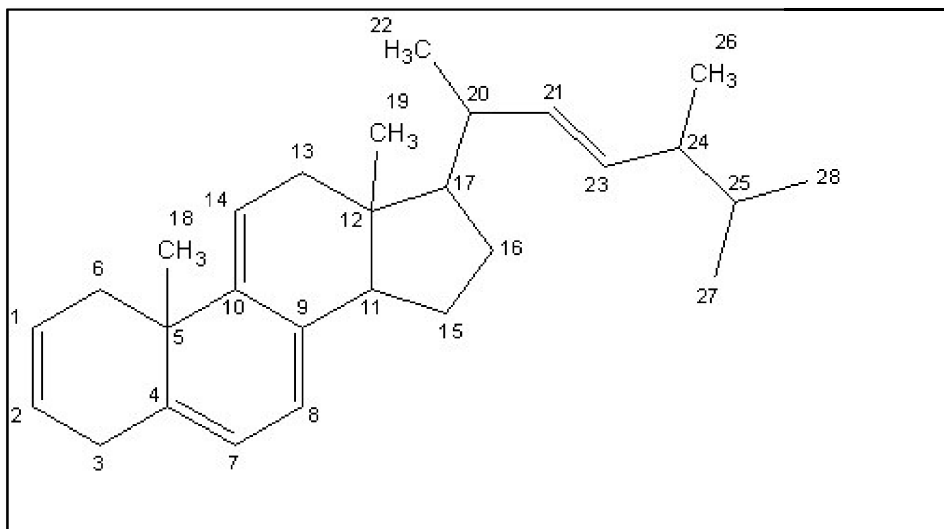


Figure 4.46 Structure of C-1: 17-(5,6-dimethylhept-3-en-2-yl)-10,13-Dimethyl-4,10,12,13,14,15,16,17-octahydro-1H-Cyclopenta[a]phenanthrene

4.13 Identification and characterization of compound C-2 isolated from fraction PF6

4.13.1 Physical characteristic of compound C-2

State: Solid powder

Color: Yellow

4.13.2 Chemical characteristic of compound C-2

In the TLC study, compound C-2 from fraction PF6 shows R_f 0.64 in the mobile phase n-Hexane: ethyl acetate: methanol (9.8:0.2:0.1), it shows yellow fluorescence in UV 366 light, after spraying with 10% methanolic KOH it shows the pink color band. (Fig. 4.47)



Figure 4.47 TLC of compound C-2

4.13.3 Spectroscopic analysis of compound C-2²⁰

4.13.3.1 IR Spectra of C-2

The IR spectra showed the characteristic absorption band at 1227cm^{-1} due to ether linkage, aromatic C-H stretching band observed between 3066cm^{-1} in IR region, –C=O stretching absorption band observed in between 1688cm^{-1} , broad absorption band obtained at 3421cm^{-1} confirms the phenolic -OH present.

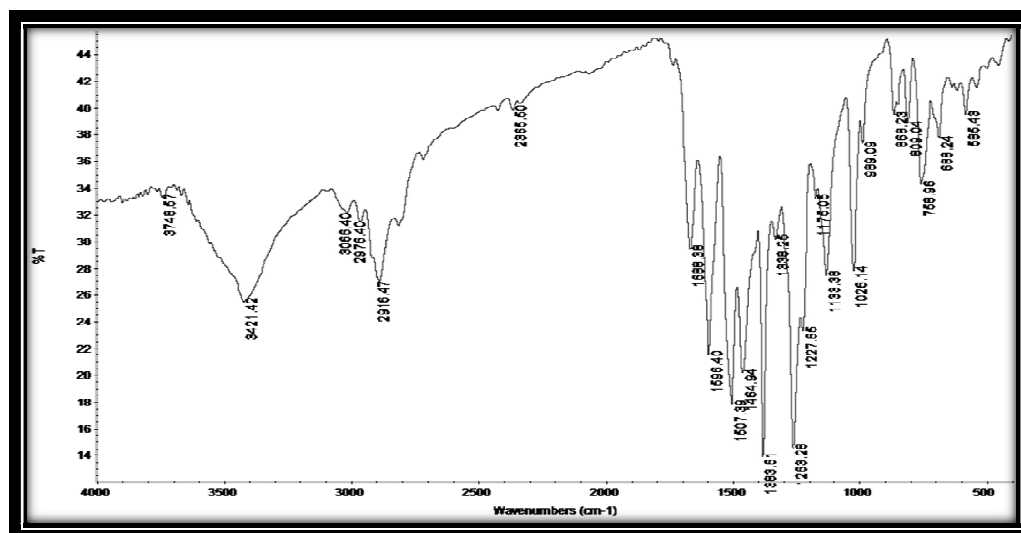


Figure 4.48 IR spectra of compound C-2

4.13.3.2 Mass Spectra of C-2

The molecular formula $C_{14}H_{10}O_4$ was established on the basis of the mass spectrum showing the molecular ion peak at m/z (relative intensity) - 242gm/mol and base peak at m/z 199gm/mol.

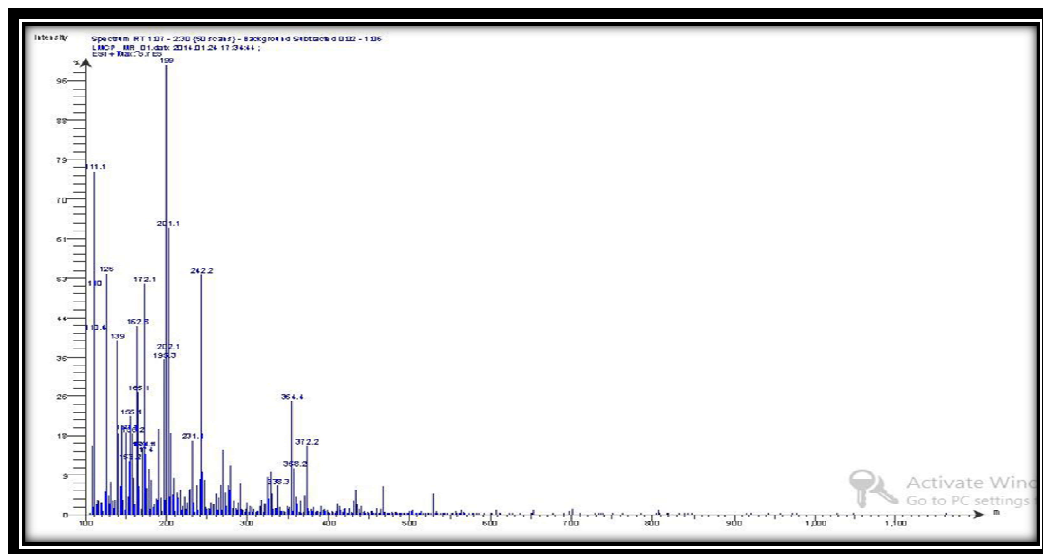
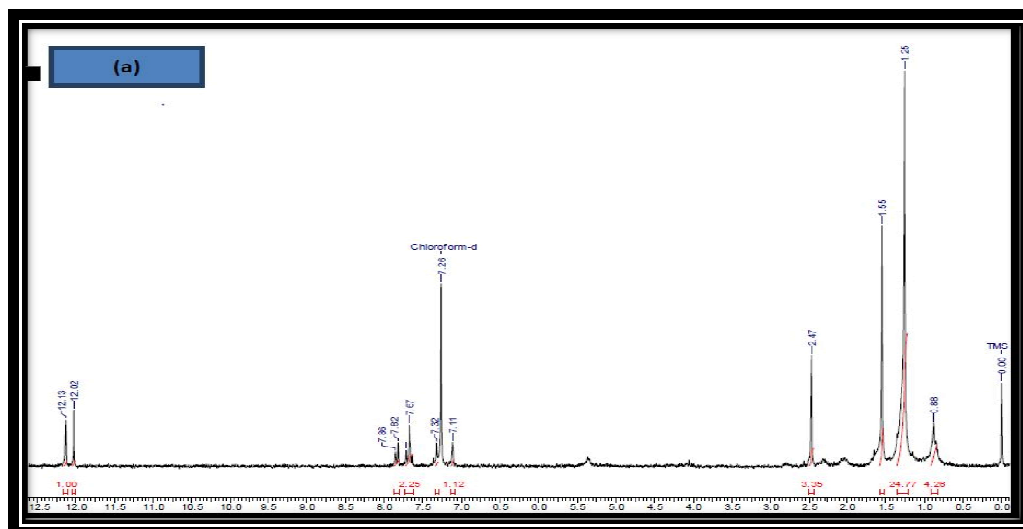
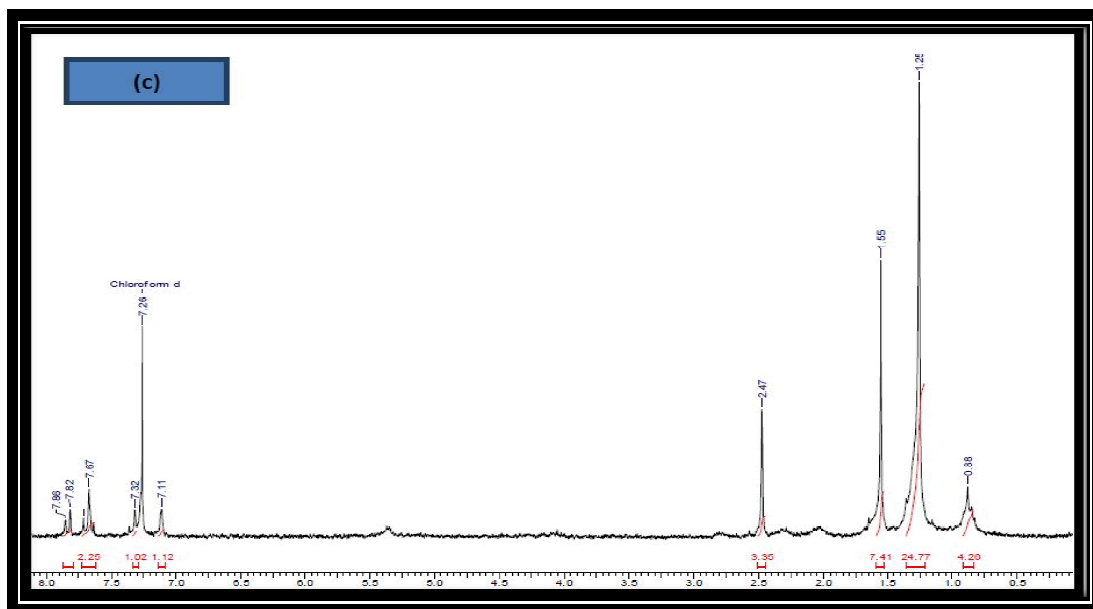
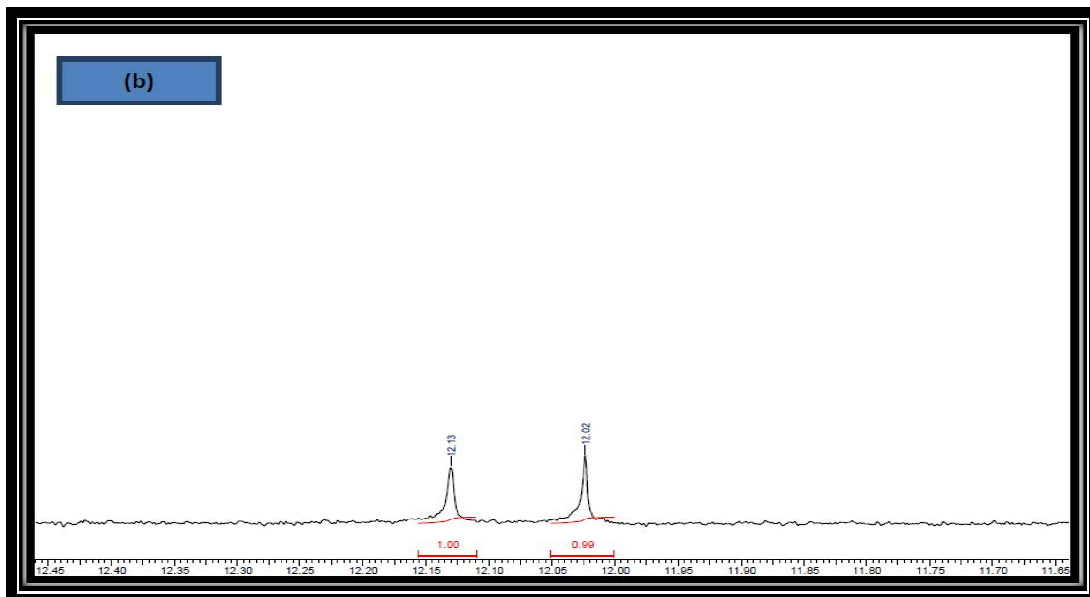


Figure 4.49 Mass spectra of compound C-2

4.13.3.3 NMR Spectra of C-2

Protons of the $-CH_3$ group were detected at 2.47ppm, All aromatic protons (Ar-H) signal observed between the ranges of 7.11-7.86ppm, Moreover, phenolic hydroxyl groups present in the proposed compound confirmed on the bases of peaks seen at $\delta=12.02$ and 12.13ppm.





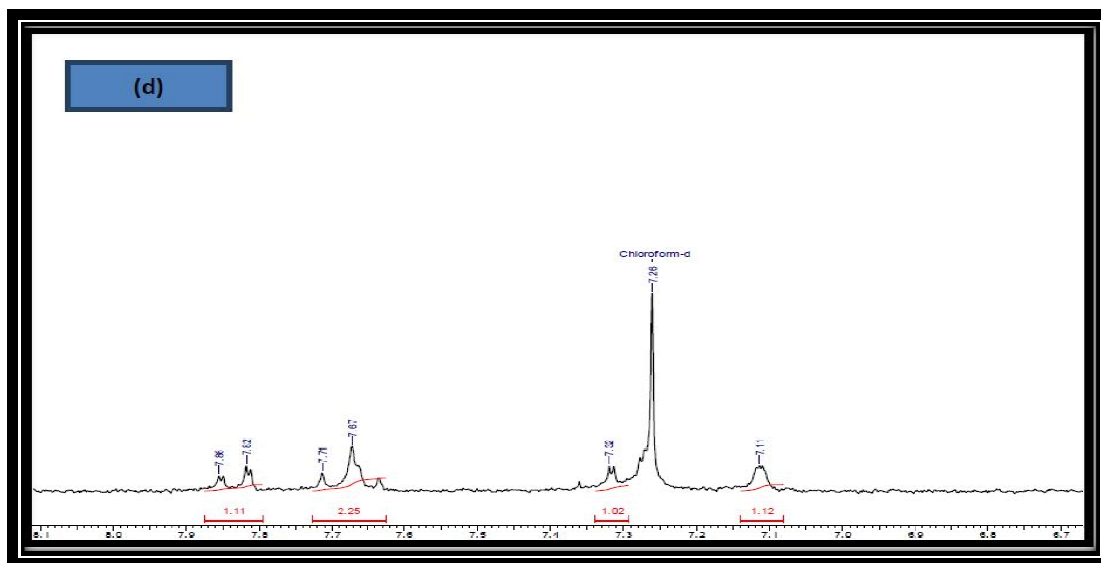


Figure 4.50 (a), (b), (c), (d) ^1H -NMR Spectra of compound C-2

4.13.4 Probable structure of compound C-2

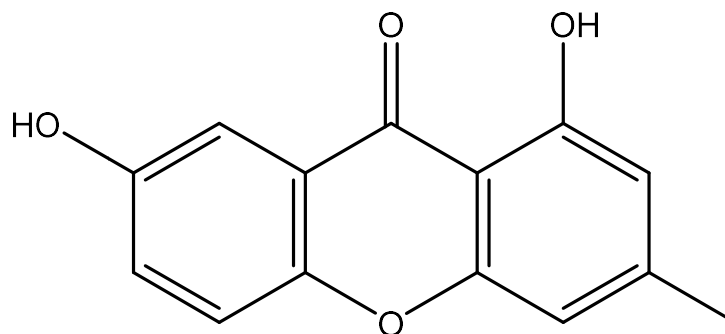


Figure 4.51 Structure C-2 : 1,7-dihydroxy-3-methyl-9H-xanthene-9-one

Molecular weight: 242gm/mol and Molecular formula: $\text{C}_{14}\text{H}_{10}\text{O}_4$

4.13.5 Quantification of C-2 by HPTLC Method

HPTLC chromatogram of C-2 was taken with Fraction PF6 and it was confirmed by scanning wavelength 254nm.

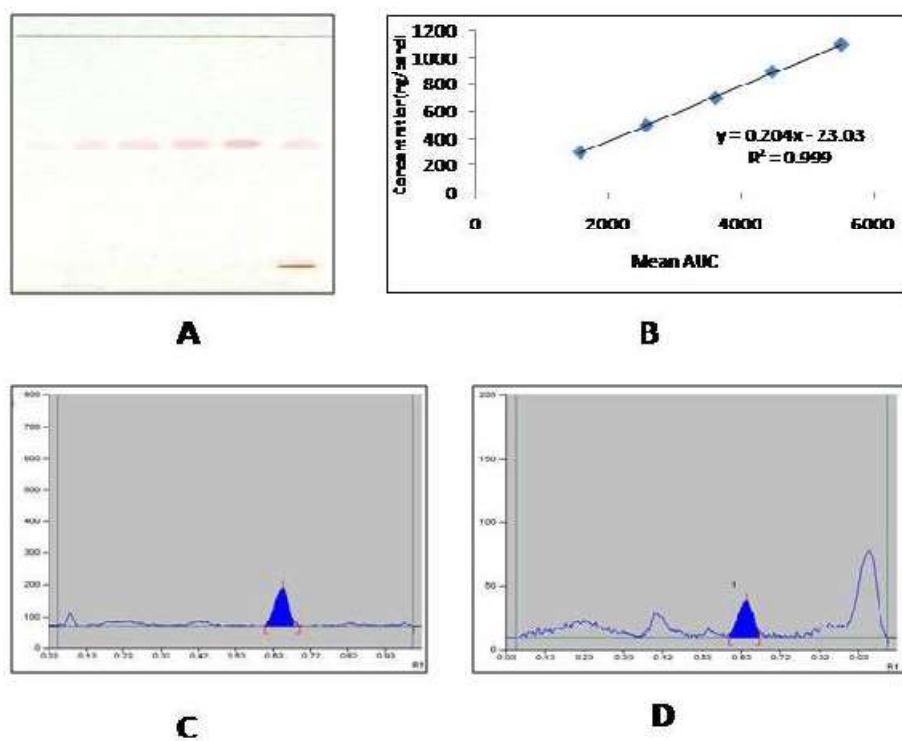


Figure 4.52 (A) HPTLC study of C-2, (B) Calibration curve of C-2, (C) chromatogram of C-2, (D) chromatogram of fraction PF6

The calibration data ranged between 300-1100ng/band. The calibration curve was obtained by plotting concentration vs. peak area. HPTLC studies revealed the purity of the compound-I resolving at Rf 0.64 and the content of compound C-2 was found to be $0.17 \pm 0.11\%$ w/w in the plant.

4.14 HRLC-MS study of A1+A2 and PF1 to PF6

Conventional methods of characterization of bioactive phytoconstituents involve a series of steps that include extraction, evaluation, chromatographic separation, and spectroscopic characterization. Hence complexity of the crude extract is reduced by using high throughput and high-resolution techniques. It is a key to pinpointing the pharmaceutically potent bioactive. HR-LC-ESI-MS/MS was used to characterize the chemical composition of a mixture of A1 and A2 extract and fractions of A1 extract of *O. bracteatum*. The representative base peak chromatogram of the mixture of A1 and A2 and fractions is depicted in Figure 4.53 and phytochemical identification data is presented in Table 4.16, 4.17, 4.18, 4.19, 4.20, 4.21, 4.22, which summarizes the tentative compounds characterized from these extracts including their retention time,

experimental m/z, mass, proposed metabolites, and molecular formula. Mixture of A1 and A2 shows presence of pyrrolizidine alkaloids, xanthone, coumarins; whereas fraction PF1 shows presence of phthalates and fatty acids, PF2 shows presence of mainly Vitamin E, Vitamin A, PF3 is rich with phytosterols, PF4 and PF5 mainly contains phenolics and flavonoid compounds, PF6 shows presence of Shikonin, coumarins, Xenthone.

Literature suggests that pyrrolizidine alkaloids, xenthones and coumarins show growth inhibitory activity against human lung cancer A549 cells²¹, 9 cis retinal possess anticancer activity by binding with cellular retinol-binding proteins²², Vitamin E and their isomer having anticancer activity²³, Ursolic acid suppressing vaccinia-related kinase 1-mediated damage repair in lung cancer cells²⁴, betulin derivatives having anticancer activity²⁵, Ferulic acid, and caffeic acid affect apoptotic signaling pathways in cancer²⁶, Flavone and flavanone are reported to have anticancer activity in breast cancer and cervical cancer cell lines²⁷, Shikonin-induced necroptosis in non-small cell lung cancer cells²⁸. Hence, we could correlate that fraction containing phytoconstituents responsible for *in-vitro* activity against lung cell cancer.

Table 4.16 List of compounds identified in the mixture of A1 and A2 by Q-Exactive Plus Biopharma

Sr. No.	Name	Molecular formula	Retention time	Mass
1	Retronecine	C8 H13 N O2	1.076	155.09444
2	Trachelanthamidine	C8 H15 N O	1.141	141.1151
3	L-Tyrosine	C9 H11 N O3	3.86	181.07361
4	Monocrotaline	C16 H23 N O6	8.046	325.15221
5	Dehydroretronecine	C8 H11 N O2	8.655	153.07868
6	2-Hydroxyphenylalanine	C9 H11 N O3	9.101	181.07361
7	2-Methyl-3H-pyrrolizin-3-one	C8H7NO	13.998	133.147
8	Gelsemine	C20 H22 N2 O2	14.827	322.16768
9	Formononetin	C16 H12 O4	17.032	268.07317
10	3,3,6,6-Tetramethyl-1,8-dioxo-2,3,4,5,6,7,8,9-octahydro-1H-xanthene-9-carboxylic acid	C18H22O	17.399	318.14632
11	3-Hydroxyfluorene	C13 H10 O	17.84	182.07311
12	17 α -Ethinylestradiol	C20 H24 O2	19.866	296.17739
13	Cafestol	C20 H28 O3	20.711	316.20348
14	7-Hydroxycoumarine	C9 H6 O3	21.424	162.03145
15	Ursolic acid	C30 H48 O3	23.464	456.36022
16	Betulin	C30 H50 O2	25.233	442.38094

**Table 4.17 List of compounds identified in the PF1 by Q-Exactive Plus
Biopharma**

Sr.No.	Name	Molecular formula	Retention time	Mass
2	12-Oxo phytodienoic acid	C18 H28 O3	21.106	292.2032
4	Docosatrienoic acid	C22 H38 O2	23.495	334.28682
5	Bis(2-ethylhexyl)adipate	C22 H42 O4	24.236	370.30754
6	Cholecalciferol	C27 H44 O	24.429	384.33876
8	Arachidonic acid	C20 H32 O2	27.706	304.23982

**Table 4.18 List of compounds identified in the PF2 by Q-Exactive Plus
Biopharma**

Sr.No.	Name	Molecular formula	Retention time	Mass
1	3-Hydroxyfluorene	C13 H10 O	18.032	182.07298
2	Polygodial	C15 H22 O2	20.822	234.16159
3	Estrone	C18 H22 O2	21.942	270.16139
4	(9cis)-Retinal	C20 H28 O	22.684	284.21349
5	Docosahexaenoic acid	C22 H32 O2	23.534	328.23982
6	D- δ -Tocopherol	C27 H46 O2	25.301	402.34911
7	Diisodecyl phthalate	C28 H46 O4	25.422	446.33902
8	Nootkatone	C15 H22 O	26.585	218.16669

**Table 4.19 List of compounds identified in the PF3 by Q-Exactive Plus
Biopharma**

Sr.No.	Name	Molecular formula	Retention time	Mass
1	Myristicin	C11 H12 O3	14.266	192.07846
2	2-Methoxyestrone	C19 H24 O3	18.525	300.17208
3	Zearalenone	C18 H22 O5	19.576	318.1461
4	8-iso Prostaglandin F2 α	C20 H34 O5	21.307	354.24001
5	β -Estradiol	C18 H24 O2	21.337	272.17726
6	D-Sphingosine	C18 H37 N O2	23.565	299.2817
7	Ursolic acid	C30 H48 O3	24.15	456.35942
8	Betulin	C30 H50 O2	24.742	442.38201

**Table 4.20 List of compounds identified in the PF4 by Q-Exactive Plus
Biopharma**

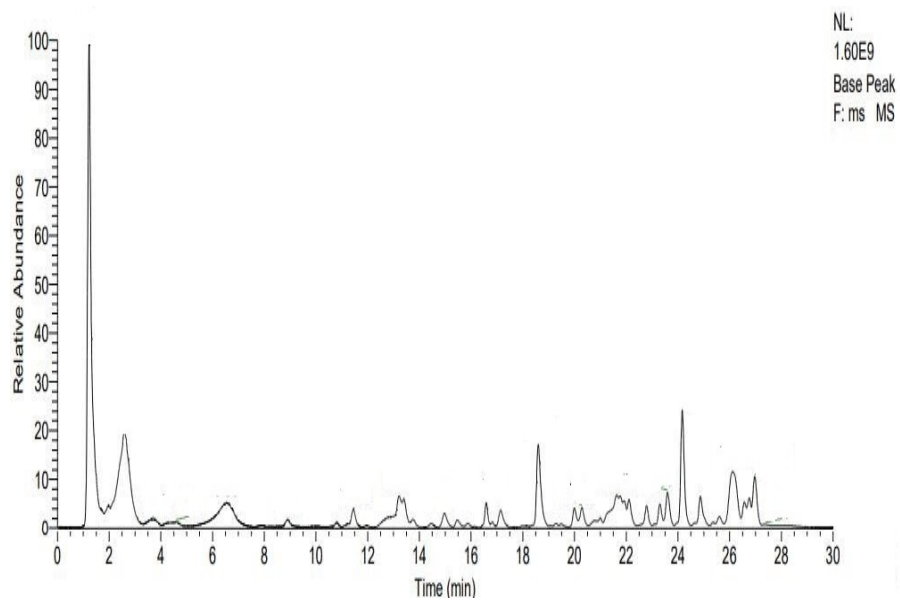
Sr.No.	Name	Molecular formula	Retention time	Mass
1	Leucine	C6 H13 N O2	1.229	131.09447
2	Vanillin	C8 H8 O3	8.937	152.04712
3	Isoferulic acid	C10 H10 O4	19.309	194.05777
4	Ferulic acid	C10 H10 O4	19.315	194.05777
5	Caffeic acid	C9 H8 O4	20.872	180.04201
6	7-Hydroxycoumarine	C9 H6 O3	20.873	162.03148
7	Sedanolid	C12 H18 O2	23.29	194.13048

**Table 4.21 List of compounds identified in the PF5 by Q-Exactive Plus
Biopharma**

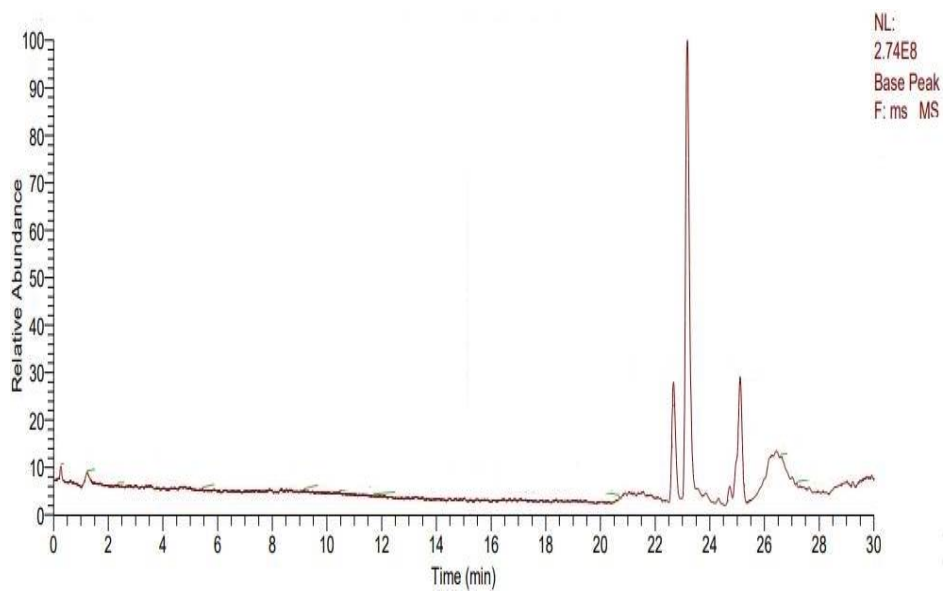
Sr.No.	Name	Molecular formula	Retention time	Mass
1	Apocynin	C ₉ H ₁₀ O ₃	8.154	166.06275
2	Flavone	C ₁₅ H ₁₀ O ₂	19.942	222.06775
3	Chalcone	C ₁₅ H ₁₂ O	20.586	208.08846
4	Flavanone	C ₁₅ H ₁₂ O ₂	20.653	224.08345
5	Biotin	C ₁₀ H ₁₆ N ₂ O ₃ S	21.362	244.0884
6	4-Methoxycinnamic acid	C ₁₀ H ₁₀ O ₃	22.848	178.06276
7	Biochanin A	C ₁₆ H ₁₂ O ₅	23.71	284.068

**Table 4.22 List of compounds identified in the PF6 by Q-Exactive Plus
Biopharma**

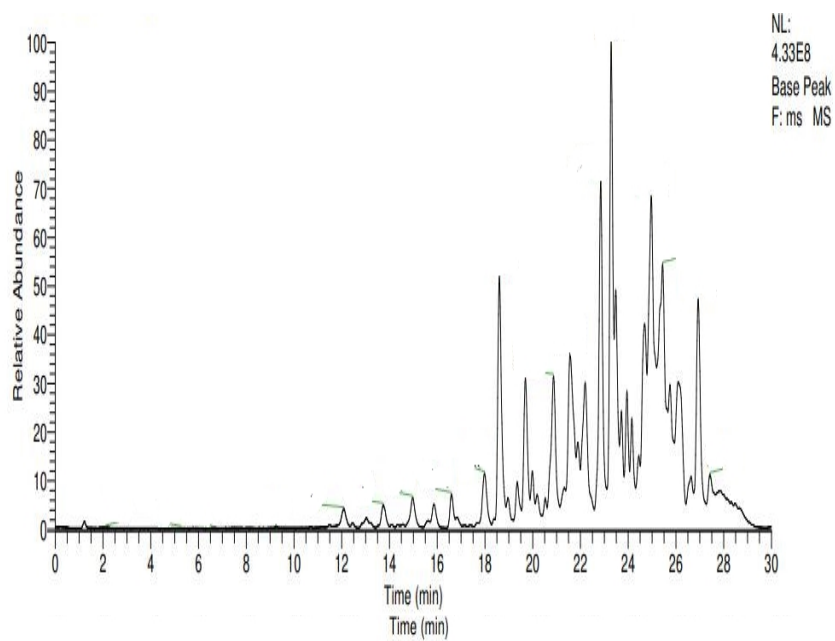
Sr.No.	Name	Molecular formula	Retention time	Mass
1	2,6-Di-tert-butyl-1,4-benzoquinone	C ₁₄ H ₂₀ O ₂	18.34	220.146
2	Licochalcone A	C ₂₁ H ₂₂ O ₄	20.572	338.15132
3	Lagochilin	C ₂₀ H ₃₆ O ₅	21.767	356.2555
4	Glycitein	C ₁₆ H ₁₂ O ₅	22.299	284.0681
5	Diosmetin	C ₁₆ H ₁₂ O ₆	23.206	300.06313
6	Shikonin	C ₁₆ H ₁₆ O ₅	25.89	288.099
7	α -Lapachone	C ₁₅ H ₁₄ O ₃	27.21	242.094



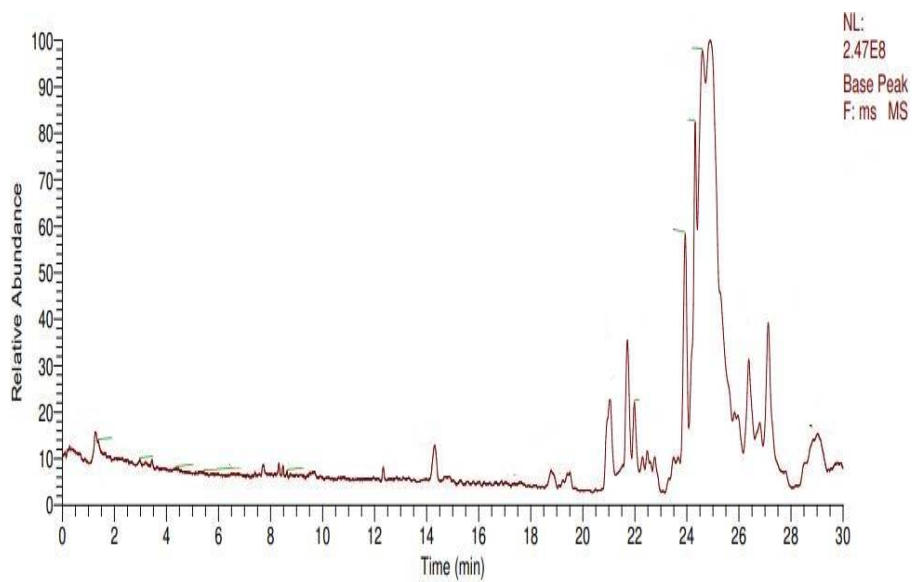
(a)



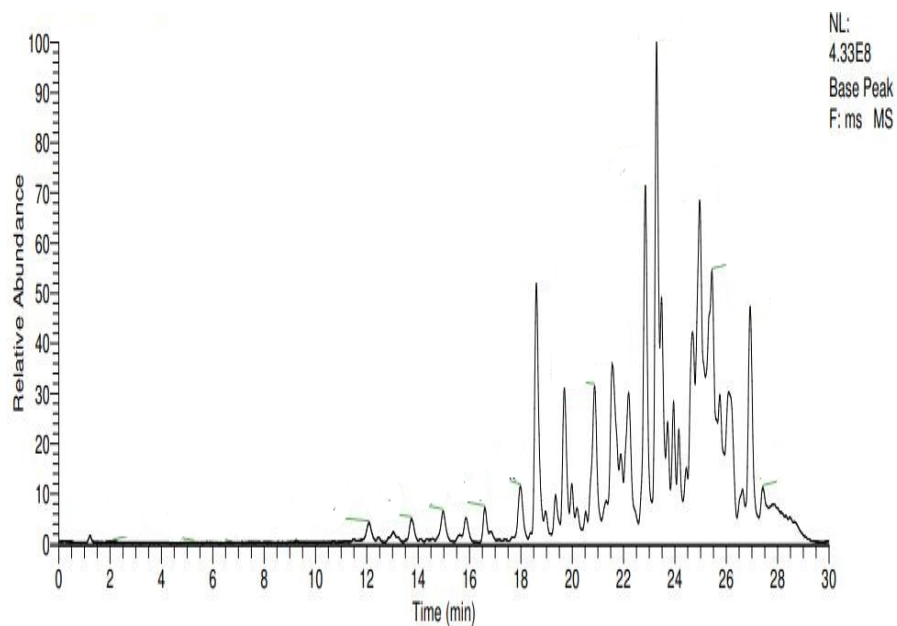
(b)



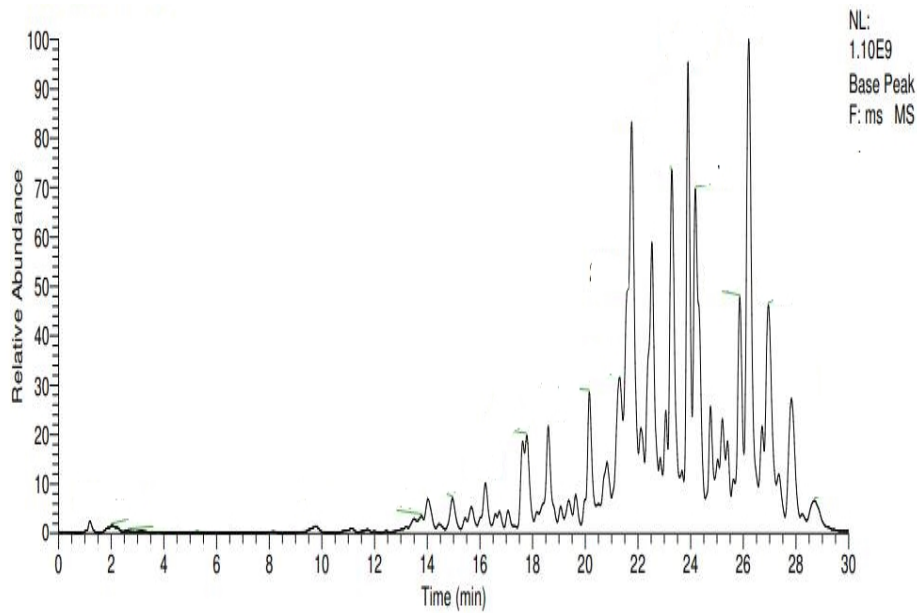
(c)



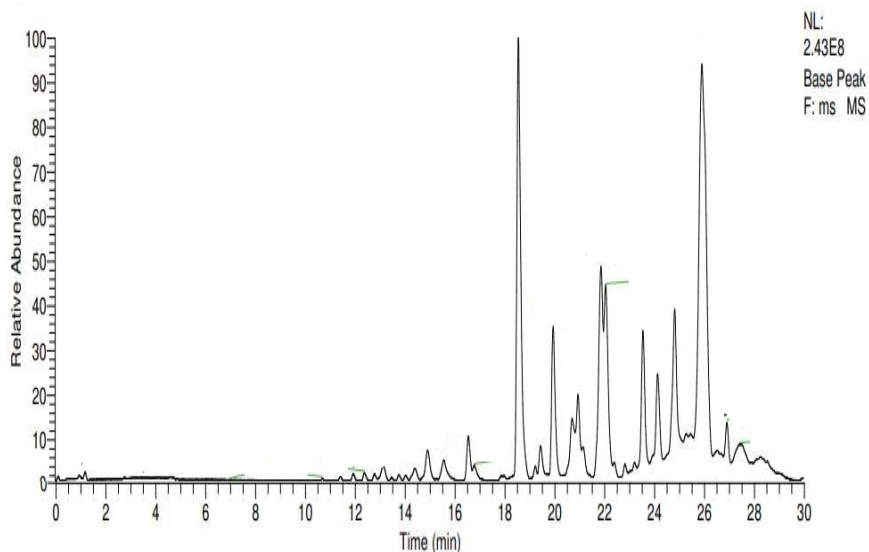
(d)



(e)



(f)



(g)

Figure 4.53 Chromatogram of extract and fractions. (a): chromatogram of mixture of A1 and A2, (b): chromatogram of fraction PF1, (c): chromatogram of fraction PF2, (d): chromatogram of fraction PF3, (e): chromatogram of fraction PF4, (f): chromatogram of fraction PF5, (g): chromatogram of fraction PF6

4.15 Identification and estimation of compounds from extract A1

4.15.1 Identification of β -sitosterol and Lupeol in PEF by TLC

Co-TLC of petroleum ether extract fraction (PEF) with standard β -sitosterol and Lupeol was carried out to identify the presence of β -sitosterol and Lupeol in PEF using Toluene: methanol (9.6:0.4) as mobile phase. In PEF purple and blue color spots were observed at the same R_f of β -sitosterol and Lupeol after spraying with anisaldehyde sulphuric acid reagent. For β -sitosterol R_f was 0.301 and for Lupeol R_f was 0.478. (Figure 4.54)

4.15.2 Estimation of β -sitosterol and Lupeol in PEF by HPTLC

HPTLC chromatogram of standard β -sitosterol and Lupeol were taken with PEF and it was confirmed by scanning at 525nm.

4.15.2.1 Calibration curves of β -sitosterol and Lupeol

The calibration data ranged between 1000-9000ng/spot for β -sitosterol and Lupeol. The calibration curve was obtained by plotting concentration vs. peak area.

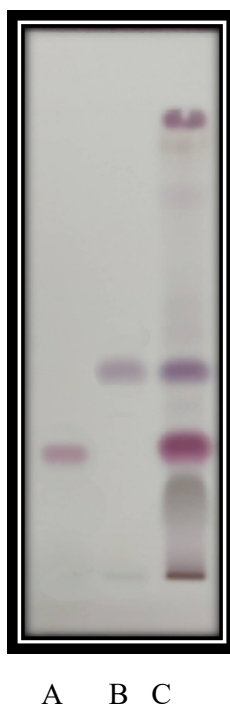


Figure 4.54 TLC of PEF (C) with standard β -sitosterol (A) and Lupeol (B)

Table 4.23 Calibration curve of β -sitosterol and Lupeol

Sr.No.	Compounds	Range (ng/spot)	Linear regression equation	r^2
1	β -sitosterol	1000-9000	$y = 2.895x + 3881$	0.999
2	Lupeol	1000-9000	$y = 3.498x + 4118$	0.999

4.15.2.2 Validation of HPTLC method for β -sitosterol and Lupeol

Linearity

The calibration curves showed linearity for both compounds with $r^2 > 0.99$. Linear regression analysis of the calibration curves of these compounds is provided in Table 4.23.

Precision

The interday precision coefficient of variation for compounds β -sitosterol and lupeol varied from 0.564 to 1.733 and 0.776 to 1.435 respectively. The intraday precision coefficient of variation for compounds β -sitosterol and lupeol varied from 0.521 to 1.109 and 0.507 to 1.217 respectively. (Table 4.24)

Table 4.24 Intra and interday precision analysis of β -sitosterol, lupeol

Marker	Concentration (ng/spot)	Intra-day precision (%CV)	Inter-day precision (%CV)
β -sitosterol	3000	0.521	0.633
	5000	1.109	1.733
	7000	0.734	0.564
Lupeol	3000	1.217	1.435
	5000	0.507	0.776
	7000	0.783	0.821

Specificity

The developed and validated method was found to be specific for quantifying compounds β -sitosterol and lupeol as distinct from their peak purity values and the absence of any other co-eluting peaks.

Limit of detection

The LODs were 218.07 and 228.68ng/spot for β -sitosterol and lupeol respectively. (Table 4.25)

Limit of Quantification

The minimum quantification limit was found to be 660.82 and 692.97ng/spot for β -sitosterol and lupeol respectively. (Table 4.25)

Recovery

The average recovery percentage was found to be 99.17% for β -sitosterol and 99.01% for lupeol. (Table 4.25)

Tablet 4.25 LOD, LOQ and recovery

Sr.No.	Compounds	LOD (ng/spot)	LOQ (ng/spot)	Recovery (%)
1	β -sitosterol	218.07	660.82	99.17
2	Lupeol	228.68	692.97	99.01

4.15.2.3 Quantification of β -sitosterol and lupeol

An external calibration procedure was applied for the quantification. The peak of compounds in a sample was identified by comparing the R_f value and UV spectra obtained in the reference standard. Both compounds were detected in PEF. (Table 4.26)

Table 4.26 Quantification (n=3) data of Extract A1

Sr.No.	Analyte	% content (w/w)
1	β -sitosterol	0.1021±0.04
2	Lupeol	0.1352±0.08

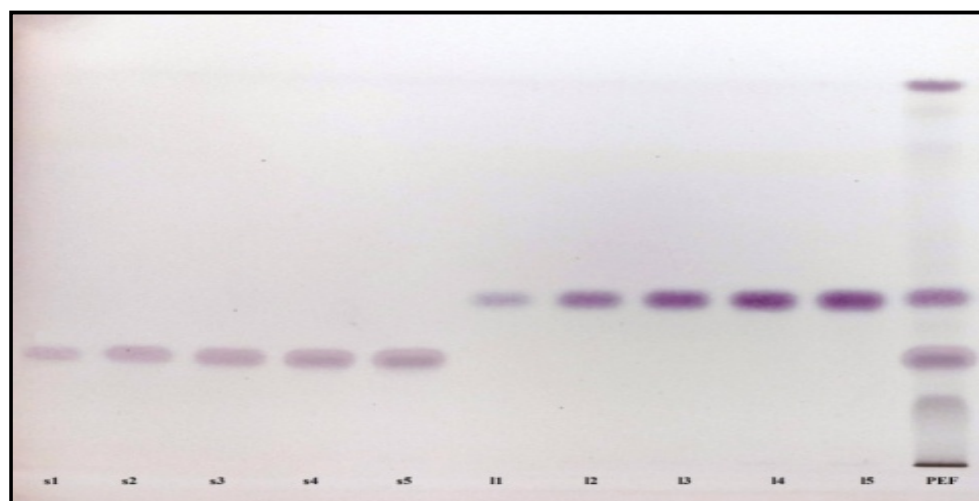


Figure 4.55 HPTLC chromatogram of standards β -sitosterol (s1 to s5) and lupeol (l1 to l5) and PEF(Petroleum ether extract fraction)

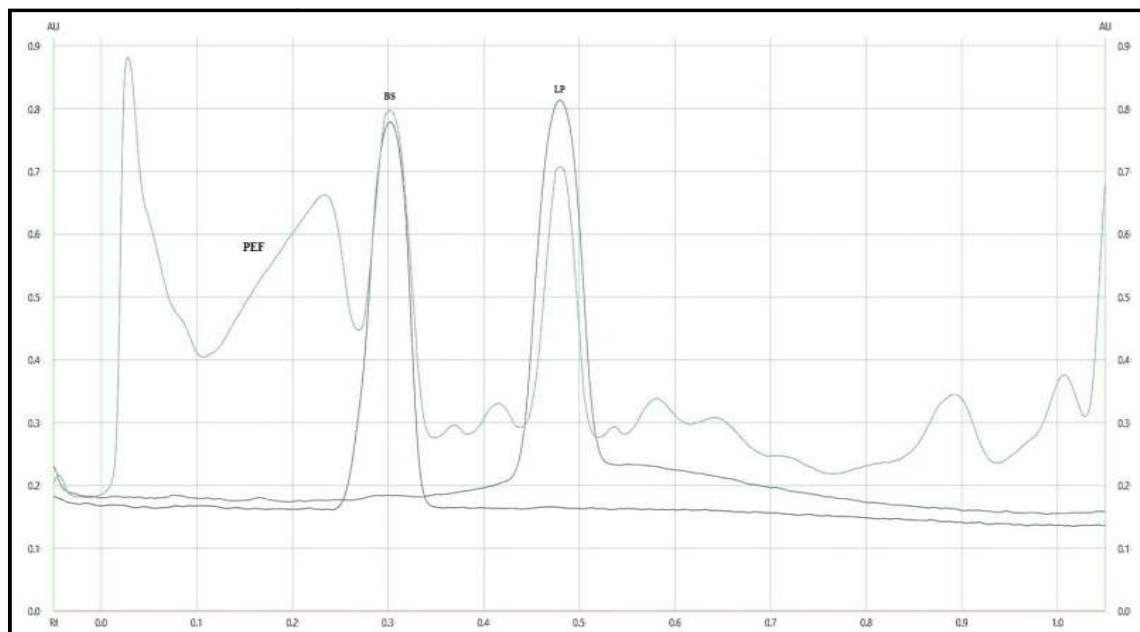
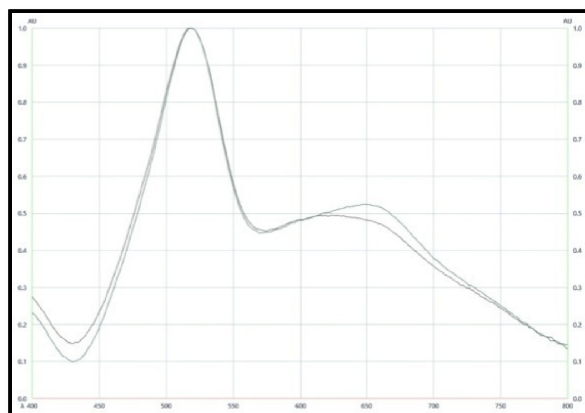
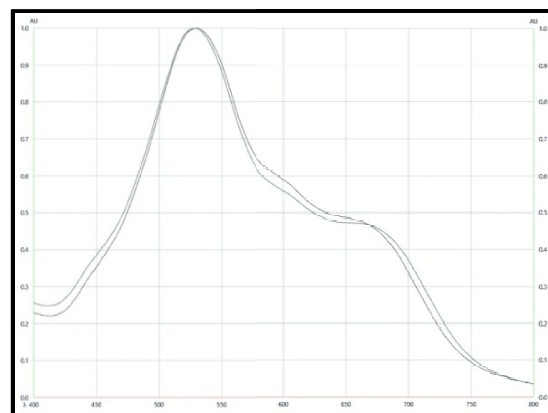


Figure 4.56 Densitometric chromatogram of standard β -sitosterol (BS), lupeol (LP) and Petroleum ether extract fraction (PEF)



(A)



(B)

Figure 4.57 Overlain spectra of β -sitosterol (A) and lupeol (B) with PEF

The fraction obtained from the extract A1 was analyzed by the proposed HPTLC method. The amount of β -sitosterol and lupeol was computed from the calibration data. The HPTLC chromatogram of β -sitosterol and lupeol are shown in Fig 4.55 to Fig. 4.57.

The method for simultaneous estimation of β -sitosterol and lupeol was validated according to the ICH guidelines. The linearity study indicated that the area was directly proportional to concentration and hence, the developed method was considered linear. Quantification was achieved with linear calibration curves at a concentration range of 1000–9000ng/spot indicating that the method is sensitive. %CV for repeatability and reproducibility study was less than 1.5 showing that the method was precise. In the robustness study, %CV was found to be less than 1.5 indicating that small changes in parameters, such as mobile phase ratio, did not show any major changes in results. The LOD and LOQ for β -sitosterol and lupeol were found to be at 218.07 and 660.82 ng and 228.68 and 692.97ng respectively. The average recoveries of β -sitosterol and lupeol were found close to 99%.

Table 4.27 Summary of validation parameters for β -sitosterol and lupeol estimation by HPTLC

Sr.No.	Parameters	β -sitosterol	Lupeol
1	Linearity range	1000-9000ng/spot	1000-9000ng/spot
2	Correlation co-efficient	0.999	0.999
3	Repeatability (%RSD)	0.721	0.676
	Reproducibility (%RSD)	0.635	0.845
	Interday precision (%CV)	0.564-1.733	0.776-1.435
	Intraday precision (%CV)	0.521-1.109	0.507-1.127
4	Accuracy %	99.02-99.32	98.83-99.11
5	Limit of Detection (ng/spot)	218.07	228.68
6	Limit of quantification (ng/spot)	660.82	692.97
7	Specificity	Specific	Specific

4.16 Identification and estimation of compounds from MEF

4.16.1 Identification of (+)catechin and (-)epicatechin in MEF by TLC

Co-TLC of a fraction of TME (MEF) with standard (+)catechin and (-)epicatechin was carried out to identify the presence of catechin and epicatechin in MEF using diisopropyl ether: ethylacetate: formic acid(9.0:0.2:0.7 v/v) as mobile phase. In MEF spots are observed at the same Rf of (+)catechin and (-)epicatechin at 280nm. For (+)catechin Rf was 0.472 and for (-)epicatechin Rf was 0.377. (Figure 4.58)

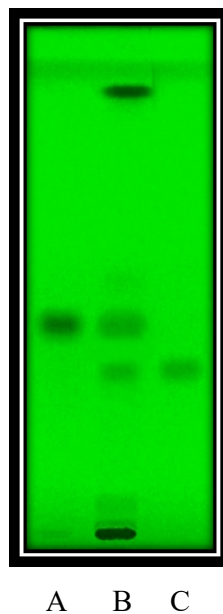


Figure 4.58 TLC of MEF (B) with standard (+)catechin (A) and (-)epicatechin (C)

4.16.2 Identification of (+)catechin and (-)epicatechin in MEF by Mass

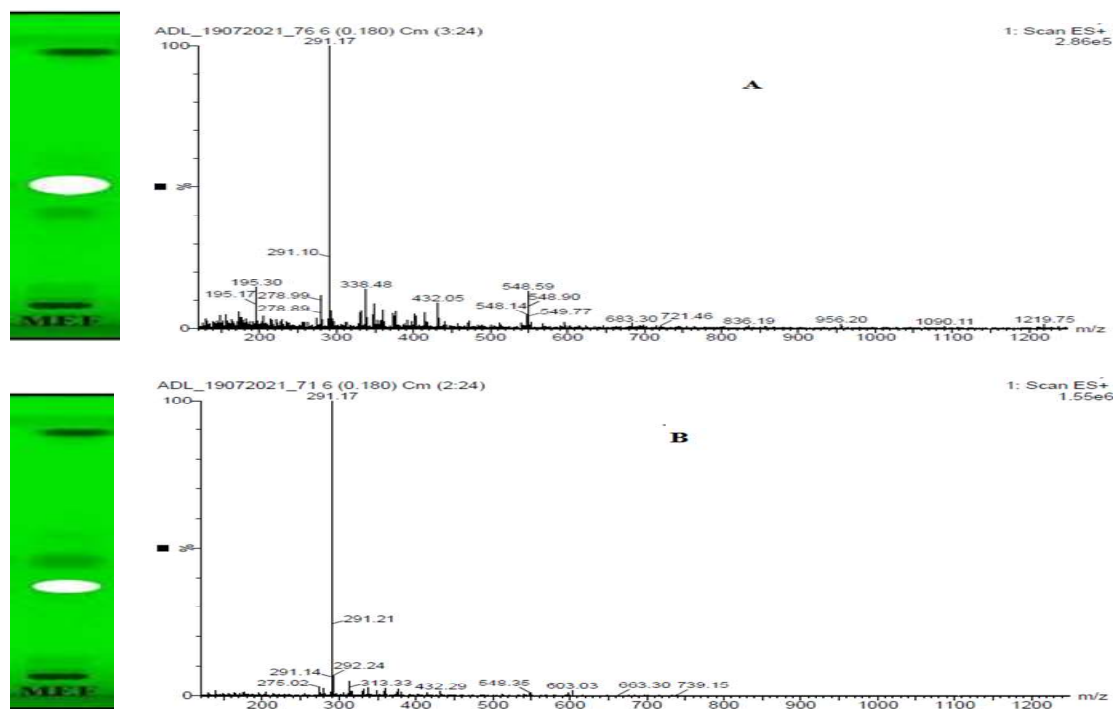


Figure 4.59 Mass spectra of (+)catechin (A) and (-)epicatechin (B) from MEF

4.16.3 Estimation of (+)catechin and (-)epicatechin in MEF by HPTLC

HPTLC chromatogram of standard (+)catechin and (-)epicatechin were taken with MEF and it was confirmed by scanning at 280 nm.

4.16.3.1 Calibration curve of (+)catechin and (-)epicatechin

The calibration data ranged between 1000-5000ng/spot for (+)catechin and (-)epicatechin. The calibration curve was obtained by plotting concentration vs. peak area.

Table 4.28 Calibration curve of (+)catechin and (-)epicatechin

Sr.No.	Compounds	Range (ng/spot)	Linear regression equation	r^2
1	(+)Catechin	1000-5000	$y = 3.185x + 4020$	0.998
2	(-)Epicatechin	1000-5000	$y = 3.049x + 3659$	0.997

4.16.3.2 Validation of HPTLC method for (+)catechin and (-)epicatechin

Linearity

The calibration curves showed linearity for both compounds with $r^2 > 0.99$. Linear regression analysis of the calibration curves of these compounds is provided in Table 4.28.

Precision

The interday precision coefficient of variation for compounds (+)catechin and (-)epicatechin varied from 0.428 to 1.316 and 0.450 to 1.266 respectively. The intraday precision coefficient of variation for compounds (+)catechin and (-)epicatechin varied from 0.467 to 1.036 and 0.497 to 1.149 respectively. (Table 4.29)

Specificity

The developed and validated method was found to be specific for quantifying compounds (+)catechin and (-)epicatechin as distinct from their peak purity values and the absence of any other co-eluting peaks.

Limit of detection

The LODs were 284.80 and 287.08ng/spot for (+)catechin and (-)epicatechin respectively. (Table 4.30)

Limit of Quantification

The minimum quantification limit was found to be 836.04 and 869.94ng/spot for (+)catechin and (-)epicatechin respectively.(Table 4.30)

Recovery

The average recovery percentage was found to be 98.86% for (+)catechin and 99.21% for (-)epicatechin. (Table 4.30)

Table 4.29 Intra and interday precision analysis of (+)catechin and (-)epicatechin

Marker	Concentration (ng/spot)	Intra-day precision (%CV)	Inter-day precision (%CV)
(+)catechin	2000	1.036	1.316
	3000	0.594	0.679
	4000	0.467	0.428
(-)epicatechin	2000	1.149	0.700
	3000	0.811	1.266
	4000	0.497	1.316

Tablet 4.30 LOD, LOQ and recovery

Sr.No.	Compounds	LOD (ng/spot)	LOQ (ng/spot)	Recovery (%)
1	(+) Catechin	284.80	863.04	98.86
2	(-) Epicatechin	287.08	869.94	99.21

4.16.3.3 Quantification of (+)catechin and (-)epicatechin

An external calibration procedure was applied for the quantification. The peak of compounds in the sample was identified by comparing the R_f value and UV spectra obtained in reference standards. Both compounds were detected in MEF. (Table 4.31)

Table 4.31 Quantification (n=3) data of (+)catechin and (-)epicatechin in MEF

Sr.No.	Analyte	% Content (w/w)
1	(+)Catechin	0.0577±0.009
2	(-)Epicatechin	0.0318±0.008

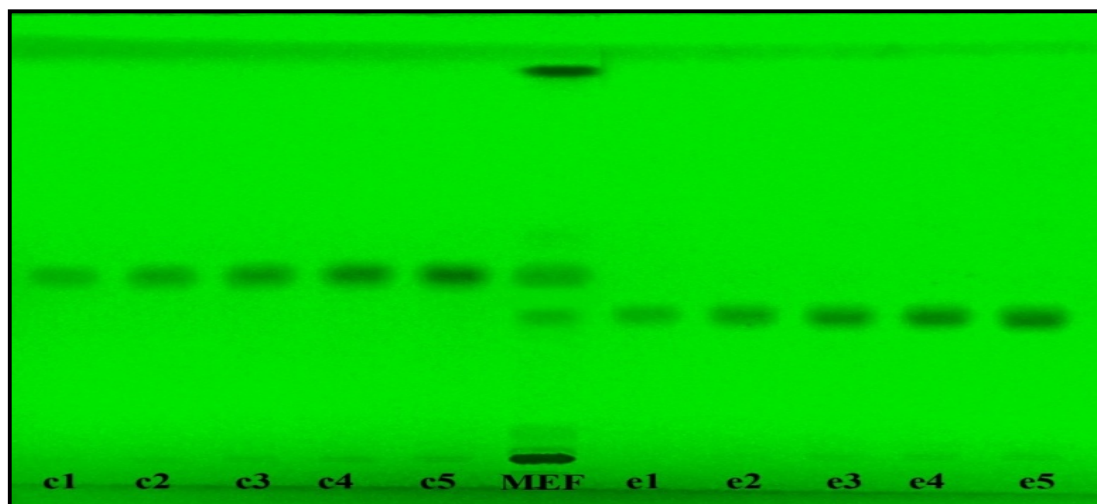


Figure 4.60 HPTLC chromatogram of standards (+)catechin (c1 to c5) and (-)epicatechin (e1 to e5) and MEF(Total methanolic extract fraction)

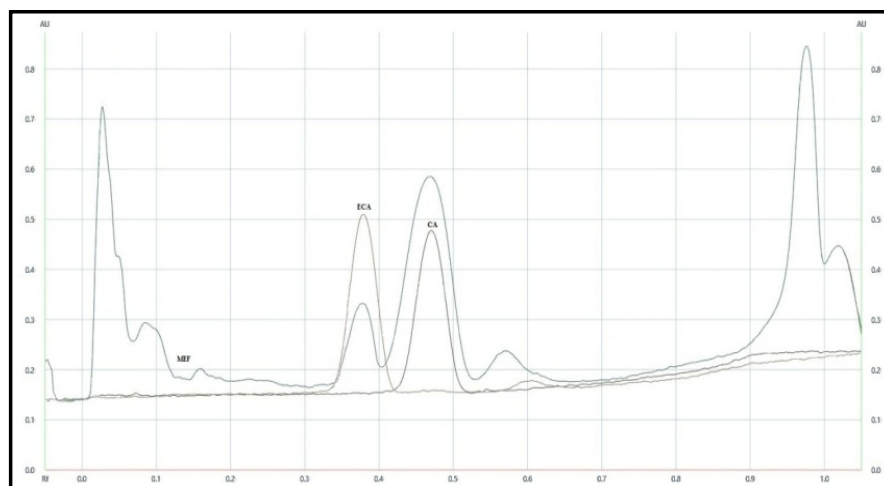


Figure 4.61 Densitometric chromatogram of standard (+)catechin and (-)epicatechin and total methanolic extract fraction (MEF)

The fraction obtained from the TME was analyzed by the proposed HPTLC method. The amount of (+)catechin and (-)epicatechin was computed from the calibration data. The HPTLC chromatogram of (+)catechin and (-)epicatechin are shown in Fig 4.60 to Fig. 4.62.

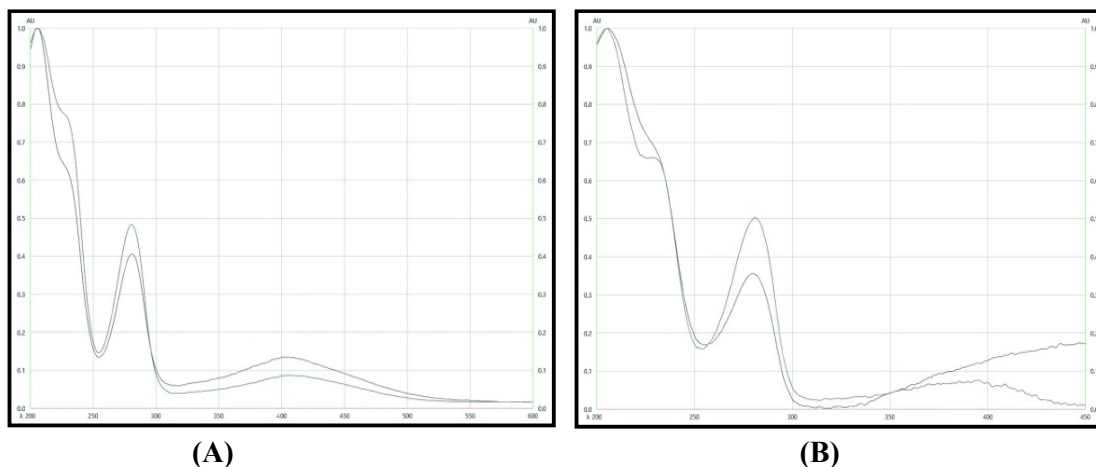


Figure 4.62 Overlain spectra of (+)catechin (A) and (-)epicatechin (B) with MEF

The method for simultaneous estimation of (+)catechin and (-)epicatechin was validated according to the ICH guidelines. The linearity study indicated that the area was directly proportional to concentration and hence, the developed method was considered linear. Quantification was achieved with linear calibration curves at a concentration range of 1000–5000 ng/spot indicating that the method is sensitive. %CV for repeatability and reproducibility study was less than 1.5 showing that the method was precise. In the robustness study, %CV was found to be less than 1.5 indicating that small changes in parameters, such as mobile phase ratio, did not show any major changes in results. The LOD and LOQ for (+)catechin and (-)epicatechin were found to be at 284.80 and 836.04ng and 287.08 and 869.94ng respectively. The average recoveries of (+)catechin and (-)epicatechin were found close to 98%.

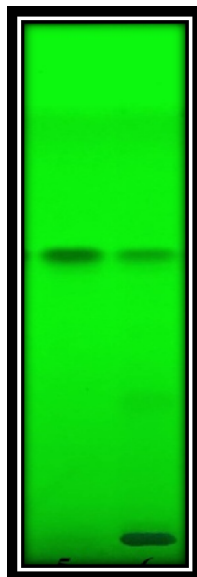
Table 4.32 Summary of validation parameters (+)catechin and (-)epicatechin estimation by HPTLC

Sr.No.	Parameter	(+) catechin	(-) epicatechin
1	Linearity range	1000-5000ng/spot	1000-5000ng/spot
2	Correlation co-efficient	0.998	0.997
3	Repeatability (%RSD)	0.670	0.562
	Reproducibility (%RSD)	0.862	0.921
	Interday precision (%CV)	0.428-1.316	0.450-1.266
	Intraday precision (%CV)	0.467-1.036	0.497-1.149
4	Accuracy %	98.79-99.93	98.83-99.48
5	Limit of Detection (ng/spot)	284.80	287.08
6	Limit of quantification (ng/spot)	836.04	869.94
7	Specificity	Specific	Specific

4.17 Identification and estimation of compound from MEF

4.17.1 Identification of kaempferol in MEF by TLC

Co-TLC of a fraction of TME (MEF) with standard kaempferol was carried out to identify the presence of kaempferol in MEF using Toluene: ethyl acetate: Formic acid (5.4:1) as mobile phase. In MEF spots are observed at the same R_f of kaempferol at 254nm. For kaempferol R_f was 0.750. (Figure 4.63)



A B

Figure 4.63 TLC of MEF (B) with standard kaempferol (A)

4.17.2 Identification of kaempferol in MEF by Mass

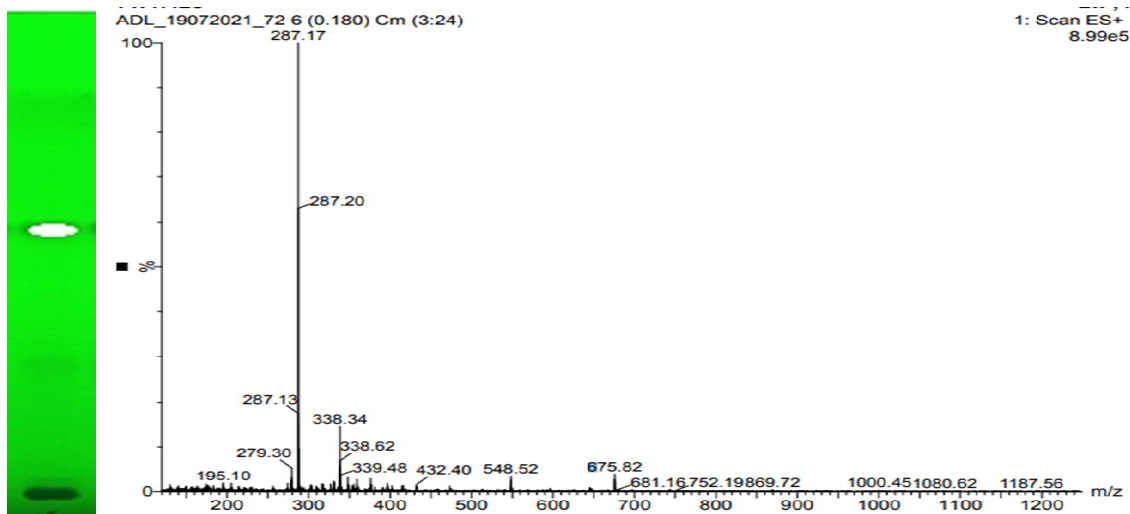


Figure 4.64 Mass spectra of kaempferol from MEF

4.17.3 Estimation of kaempferol in MEF by HPTLC

HPTLC chromatogram of standard kaempferol was taken with MEF and it was confirmed by scanning at 254nm.

4.17.3.1 Calibration curve of kaempferol

The calibration data ranged between 500-2500ng/spot for kaempferol. The calibration curve was obtained by plotting concentration vs. peak area

Table 4.33 Calibration curve of *kaempferol*

Sr.No.	Compound	Range (ng/spot)	Linear regression equation	r ²
1	Kaempferol	500-2500	y = 6.15x-9	0.998

4.17.3.2 Validation of HPTLC method for kaempferol**Linearity**

The calibration curves showed linearity for the compound with r²>0.99. Linear regression analysis of the calibration curves of the compound is provided in Table 4.33.

Precision

The interday precision coefficient of variation for kaempferol varied from 0.643 to 1.515. The intraday precision coefficient of variation for kaempferol varied from 0.470 to 1.202. (Table 4.34)

Table 4.34 Intra and interday precision analysis of kaempferol

Marker	Concentration (ng/spot)	Intra-day precision (%CV)	Inter-day precision (%CV)
Kaempferol	1000	1.202	0.883
	1500	0.470	1.515
	2000	0.895	0.643

Specificity

The developed and validated method was found to be specific for quantifying kaempferol as distinct from their peak purity values and the absence of any other co-eluting peaks.

Limit of detection

The LOD for kaempferol was found to be 111.91ng/spot (Table 4.35)

Limit of Quantification

The minimum quantification limit for kaempferol was found to be 339.14ng/spot. (Table 4.35)

Recovery

The average recovery percentage of kaempferol was found to be 98.95%. (Table 4.35)

Tablet 4.35 LOD, LOQ and recovery

Sr.No.	Compounds	LOD (ng/spot)	LOQ (ng/spot)	Recovery (%)
1	kaempferol	111.91	339.14	98.95

4.17.3.3 Quantification of kaempferol

An external calibration procedure was applied for the quantification. The peak of compound in sample was identified by comparing the R_f value and UV overlaid spectra of test spot and reference standard. Kaempferol was confirmed in MEF. (Table 4.36)

Table 4.36 Quantification (n=3) data of MEF

Sr.No.	Analyte	% Content (w/w)
1	Kaempferol	0.0286±0.008

The fraction obtained from the TME was analyzed by the proposed HPTLC method. The amount of kaempferol was computed from the calibration data. The HPTLC chromatogram of kaempferol is shown in Fig 4.65 to Fig. 4.67.

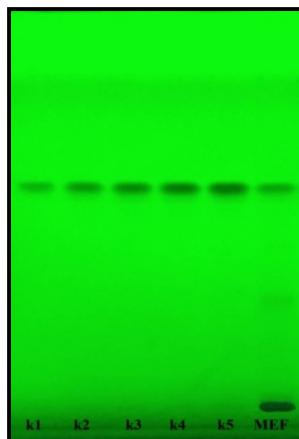


Figure 4.65 HPTLC chromatogram of standard kaempferol (k1 to k5) and MEF(Total methanolic extract fraction)

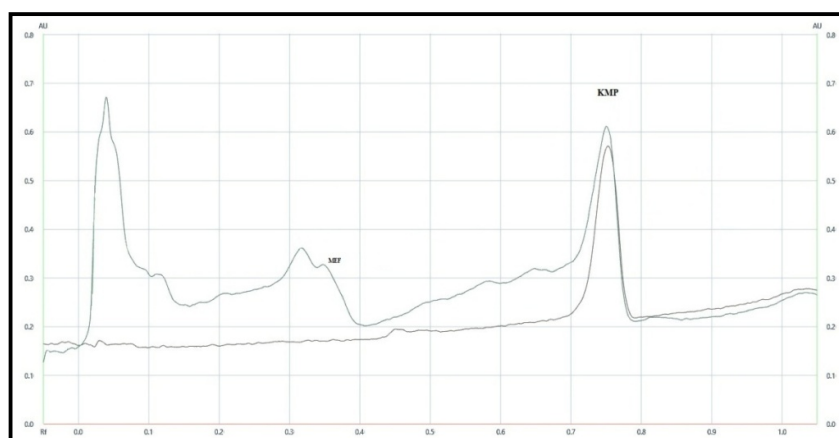


Figure 4.66 Densitometric chromatogram of standard kaempferol and total methanolic extract fraction (MEF)

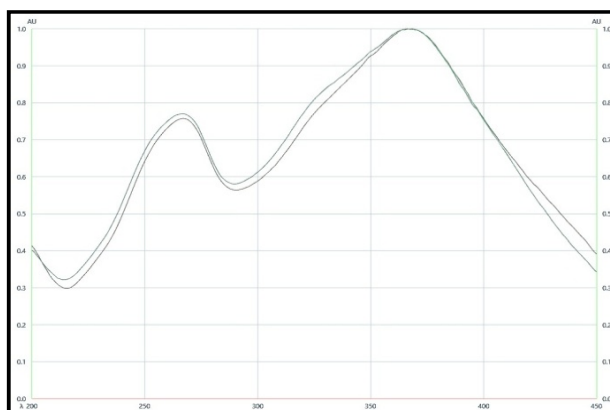


Figure 4.67 Overlain spectra of kaempferol with MEF

Table 4.37 Summary of validation parameters kaempferol estimation by HPTLC

Sr.No.	Parameters	Kaempferol
1	Linearity range	500-2500ng/spot
2	Correlation co-efficient	0.998
3	Repeatability (%RSD)	0.834
	Reproducibility (%RSD)	0.754
	Interday precision (%CV)	0.634-1.515
	Intraday precision (%CV)	0.470-1.202
4	Accuracy %	98.95
5	Limit of Detection (ng/spot)	111.91
6	Limit of quantification (ng/spot)	339.14
7	Specificity	Specific

The method for the estimation of kaempferol was validated according to the ICH guidelines. The linearity study indicated that the area was directly proportional to concentration and hence, the developed method was considered linear. Quantification was achieved with linear calibration curves at a concentration range of 500–2500ng/spot indicating that the method is sensitive. %CV for repeatability and reproducibility study was less than 1.5 showing that the method was precise. In the robustness study, %CV was found to be less than 1.5 indicating that small changes in parameters, such as mobile phase ratio, did not show any major changes in results. The LOD and LOQ for kaempferol were found to be at 111.91 and 339.14ng respectively. The average recovery of kaempferol was found close to 98%.

REFERENCES

1. The Ayurvedic pharmacopoeia of India. Government of India, Ministry of health and family Welfare department of AYUSH, New Delhi, 2007; 1(III): pp55-56.
2. Bhatti M Z, Ali A, Ahmad A, Saeed A, Malik S A. Antioxidant and phytochemical analysis of *Ranunculus arvensis* L. extracts. BMC Res Notes. 2015;(8):279
3. Habu J B, & Ibeh B O. *In vitro* antioxidant capacity and free radical scavenging evaluation of active metabolite constituents of newbouldialaervis ethanolic leaf extract. Biol Res. 2015;48(1):16.
4. Rieser M J, Gu Z M, Fang X P, Zeng L, Wood K V, McLaughlin J L. Five novel mono-tetrahydrofuran ring acetogenins from the seeds of *Annona muricata*. J Nat Prod. 1996;59:100–8.
5. Finney D, Probit analysis: a statistical treatment of the sigmoid response curve, Cambridge University Press, Cambridge.1952.
6. Finney D. Probit analysis, third ed. Cambridge University Press, Cambridge.1971.
7. Mosmann T. Rapid colorimetric assay for cellular growth and survival: application to proliferation and cytotoxicity assays. J. Immunol. Methods. 1983; 65(1):55–63.
8. Kumar N, Kumar R, Kishore K. Onosma L.: A review of phytochemistry and ethnopharmacology. Pharmacogn Rev. 2013;7(14):140-51.
9. Farooq U, Yanjun P, Disasa D, Qi J. Novel Anti-Aging Benzoquinone Derivatives from *Onosmabracteatum* Wall. Molecules 2019; 24:1-9.
10. Pijuan J, Barcelo C, Moreno D F, Maiques O, Siso P, Marti R.M et.al., *In vitro* Cell Migration, Invasion, and Adhesion Assays: From Cell Imaging to Data Analysis. Front. Cell Dev. Biol. 2019; 7:107
11. Badmus J A, Ekpo O E, Hussein A A, Meyer M, Hiss D C. Antiproliferative and Apoptosis Induction Potential of the Methanolic Leaf Extract of *Holarrhena floribunda* (G. Don). Evid Based Complement Alternat Med. 2015;756482

12. Tice R R, Agurell E, Anderson D, Burlinson B, Hartmann A, Kobayashi H, et al. Single cell gel/comet assay: guidelines for in vitro and in vivo genetic toxicology testing. *Environ Mol Mutagenesis*. 2000;35:206–21
13. Efenberger-Szmechtyk M, Nowak A, Nowak A. Cytotoxic and DNA-Damaging Effects of *Aronia melanocarpa*, *Cornus mas*, and *Chaenomeles superba* Leaf Extracts on the Human Colon Adenocarcinoma Cell Line Caco-2. *Antioxidants*. 2020; 9(11):1030
14. Charaka Samhita, Shri Gulabkunverba Ayurvedic Society, Jamnagar, Ayurvedic Mundranalaya, Jamnagar 1949; 4: 1952
15. Sharma P V, Dravyaguna-Vijnana, Vol II, Chaukhambhabharati academy, Varanasi, 12th edition, 1991; 256-258.
16. Chunekar K C. Bhavaprakash Nighantu. Commentary. A.M.S. Edited By Dr. G.S. Pandey, A.M.S. Chaukhambha Bharti Academy Publisher Varanasi. Pp 472-7.
17. Kaiyadev Nighantu. Edited And Translated By Prof. Priyavrata Sharma And Dr. Guru Prasad Sharma. Chaukhambha Orientalia Varanasi. pp.136.
18. Fadok V A, Voelker D R, Campbell P A, Cohen J J, Bratton D L, Henson P M. Exposure of phosphatidylserine on the surface of apoptotic lymphocytes triggers specific recognition and removal by macrophages. *J. Immunol.* 1992;148(7):2207–2216
19. Hsu Y L, Chia C C, Chen P J, Huang S E, Huang S C, Kuo P L. Shallot and licorice constituent isoliquiritigenin arrests cell cycle progression and induces apoptosis through the induction of ATM/p53 and initiation of the mitochondrial system in human cervical carcinoma HeLa cells. *Mol. Nutr. Food Res.* 2009;53(7):826–835.
20. Pavia D L, Lampman G M, Kriz G S, Introduction to spectroscopy a guide for student of organic chemistry, 3rd edition, Thomson learning academic resource center.
21. Wu J, Dai J, Zhang Y, Wang J, Huang L, Ding H et al. Synthesis of Novel Xanthone Analogues and Their Growth Inhibitory Activity Against Human Lung Cancer A549 Cells. *Drug design, development and therapy*. 2019;13:4239-4246

22. Constantinou C, Papas A, Constantinou AI. Vitamin E and cancer: An insight into the anticancer activities of vitamin E isomers and analogs. *Int J Cancer*. 2008;123(4):739-52
23. Doldo E, Costanza G, Agostinelli S, Tarquini C, Ferlosio A, Arcuri G et.al., Vitamin A, *Cancer Treatment and Prevention: The New Role of Cellular Retinol Binding Proteins*, *Biomed Res Int*. 2015; 624627.
24. Kim S H, Ryu H, Lee J, Shin J, Harikishore A, Jung H et.al., Ursolic acid exerts anti-cancer activity by suppressing vaccinia-related kinase 1-mediated damage repair in lung cancer cells. *Sci Rep*. 2015; 5:14570.
25. Kommera H, Kaluderovic G N, Kalbitz J, Paschke R. Synthesis and Anticancer Activity of Novel Betulinic acid and Betulin Derivatives. *Arch Pharm*. 2010; 343(8):449-57.
26. Gupta A, Singh A K, Loka M, Pandey A K, Bishayee A. Ferulic acid-mediated modulation of apoptotic signaling pathways in cancer. *Adv. Protein Chem. Struct. Biol.* 2021 ; 125:215-257
27. Mallick N, Singh M, Parveen R, Khan W, Ahmad S, Najm M Z et.al., HPTLC Analysis of Bioactivity Guided Anticancer Enriched Fraction of Hydroalcoholic Extract of *Picrorhizakurroa*. *Biomed Res. Int.* 2015; 513875
28. Kim H J, Hwang K E, Park DS. et al. Shikonin-induced necroptosis is enhanced by the inhibition of autophagy in non-small cell lung cancer cells. *J Transl Med* 2017; 15:123.

Chapter 5

Summary & Conclusion

SUMMARY & CONCLUSION

Onosma bracteatum was collected, authenticated, and used for the present study. Important features to consider for morphological identification include twisted and rough stems and roots, a fibrous fracture, and a brown color. Additionally, the flowers of *O. bracteatum* exhibit a deep blue to purplish color, while the bracts are lanceolate and hairy. Microscopical analysis of the powder revealed the presence of cork cells, xylem vessels, long, unicellular warty trichomes, rosettes of calcium oxalate crystals, and hexagonal and star-shaped pollen. These characteristics serve as key features for the identification of the *O. bracteatum* plant. Furthermore, the plant was subjected to proximate analysis and compared with Ayurvedic pharmacopoeial standards for further identification.

The utilization of bioactivity-guided fractionation and isolation, in conjunction with chromatographic separation techniques, is extensively employed for the discovery of lead compounds from plants. Preliminary phytochemical screening, as well as in vitro antioxidant activity and cytotoxicity assessments (including Brine shrimp lethality assay and MTT assay in A549 and NCI-H23 cell lines), were found to be helpful in guiding the extraction and fractionation processes of the total methanolic extract. Furthermore, successive solvent extraction of the powder was performed using the Soxhlet extraction method to collect solvent extracts ranging from non-polar to polar.

The bioactivity-driven isolation approach has played a significant role in the discovery of various plant-derived natural products, including anticancer agents such as camptothecin from *Camptotheca acuminata* and paclitaxel from *Taxus brevifolia*. The assessment of apoptosis is a crucial parameter in studying anticancer activity. The apoptosis profile comprises several assays, including the MTT assay to evaluate cytotoxicity, the scratch assay to analyze cell migration, the annexin V assay to detect cells in different stages of apoptosis, the caspase 3/7 assay to assess the activity of caspase enzymes, and the comet assay to evaluate cellular DNA damage. It was observed that the petroleum ether and chloroform extracts displayed the most pronounced apoptosis activity on lung cancer cell lines. Further more the apoptosis profile of the mixture of pet ether and chloroform extract exhibited synergistic activity on both cell lines. Consequently, this combination presents potential for further

investigation in formulation studies. However, as our project primarily emphasizes bioactivity-guided compound isolation rather than formulation. Hence, column chromatography was performed solely on the petroleum ether extract to obtain fractions. Subsequently, all fractions underwent apoptosis profile analysis.

All fractions and the mixture of petroleum ether and chloroform exhibited significant antiproliferative activity and antimigratory activity, as determined by the wound scratch assay. Additionally, they demonstrated activation of the caspase 3/7 enzyme, and increased cell population in early and late apoptotic cell stage as determined by Annexin V assay. Furthermore, the mixture of petroleum ether and chloroform, as well as fraction PF5 and PF6, induced cell death and genotoxic effects, which were confirmed by DNA damage observed in the comet assay. HPLC-MS analysis revealed that the active extract and fractions were enriched with alkaloids, shikonin, xanthenes, sterols, flavonoids, phenolics, and coumarins.

HPTLC has been extensively utilized for the simultaneous assay of multiple components in extracts, fractions, and multicomponent formulations. Through TLC studies, we have successfully identified β -sitosterol, lupeol, catechin, epicatechin, and kaempferol in extract/fraction using co-TLC with standard. β -sitosterol and lupeol were simultaneously estimated in the pet ether fraction of *O.bracteatum* by a simultaneous HPTLC method tailored and validated according to ICH guidelines. Similarly, a customized HPTLC-MS method was developed to concurrently estimate the epimer (+)catechin and (-)epicatechin in the total methanolic extract fraction of *O. bracteatum*. Additionally, the estimation of kaempferol in the total methanolic extract fraction of *O. bracteatum* was carried out using an HPTLC-MS method. All three methods exhibited excellent band resolution and demonstrated simplicity, precision, and reproducibility, making them suitable for routine analysis of this commercially valuable medicinal plant.

The current study holds significant importance as it aims to provide scientific validation for the traditional medicinal claims associated with the plant extracts and fractions. The observed anticancer activity of the extract and fractions can be attributed to the presence of isolated and identified phytochemicals, which include alkaloids, shikonin, xanthenes, sterols, flavonoids, phenolics, and coumarins. Moreover, many of compounds only identified in our study, that need to isolate and

tested for further bioactivity. Identification of compounds from specific fractions suggests further isolation and exploration of the bioactivity of a new lead molecule from plants for future research by researchers.

Appendix A: Authentication certificate of *Onosma bracteatum* Wall.


Herbal Research & Development Institute (HRDI)
उद्योग-सुटी शोध एवं विकास संस्थान (एचआरडीआई)
Mandal, Gopeshwar - 246 401
मण्डल, गोपेश्वर - 246 401
Phone: 01372 254230, Fax: 01372-254233, website: hrddi.org Email: director_hrddi@yahoo.in

Ref. No. Gopeshwar/HRDI/ Herbarium /2015-16 Dated, 10 February 2016

CERTIFICATE

This is to certify that the herbarium specimens prepared by Department of Pharmacognosy, L. M. College of Pharmacy are as follows:

Voucher No.	Botanical Name	Family
PCOG/2016/1	<i>Hippophae salicifolia</i>	Elaeagnaceae
PCOG/2016/2	<i>Juniperus indica</i>	Cupressaceae
PCOG/2016/3	<i>Pleurospermum angelicoides</i>	Apiaceae
PCOG/2016/4	<i>Rumex napelensis</i>	Polygonaceae
PCOG/2016/5	<i>Onosma bracteatum</i>	Boraginaceae


(Dr. V. P. Bhatt)
(Scientist)

LIST OF PUBLICATIONS

- 1) Aruna M Rajapara, Vijay P Bhatt and Mamta B Shah. Phytochemical and Pharmacological Investigation on *Onosma bracteatum* Wall. Asian Journal of Biological and Life Sciences, 2021,10,1,141-149. DOI:10.5530/ajbls.2021.10.21
- 2 Aruna M. Rajapara, Mamta B. Shah. THE GENUS ONOSMA L.: A COMPREHENSIVE REVIEW. EPRA International Journal of Research and Development (IJRD). DOI: <https://doi.org/10.36713/epra9023>
- 3 Aruna Rajpara, Mamta B. Shah, Noopur Gandhi, Vijay Bhatt. Simultaneous determination of epimers ((+)-catechin and (-)-epicatechin) in *Onosma bracteatum* Wall. using the HPTLC-MS method. Journal of Planer chromatography-Modern TLC. DOI:10.1007/s00764-022-00157-5

Gujarat Technological University

PhD Viva Voce Report

TITLE OF THE THESIS:

Bioactivity guided extraction and fractionation of *Onosma bracteatum* with specific reference to its anti-cancer activity against lung cell cancer.

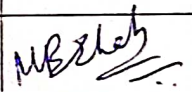


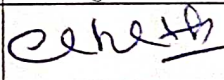
Name of the Scholar	Enrollment No.	Day & Date of Public Viva Voce	Discipline/ Branch	Venue
Arunabehn Mavjibhai Rajapara	149997390002	30 th April 2024, Tuesday	Pharmacy	GTU Gandhinagar

Based on the thesis defense of above mentioned PhD Thesis, the overall recommendation on the thesis is as follows (Please tick any one of the following option):

- The performance of the candidate was satisfactory. We recommend that he/she be awarded the PhD Degree.
- Any further modifications in research work recommend by the panel after 3 months from the date of first viva-voce upon request of the Supervisor or request of Independent Research Scholar after which viva-voce can be re-conducted by the same panel again. The suggestions for improving the thesis based on the discussions during the oral examination is detailed in a separate sheet to be incorporated in the thesis.
- The performance of the candidate was unsatisfactory. We recommend that he/she should not be awarded the PhD Degree. A separate sheet is enclosed describing unsatisfactory performance.

Further, it is certified that the examiner who participated in the thesis defense through electronic medium (if any), have confirmed the above recommendation after the viva-voce (through email as attached; if any) and the same may be considered sufficient record for acceptance.

BOARD OF EXAMINERS:

Sl No	Name	Designation	Institute	Signature
1.	Dr. Mamta B Shah	Supervisor/ Co-Supervisor*	L.M.College of Pharmacy	
2.	Dr. Jagannath Sahoo	External Examiner 1	NMIMS University, Mumbai	 30/4/24
3.	Dr. Johnson Stanslas	External Examiner who participated through e- medium (if any)	Universiti Putra Malaysia, Selangor, Malaysia	 30/4/24
4.	Dr.N.R. Sheth	DPC Member	Ex-Vice chancellor, GTU	

Encl.:

- 1) Separate sheet for suggestions / comments on the thesis (if any) endorsed by the Supervisor/ Co-Supervisor and the external examiners. The same to be provided to the scholar for revision/ modification in the thesis.
- 2) Email of external examiner (if any) who participated in the thesis defense through electronic medium.
- 3) Undertaking for final submission of hard copy of Ph.D. thesis & CD.

For Office Use Only (Strike off whichever is not applicable)-Notification to / not to be issued

Honorable Vice Chancellor